MUTATIONAL ANALYSIS OF CD127 AND ITS ROLE IN IMMUNOLOGICAL DISEASES

Marko Cavar

A thesis submitted to the
Faculty of Graduate and Postdoctoral Studies
in partial fulfillment of the requirements for the
Master of Science (M.Sc.) degree in Microbiology and Immunology.

Department of Biochemistry, Microbiology, and Immunology
Faculty of Medicine
University of Ottawa

ABSTRACT

Interleukin (IL) -7 is an essential non-redundant cytokine that influences T-cell differentiation, proliferation, homeostasis and T-cell functions. In T-cells, IL-7 signals are transduced via IL-7's heterodimeric receptor composed of a common, γ chain (CD132) and an IL-7 specific, α chain (CD127). In light of the many roles that IL-7 plays in T-cell biology, it is no surprise that CD127 expression is tightly regulated in T-cells.

In this study, I explore the effects that disease specific mutations in CD127 have on CD127 expression, regulation and signal transduction using an *in vitro* T-cell model. Here I specifically examined four disease associated mutations of CD127: P132S associated with severe combined immunodeficiency; L242_L243insNPC associated with T-cell acute lymphoblastic leukemia; I356V & T244I associated with autoimmune diseases like multiple sclerosis, rheumatoid arthritis and type 1 diabetes. In developing my model, I decided to use Jurkat cells because they expressed high endogenous surface levels of CD132, low endogenous surface levels of CD127 and endogenous STAT5. Jurkat cells were transduced with lentiviruses that induced expression of either WT or one of the four mutant CD127.

I found that transduced Jurkat cells produced the WT and all four mutant CD127 proteins. I also found that wild type CD127, I356V, L242_L243insNPC and T244I mutant CD127 proteins were all expressed at the same level on the cell surface. However, I could not detect P132S mutated CD127 protein in its native state on the surface or intracellularly. I also found no differences between the mutant CD127 and wild type CD127 with regards to the level of soluble CD127 transcripts. I found that cell lines expressing L242_L243insNPC, I356V and T244I mutant CD127 protein, down-regulated surface CD127 at high IL-7 doses (25ng/mL) to the same extent as in the cell line expressing wild type CD127 protein. Interestingly, at the low IL-7 dose (1ng/mL) these mutant CD127 cell lines down-regulated surface CD127 to a lesser degree the wild type CD127 cell line.

Further studies are required to elucidate whether P132S mutated CD127 is expressed on the surface and if T224I and I356V mutations in CD127 enhance signaling. By understanding CD127 dysregulation and dysfunction in disease states, we can potentially develop therapeutics that can return the function of CD127 to normalcy.

ACKNOWLEDGEMENTS

First, I would like to thank my PI, Dr. Paul A. MacPherson, for taking me on as a student. Paul is a brilliant and creative scientist, who has guided me through my two year journey into basic research. Paul has taught me various aspects of basic research from how to approach experimental design to analyzing data to grant writing and more. Paul has inspired me to work hard and aim high in life.

I owe much of my successes to my friend, lab mate and mentor, Dr. Elliott Faller. Elliott is one of the most knowledgeable and creative people I know. He has immensely helped me during the last two years in troubleshooting my experiments, teaching me lab techniques like flow cytometry and in analyzing data. I will miss the lunches with Elliott.

I would like to thank my TAC committee members, Drs. Jonathan Angel and Robin Parks, for their helpful discussions.

I would like to thank Nischal Ranganath for the many helpful discussions on my project, and for the support to complete my project and pursue my studies in pharmacy. Your friendship helped keep me sane when during the difficult moments.

I would like to thank my family, especially my mother, Darka Cavar and father, Nedo Cavar. Their support and love during the last two years kept me going during the difficult moments.

Lastly, I would like to thank Maria del Mar Sanchez Vidales for providing helpful discussions during my project. Maria's support kept me going during difficult moments. Her positivity and work ethic is inspiring. Having her in my corner is truly a blessing.

TABLE OF CONTENTS

LIST OF ABBREVIATIONS viii
LIST OF FIGURES xii
LIST OF TABLES xiii

CHAPTER 1: INTRODUCTION 1

1.1 Interleukin-7 and its receptor 2
1.1.1 Interleukin-7 2
1.1.2 Interleukin-7 receptor 2
1.2 Interleukin-7 role in T-cell biology 3
1.2.1 Interleukin-7 role in thymopoiesis 4
1.3 Interleukin-7 unique α chain, CD127 4
1.4 IL-7 signal transduction 9
1.4.1 Signaling through the JAK/STAT5 pathway 9
1.4.2 Signaling through the PI3K pathway 12
1.5 CD127 regulation 12
1.6 CD127 in immunological diseases 13
1.6.1 CD127 in SCID 16
1.6.2 CD127 in T-ALL 17
1.6.3 CD127 in autoimmune diseases 17
Hypothesis and Objectives 19

CHAPTER 2: MATERIALS AND METHODS 20

2.1 $CD8^+$ T-cell isolation 21
2.2 Cell culture 21
2.3 Development of cell lines that stably express WT or mutant CD127 22
2.3.1 Lentiviral system 23
2.3.2 Production of transfer vector: pWPI/MOCK/Neo 23
2.3.2.1 Restriction digestion of pWPI/hPLK2WT/Neo with BamHI 23
2.3.2.2 Gel electrophoresis and isolation of pWPI/-/Neo backbone 24
2.3.2.3 Self-ligation of pWPI/-/Neo vector backbone 24
2.3.2.4 Transformation of pWPI/MOCK/Neo into XL Gold Ultracompetent bacteria 27
2.3.3 Production of transfer vector: pWPI/CD127WT/Neo 27
2.3.3.1 Restriction digestion of pWPI/hPLK2WT/Neo and pCMV6-CD127 with XmaI 28
2.3.3.2 Restriction digestion of XmaI linearized pWPI/hPLK2WT/Neo with BamHI 28
2.3.3.3 Restriction digestion of XmaI linearized pCMV6-CD127 with BglII 28
2.3.3.4 Gel electrophoresis and isolation of pWPI/-/Neo backbone and CD127 fragment 29

2.3.3.5 Ligation of CD127 fragment with the pWPI/-/Neo vector backbone 29
2.3.3.6 Transformation of pWPI/CD127WT/Neo into XL Gold Ultracompetent bacteria 29
2.3.4 Production of the four CD127 mutants in pWPI/CD127WT/Neo transfer vectors 32
2.3.4.1 Site directed mutagenesis (SDM) to create four CD127 mutants 32
2.3.4.2 Transformation of the four CD127 mutants 36
2.3.5 Amplification of positive bacterial colonies and isolation of plasmids 36
2.3.6 DNA sequencing to confirm the wild type CD127 cDNA was incorporated into the open reading frame of pWPI/-/Neo and to confirm the four mutation of CD127 36
2.3.7 Production and harvesting of lentiviruses 37
2.3.7.1 Transfection of HEK293T cells with envelope, packaging and transfer vectors 37
2.3.7.2 Detection of lentiviruses 38
2.3.7.3 Harvesting the six different lentiviruses produced 38
2.3.8 Lentiviral transduction and selection of Jurkat cells that stably express wild type or mutant CD127 38
2.3.8.1 Coating of 6-well plate with RetroNectin® for lentiviral transduction 38
2.3.8.2 Lentiviral transduction of Jurkat cells 39
2.3.8.3 Selection of transduced Jurkat cells 39
2.4 Western blot analysis 40
2.5 Flow cytometry 42
2.5.1 Surface CD132 and CD127 42
2.5.2 Alternative staining protocols for surface CD127 43
2.5.3 Intracellular staining protocol for CD127 44
2.5.4 pSTAT5 staining protocol 44
2.5.5 Acquisition and analysis for flow cytometry 45
2.6 Comparing levels of transcript encoding soluble CD127 versus total CD127 in cell lines expressing WT or mutant CD127 45
2.6.1 Total RNA isolation 45
2.6.2 cDNA synthesis 46
2.6.3 Real-Time PCR 46
2.6.3.1 Analysis of RT-PCR data 49

CHAPTER 3: RESULTS 50

3.1 Development of an *in vitro* model to study the effect that disease specific mutations have on CD127 expression, regulation and signal transduction 51

3.1.1 All four lymphoblastic cell lines expressed high surface levels of endogenous CD132 51
3.1.2 A3, CEM and Jurkat cells expressed low surface levels of endogenous CD127 54
3.1.3 A3 cells were unsuitable for the T-cell model because they are resistant to G418 sulfate mediated cell death 54
3.1.4 CEM and Jurkat cell lines expressed endogenous STAT5 54
3.1.5 CEM cells were unsuitable for the T-cell model because they were difficult to culture and readily died 59
3.1.6 Parental Jurkat cells were unresponsive to IL-7 stimulation 59
3.1.7 Transducing Jurkat cells with WT or mutant CD127 genes to develop our T-cell models 62
3.1.8 Jurkat cells transduced with WT or mutant CD127 genes produced CD127 proteins 62
3.2 CD127 protein expression in Jurkat cells transduced with wild type or mutant CD127 genes 66
3.2.1 CD127 protein with I356V, L242_L243insNPC and T244I mutations are detected on the surface of established cell lines 66
3.2.2 CD127 containing the P132S mutation cannot be detected by flow cytometry on the cell surface 69
3.2.3 P132S mutated CD127 protein cannot be detected intracellularly by flow cytometry 69
3.3 Examining the established mutant cell lines for CD127 transcripts 74
3.3.1 The four mutant CD127 cell lines have no significant fold differences in the transcript levels of soluble CD127 (sCD127) compared to the CD127WT cell line 74
3.4 Surface CD127 down-regulation is altered in the I356V, insNPC and T244I cell lines compared to the down-regulation in the CD127WT cell line 76
3.4.1 Surface CD127 is down-regulated in the CD127WT, I356V, insNPC and T244I Jurkat cell lines in response to IL-7 76
3.5 Examining the established mutant cell lines for altered IL-7 signal transduction 83
3.5.1 In IL-7 stimulated cell lines, pSTAT5 cannot be detected above background signal 83

CHAPTER 4: DISCUSSION 87

4.1 Development of an *in vitro* model to study the effect that disease specific mutations have on CD127 expression, regulation and signal transduction 88
4.2 Wild type and CD127 proteins containing the I356V, L242_L243insNPC and T244I mutations are all expressed on the cell surface while P132S could not be detected by flow cytometry 94

4.3 CD127 cell lines express mRNA transcripts encoding the full length and soluble CD127 isoforms and there is no difference in the relative level of transcript encoding soluble CD127 between the mutants and the wild type CD127 95
4.4 Surface CD127 protein is down-regulated on the CD127WT cell line when stimulated with IL-7 97
4.5 Surface CD127 protein is down-regulated on I356V, insNPC and T244I cell lines when stimulated with high doses (>10ng/mL) of IL-7 98
4.6 The established cell lines had high basal levels of pSTAT5 and thus IL-7 signaling could not be measured by flow cytometry 100

CHAPTER 5: CONCLUSION 103

REFERENCES 106
APPENDICES 112
CURRICULUM VITAE 126

LIST OF ABBREVIATIONS

Amino Acids

Amino Acid	Three letter abbreviation	One letter abbreviation
Glycine	Gly	G
Alanine	Ala	A
Valine	Val	V
Leucine	Leu	L
Isoleucine	Ile	I
Proline	Pro	P
Phenylalanine	Phe	F
Tyrosine	Tyr	Y
Tryptophan	Trp	W
Serine	Ser	S
Threonine	Thr	T
Cysteine	Cys	C
Methionine	Met	M
Asparagine	Asn	N
Glutamine	Gln	Q
Lysine	Lys	K
Arginine	Arg	R
Histadine	His	H
Aspartate	Asp	D
Glutamate	Glu	E

Name used to refer to Jurkat cell lines that were selected:

Name of Jurkat cell line	Gene of Interest Expressed
MOCK	No Gene of Interest (except neomycin resistance gene from IRES)
CD127WT	Wild type CD127; and neomycin resistance gene
P132S	CD127 with mutation P132S; and neomycin resistance gene
I356V	CD127 with mutation I356V; and neomycin resistance gene
insNPC	CD127 with insertion mutation L242_L243insNPC; and neomycin resistance gene
T244I	CD127 with mutation T244I; and neomycin resistance gene

α	—	Alpha
Å	—	Angstrom (1E-10 meters)
aa	—	Amino acids
AKT	—	alpha serine/threonine-protein kinase
Amp	—	Ampicillin
ATCC	—	American Type Culture Collection
ATP	—	Adenosine triphosphate
β	—	Beta
Bad	—	Bcl-2 - associated death promoter (pro-apoptotic)
Bax	—	Bcl-2 - associated X protein (pro-apoptotic)
bp	—	Base pairs
Bcl-2	—	B-cell lymphoma 2 (anti-apoptotic)
Bcl-X_L	—	B-cell lymphoma-extra large (anti-apoptotic)
Bim	—	Bcl-2 like protein 1 (pro-apoptotic)
BSA	—	Bovine serum albumin
°C	—	Degrees Celsius
CD25	—	Cluster of differentiation 25, interleukin-2 receptor α chain
CD127	—	Cluster of differentiation 127, interleukin-7 receptor unique α chain
CD132	—	Cluster of differentiation 132, common γ chain
CDK	—	Cyclin-dependent kinases
cDNA	—	complementary deoxyribonucleic acid
CIP	—	Calf intestinal alkaline phosphatase
CIS	—	Cytokine-Inducible SH2-Containing Protein
cm	—	Centimeter
CMV	—	Cytomegalovirus
c-Myb	—	myeloblastosis proto-oncogene protein
CO_2	—	Carbon dioxide
Ct	—	Threshold Cycle
δ	—	Delta
DMEM	—	Dulbecco's Modified Eagles Medium
DN	—	Double negative
DNA	—	Deoxyribonucleic acid
DP	—	Double positive
DTT	—	Dithiothreitol (reducing agent)
EDTA	—	Ethylenediaminetetraacetic acid
et al.	—	"And others"
FERM	—	Four-point-one, ezrin, radixin, moesin domains (binding domain)
FoxO3	—	Forkhead box O3, transcription factor
FWD	—	Forward
γ	—	Gamma
g	—	Grams
GLUT1	—	Glucose transporter 1
GWAS	—	Genome wide association studies
HCl	—	Hydrochloric Acid
HI FBS	—	Heat inactivated fetal bovine serum
HIV	—	Human immunodeficiency virus
H_2O	—	Water

HRP	—	Horseradish Peroxidase
IL	—	Interleukin
IL-7R	—	Interleukin 7 receptor
IL-7Rα	—	Interleukin 7 receptor α chain (CD127)
IL-2Rα	—	Interleukin 2 receptor α chain (CD25)
IFN	—	Interferon
IRES	—	Internal ribosomal entry site
JAK	—	Janus kinase
Kb	—	Kilo bases
Kbp	—	Kilo basepairs
KCl	—	Potassium chloride
K_d	—	Dissociation constant
kDa	—	Kilo Daltons
L	—	Litres
LB	—	Luria broth
MACS	—	Magnet assisted cell sorting
MCL-1	—	Myeloid Cell Leukemia factor 1 (anti-apoptotic)
memCD127	—	Membrane bound CD127
µg	—	Micrograms
$MgCl_2$	—	Magnesium chloride
µL	—	Microlitres
mL	—	Millilitres
µm	—	Micrometer
mM	—	Millimolar
MS	—	Multiple sclerosis
mRNA	—	messenger RNA
NaCl	—	Sodium Chloride
Neo	—	Neomycin
ng	—	Nanograms
NDS	—	Normal donkey serum
NGS	—	Normal goat serum
NK	—	Natural killer
NP-40	—	Nonidet P-40
nM	—	Nanomolar
OHRI	—	Ottawa hospital research institute
pAKT	—	phosphorylated AKT
PBMC	—	Peripheral blood mononuclear cells
PBS	—	Phosphate buffered saline
PCR	—	Polymerase chain reaction
PDK-1	—	Phosphoinositide-dependent kinase-1
PE	—	Phycoerythrin
PES	—	polyethersulfone
PFA	—	Para formaldehyde
pg	—	Picograms
pM	—	Picomolar
PI	—	Propidium iodide

PI3K	—	Phosphoinositide 3-kinase
PIP2	—	Phosphatidylinositol 4,5-bisphosphate
PIP3	—	phosphatidylinositol (3,4,5)-trisphosphate
pSTAT5	—	phosphorylated STAT5 (phospho-STAT5)
PVDF	—	Polyvinylidene Fluoride
RA	—	Rheumatoid arthritis
REV	—	Reverse
RNA	—	Ribonucleic acid
rpm	—	revolutions per minute
RPMI 1640	—	Roswell Park Memorial Institute 1640 (media)
RPS18	—	Ribosomal protein S18
RT	—	Real time
sCD127	—	soluble CD127
SCID	—	severe combined immunodeficiency
SDM	—	Site directed mutagenesis
SDS	—	Sodium dodecyl sulfate
SH2	—	Src Homology 2
SLE	—	Systemic lupus erythematosus
SNP	—	Single nucleotide polymorphism
SP	—	Single positive
SOCS2	—	Suppressor of cytokine signaling 2
STAT5	—	Signal transducer and activator of transcription 5
T1D	—	Type 1 diabetes
T-ALL	—	T-cell acute lymphoblastic leukemia
Tat	—	Transactivator of transcription
TCR	—	T-cell receptor
TBST	—	Tris-buffered saline with Tween-20
U	—	Units
V	—	Volts
V(D)J	—	Variable, Diversity, and Joining regions
WT	—	Wild type

LIST OF FIGURES

Figure 1: Structure of the interleukin-7 receptor 6

Figure 2 : Interleukin-7 signal transduction 10

Figure 3 : Schematic showing the location of the four mutations on CD127 14

Figure 4 : Sub-cloning strategy to produce the empty transfer vector: pWPI/MOCK/Neo 25

Figure 5 : Sub-cloning strategy to produce the transfer vector: pWPI/CD127WT/Neo 30

Figure 6 : Cloning strategy to produce CD127 mutants in the transfer vector: pWPI/CD127WT/Neo 34

Figure 7 : A3, CEM, Jurkat and SupT1 cell lines express high surface levels of endogenous CD132 relative to primary human CD8+ T-cells 52

Figure 8 : A3, CEM and Jurkat cells have the lowest surface expression of endogenous CD127 relative to primary human $CD8^+$ T-cells 55

Figure 9 : STAT5 is endogenously expressed by both Jurkat and CEM cell lines 57

Figure 10 : Jurkat cells do not phosphorylate STAT5 in response to IL-7 (10ng/µL) 60

Figure 11: Transduced Jurkat cell lines stably express wild type CD127 and mutant CD127 genes 64

Figure 12 : CD127WT, I356V, L242_L243insNPC and T244I transduced Jurkat cells have significantly higher surface expression of CD127 relative to the MOCK vector transduced Jurkat cells 67

Figure 13 : P132S mutant CD127 protein cannot be detected on the surface of cells by three different monoclonal anti-CD127 antibodies or by a polyclonal anti-CD127 antibody 70

Figure 14 : Intracellular CD127 protein cannot be detected in P132S - Jurkat cell line 72

Figure 15 : The four mutant CD127 cell lines have no significant differences in relative mRNA expression levels of soluble CD127 (sCD127) compared to the CD127WT cell line 77

Figure 16 : CD127 is down-regulated on the surface of the CD127WT, I356V, insNPC and T244I cell lines in a dose and time dependent manner 81

Figure 17 : pSTAT5 cannot be detected above background in the CD127 expressing cell lines when stimulated with IL-7 (10ng/mL) 85

LIST OF TABLES

Table 1 : Primer sequences used in QuikChange II XL SDM kit to produce four different mutants of CD127 in the pWPI/CD127WT/Neo plasmid 33

Table 2 : Primers used in real time PCR experiments to quantify the relative amounts of total CD127, soluble CD127 and RPS18 transcripts 48

CHAPTER 1: INTRODUCTION

1.1 Interleukin-7 and its receptor

Interleukin-7 (IL-7) is a non-redundant cytokine that has essential roles in human T-cell development, survival, proliferation and differentiation [1-3]. In 1988, IL-7 was first discovered and was initially characterized as a protein that could stimulate proliferation of murine B-cell precursors ($B220^+$ Surface Ig^-) [1, 2, 4]. Other early research indicated that mice lacking IL-7 or the IL-7 receptor's unique α chain (CD127) had reduced numbers and impaired development of B and T-cells [1-3, 5, 6]. Since then IL-7 and its roles in T-cell biology have been extensively studied across multiple species [1, 2, 7].

1.1.1 Interleukin-7

Human IL-7 is a 25kDa glycoprotein; that is encoded on a 72Kb gene located on chromosome 8(q12-q13) [1, 2]. The protein structure of IL-7 is composed of four α-helix subunits that surround a hydrophobic core, a structure that is conserved amongst a variety of cytokines [1, 2, 8]. IL-7 is produced by a wide range of cells including thymic and bone marrow stromal cells, intestinal epithelium, keratinocytes, hepatocytes, endothelial cells, peripheral and follicular dendritic cells, smooth muscle cells and fibroblasts [1, 2]. In healthy adults, the circulating levels of IL-7 in plasma range from 0.3 to 8.4 pg/mL [9]. IL-7 has been shown to have a very strong binding affinity (K_d=40pM) to its receptor (IL7R) [1].

1.1.2 Interleukin-7 receptor

The IL-7 receptor (IL7R) is a heterodimer composed of a unique α chain subunit (CD127) and the common γ chain subunit (CD132) [1, 2]. Each subunit is independently expressed on the surface of cells [1, 2]. CD127 specifically binds to IL-7, while CD132 is shared amongst the common γ chain cytokines: IL-2, IL-4, IL-7, IL-9, IL-15, and IL-21 [1,

2, 5]. The binding of IL-7 to this heterodimeric receptor initiates two main signal transduction pathways in T-cells: JAK/STAT5 and Phosphoinositide 3-kinase (PI3K) (see below) [1, 2, 10].

1.2 Interleukin-7 role in T-cell biology

In human T-cells, IL-7 stimulation has been shown to induce a variety of effects. IL-7 stimulation directly promotes proliferation in naive and memory T-cell populations and in thymocytes from various stages of thymopoiesis [1, 10-13]. This proliferative effect occurs because IL-7 stimulation up-regulates the expression of telomerase and promotes progression from the G_0 phase to the S phase of the cell cycle [1, 14]. IL-7 stimulation also increases glucose uptake in T-cells by up-regulating glucose transporter-1 (GLUT1) [10]. The increase in glucose uptake satisfies the metabolic needs of T-cells undergoing proliferation. In addition, IL-7 stimulation enhances the survival of naive and memory T-cells, and thymocytes from various stages of thymopoiesis by up-regulating anti-apoptotic factors like Bcl-2, Bcl-X_L and MCL-1, and by down-regulating pro-apoptotic factors like Bad, Bax and Bim [1, 10, 15]. Finally, IL-7 stimulation enhances the cytolytic potential of effector T-cells by up-regulating perforin at the mRNA and protein level and IFNγ production [10, 16-19].

IL-7 also indirectly up-regulates proliferation and survival of antigen stimulated effector T-cells by up-regulating the surface expression of CD25 (IL-2Rα) [15, 17, 20]. Increases in IL2Rα expression on antigen stimulated effector T-cells allows for IL-2 signaling to occur and induce proliferation and survival [20].

1.2.1 Interleukin-7's role in thymopoiesis

In thymopoiesis, thymocytes begin as early T-cell progenitors that become double negative (DN; $CD4^-CD8^-$) cells, then double positive (DP; $CD4^+CD8^+$) cells and finally as single positive (SP; $CD4^+$ or $CD8^+$) T-cells [3]. IL-7 has been shown to be critical for the survival and proliferation of DN T-cells [1, 21-23]. Without IL-7 signaling, thymocytes remain as early T-cell progenitors and do not undergo development [3, 22]. Deletions of the IL7Rα gene in mice cause the thymus to be 100-fold smaller [3]. In these CD127 deficient mice, the over-expression of Bcl-2 transgene or deletion of Bax gene causes partial rescue of thymocyte development and survival [22]. In DN cells, IL-7 signaling is found to be crucial to V(D)J rearrangement of the TCR β, γ and δ genes [1, 21, 22, 24]. IL-7 activation of STAT5 causes histone acetylation of γ and δ loci allowing for the chromatin to become accessible to recombinases (RAG proteins), which rearrange the V(D)J segments in the TCR genes [1, 22]. Boudil *et al.* have also found that mice that lack the IL-7 gene undergo TCR α gene rearrangement prematurely in DN cells, opposed to normally undergoing gene rearrangement in early DP cells [24]. Whether IL-7 signaling is directly involved in TCR α gene arrangement has yet to be fully elucidated.

1.3 Interleukin-7 receptor unique α chain, CD127

The CD127 gene is 19.79kb long and is located on chromosome 5(p13) [1, 25]. The gene contains 8 exons that encode for a 459 amino acid (aa) long, single pass transmembrane protein [1, 2, 25]. Exons 1 to 5 encode for the extracellular region (aa 1-239) of CD127; exon 6 encodes for the transmembrane region (aa 240-264); and exons 7 and 8 encode for the cytoplasmic region (aa 264-459) [1, 2, 25].

The molecular weight of full length CD127 is calculated to be 49.5kDa; however due to differing levels of glycosylation the molecular weight can vary from 50 to 92 kDa [1]. Glycosylation of CD127 has been shown to enhance the binding affinity of IL-7 by 300-fold [27, 28]. This effect is attributed to glycosylation stabilizing the interactions between CD127 and CD132 and by shifting CD127 towards a state that could more readily interact with IL-7 [27, 28].

The extracellular region of CD127 includes two type-III fibronectin-like domains linked by a 3_{10} helical linker, two pairs of conserved cysteine residues that stabilize the structure of the extracellular region by forming disulfide bridges, and a Trp-Ser-X-Trp-Ser (WS-X-WS) motif that is necessary for the proper folding of the extracellular region [1, 2].

The cytoplasmic region is composed of four domains: Box1, acidic, serine-rich and C-terminal [1]. The FERM and SH2 domains of Janus Kinase (JAK)-1 are known to bind to the Box1 domain of CD127 [29]. In studies where the Box1 domain in CD127 was deleted there was no phosphorylation of JAK-1 when cells were stimulated with IL-7 [1]. Src kinases like $p59^{fyn}$ and $p56^{lck}$ are known to bind to the acidic domain of CD127; however the activation of Src kinases are not dependent on IL-7 signaling in T-cells [1, 30]. The C-terminal domain contains three tyrosine residues: Y401, Y449, Y456 [1]. The SH2 domains on STAT5 and the regulatory subunit, p85, of PI3K are known to dock to the phosphorylated Y449 residue on CD127 [1, 2, 30, 31]. Researchers have observed that mutations of Y449 prevent the docking and subsequent phosphorylation of STAT5 and p85; which resulted in a loss of IL-7 signal transduction [1]. See figure 1 for IL-7R structure.

Figure 1: Structure of the interleukin-7 receptor

This receptor is composed of two single pass transmembrane subunits. The unique α chain, CD127, is highly specific to IL-7. The extracellular region (blue) of CD127 is 239 amino acids long and has two type-III fibronectin domains which are linked together by a 3_{10} helical linker peptide. The transmembrane region (orange) of CD127 is 25 amino acids long. The cytoplasmic region of CD127 is 195 amino acids long. It is composed of four domains: Box1 (red), acidic domain (light purple), serine-rich domain (purple) and C-terminal domain (dark purple). JAK-1 binds to CD127 at the Box1 domain. The C-terminal domain contains three conserved tyrosines at 401, 449 and 456. Shown in green is the common γ chain subunit, CD132. This subunit is shared with common γ chain cytokines: IL-2, IL-4, IL-7, IL-9, IL-15, & IL-21. CD132 has two type-III fibronectin domains in its extracellular region. JAK-3 binds to CD132's cytoplasmic region.

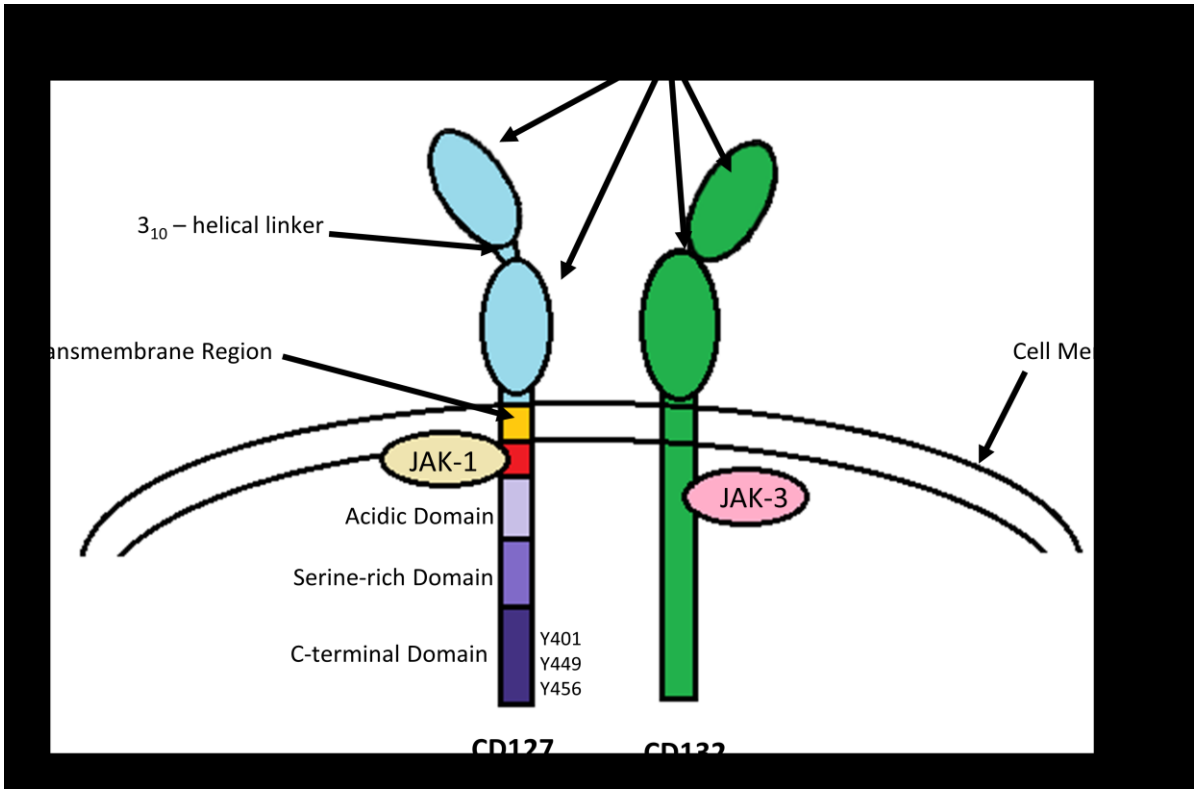
3_{10} – helical linker
ansmembrane Region
Cell Me
JAK-1
JAK-3
Acidic Domain
Serine-rich Domain
C-terminal Domain
Y401
Y449
Y456
CD127
CD132

While translation of full length membrane bound CD127 (mCD127) is most prevalent; others have found soluble CD127 (sCD127) in serum [4, 25, 26]. Soluble CD127 is translated from an mRNA transcript that excludes exon 6 [4, 25, 26]. DNA sequencing analysis reveals that only the full length CD127 is encoded in the genome and that alternative splicing of the full length CD127 gene results in the exclusion of exon 6 leading to the sCD127 isoform [1, 25].

CD127 is highly expressed on naive and memory T-cells where IL-7 is presumed to provide a survival signal through up-regulation of Bcl2 [1]. In contrast, CD127 expression is down-regulated on effector T-cells following stimulation through the TCR or other common γ chain cytokines [23]. CD127 is also highly expressed at all stages of T-cell development except in DP thymocytes [1, 2]. There are two hypotheses, altruistic or inhibitory, as to why the DP cells in thymopoiesis lack CD127. In the altruistic hypothesis, the leading T-cell in thymopoiesis (DP cells) has already benefited from the effects of IL-7 so it down-regulates CD127; this allows the trailing T-cell (DN cells) to interact with the limited amount of IL-7 left and benefit from IL-7 mediated effects [21]. In the inhibitory hypothesis, it is suggested that CD127 expression on early DP cells sends an inhibitory signal to the thymocyte to halt T-cell development; hence DP cells down-regulate expression of CD127 as a means of preventing the transduction of an inhibitory signal that halt thymocyte development [21]. These hypotheses have yet to be tested. CD127 can also be found to a lesser degree on NK precursors, bone marrow derived macrophages, developing B-cells, human endothelial cells, and a variety of cancer cells [1].

1.4 Interleukin-7 signal transduction

IL-7 initially binds to CD127 at a 1:1 ratio which leads to the recruitment of CD132 [1, 2, 27]. Once IL-7 is bound to the extracellular regions of both CD127 and CD132, the receptor subunits undergo a conformational change that brings their cytoplasmic regions in close proximity to each other (27Å) [1, 2, 27]. As the subunits come in close proximity, JAK-1 which is associated with CD127 and JAK-3 which is associated with CD132 will trans-phosphorylate each other, thereby activating the kinases [1, 2]. Activated JAKs will then phosphorylate Y449 on CD127 forming a docking site for STAT5 and p85 [1, 2]. See figure 2 for schematic of IL-7 signal transduction.

Interestingly, CD127 and CD132 are also known to form heterodimers even without IL-7 binding; however no conformational changes take place in these heterodimers and the cytoplasmic regions on each subunit remain sufficiently far apart (110Å) such that JAK-1 and JAK-3 are not trans-activated [32].

1.4.1 Signaling through the JAK/STAT5 pathway

Once STAT5 binds to the phosphorylated Y449 residue of CD127, either JAK-1 and/or JAK-3 will phosphorylate STAT5 [1, 10]. Phosphorylated STAT5 (pSTAT5) will then dimerize in the cytoplasm [1]. pSTAT5 dimers then trans-locate into the nucleus were they induce gene transcription to up-regulate pro-survival proteins (Bcl-2) and cytolytic proteins (perforin); induce proliferation, glucose uptake (GLUT1) and V(D)J rearrangement in thymocytes [1, 10].

Figure 2: Interleukin-7 signal transduction

(1) IL-7 first binds to CD127 which in turn causes the recruitment of CD132. As CD127 and CD132 come into close proximity, JAK-1 bound to CD127 and JAK-3 bound to CD132 trans-phosphorylate each other. Once activated the Janus kinases phosphorylate Y449 on CD127. (2) STAT5 docks to the phosphorylated Y499 (pY449) and is phosphorylated by JAK-1. (3) Phosphorylated STAT5 (pSTAT5) molecules dimerize in the cytosol. (4) pSTAT5 dimers trans-locate into the nucleus and induce gene transcription to up-regulate pro-survival proteins (Bcl-2) and cytolytic proteins (perforin); induce proliferation, glucose uptake (GLUT1) and V(D)J rearrangement. (5) Inactive PI3K's p85 subunit docks to pY449 and gets phosphorylated by JAK-3, thereby activating PI3K. (6) Active PI3K then phosphorylates PIP2 at the cell membrane. (7) PIP2 becomes PIP3. PDK-1 binds to PIP3 and becomes activated. (8) Activated PDK-1 phosphorylates AKT. (9) Activated AKT then inhibits pro-apoptotic factors (Bim) and induces up-regulation of pro-survival proteins (Bcl-2), proliferation and glucose uptake (GLUT1).

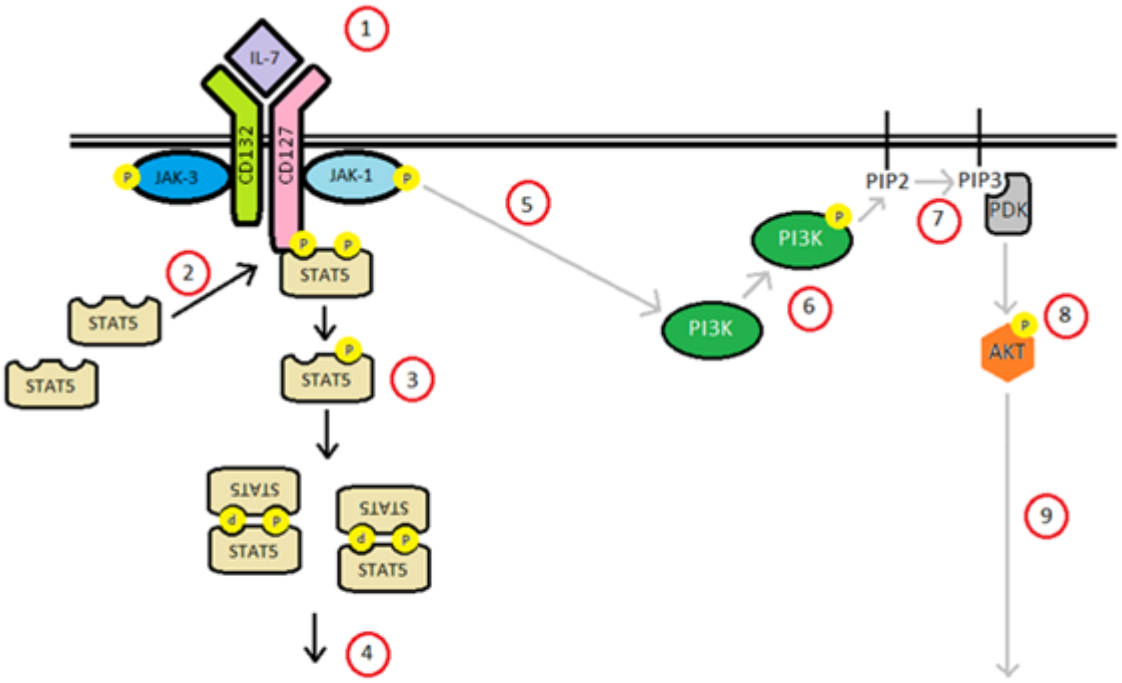

Proliferation – Survival – Enhance Cytolytic Capacity - Differentiation

1.4.2 Signaling through the PI3K pathway

Phosphoinositide 3-kinase (PI3K) pathway is another signaling pathway induced by IL-7 binding to its receptor [1, 30]. PI3K contains a regulatory subunit, p85 that inhibits PI3K activity by binding to the catalytic subunit, p110 [1, 30, 31]. Once p85 docks to the phosphorylated Y449 residue on CD127, JAK-3 will phosphorylate p85 [1, 30]. Phosphorylation of p85 results in its dissociation from p110 of PI3K [30, 31].

Activated PI3K begins a signaling cascade that leads to the phosphorylation of AKT (pAKT) [1, 10]. pAKT then phosphorylates the pro-apoptotic protein Bad causing it to be sequestered and inhibited by 14-3-3 proteins in the cytosol [1]. Active PI3K also phosphorylates the transcription factor FoxO3 and prevents it from translocating to the nucleus [1]. As such, phosphorylated FoxO3 cannot up-regulate the expression of pro-apoptotic protein Bim or the cell cycle inhibitor $p27^{kip1}$ [1]. Activated PI3K also phosphorylates $p27^{kip1}$ causing it to be degraded; thus allowing cyclin-dependent kinases (CDKs) to become active and trigger the cell to progress from G_0 to S phase of the cell cycle [1]. GLUT1 has been shown to be up-regulated by the PI3K pathway in IL-7 stimulated $CD8^+$ T-cells [10]. Anti-apoptotic proteins like Bcl-2, Bcl-X_L and MCL-1 have also been shown to be up-regulated through the IL-7 dependent PI3K pathway [1, 2, 10].

1.5 CD127 regulation

Our lab has shown that on resting primary CD8 T-cells, CD127 has a half-life of 55 hours and is continuously endocytosed and recycled back to the surface [33]. A small percentage of CD127 endocytosed is shunted to lysosomes for degradation, while the majority returns to the cell surface [33]. Degraded proteins are replaced by *de novo* synthesis of CD127, thereby keeping the level of CD127 on the surface constant [33].

Our lab has also shown that when IL-7 binds to its receptor CD127 surface expression is down-regulated at the protein and mRNA levels [34]. IL-7 bound CD127 is rapidly endocytosed and degraded by proteosomes [34]. Proteosomal degradation is targeted towards CD127 with Y449 phosphorylated [34]. Through activation of STAT5, IL-7 signaling induces the transcription of SOCS2, CIS and c-Myb [35]. SOCS2 and CIS proteins bind to phosphorylated CD127 in the endosomes and recruit ubiquitin ligases that direct CD127 to the proteosomes for degradation [35]. c-Myb in turn binds to the CD127 gene promoter and represses CD127 transcription thus preventing *de novo* synthesis of CD127 [34, 35]. The down-regulation of CD127 at the protein and mRNA levels were shown to be independent mechanisms [34].

1.6 CD127 in immunological diseases

In light of the roles that IL-7 has in T-cell biology, our lab has been interested in how CD127 expression, regulation and signaling are affected in various diseases states. Our lab has for a number of years studied IL-7 and CD127 on T-cells in the context of HIV pathogenesis. Our lab was amongst the first to show that CD127 expression was reduced on $CD8^+$ T-cells from patients with uncontrolled HIV viral replication [36]. Our lab has also shown that the HIV Tat protein causes IL-7 independent down-regulation and degradation of CD127 [13, 19]. Tat induced down-regulation of CD127 results in decreased proliferation and perforin synthesis in $CD8^+$ T-cell [19].

In this report, I set out to examine the effect that disease associated mutations have on CD127 expression, regulation and signaling. Herein I focus on four mutations in CD127: P132S, L242_L243insNPC, T244I and I356V (Figure 3). These mutations have been

Figure 3: Schematic showing the location of the four mutations in CD127

P132S is in the extracellular region and is associated with severe combined immunodeficiency. L242_L243insNPC is in the transmembrane region and is associated with T-cell acute lymphoblastic leukemia. T244I is located in the transmembrane region and is associated with autoimmune diseases like multiple sclerosis, type I diabetes, sarcoidosis, systemic lupus erythematosus and rheumatoid arthritis. I356V is in the cytoplasmic region and is associated to multiple sclerosis.

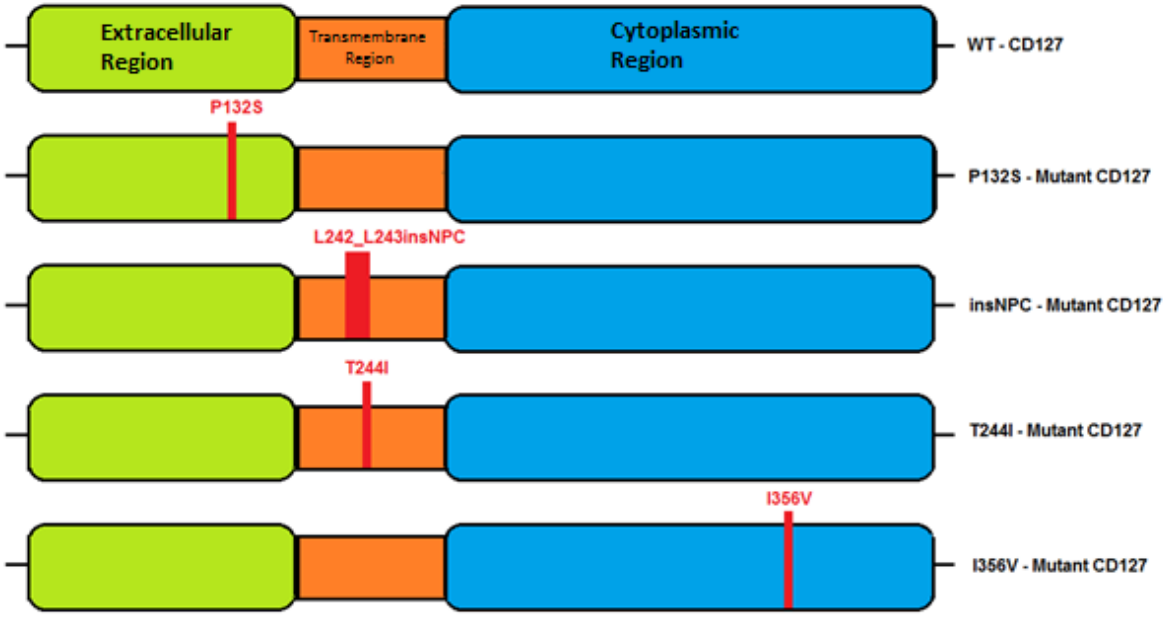
Extracellular Region
Transmembrane Region
Cytoplasmic Region
WT - CD127
P132S
P132S - Mutant CD127
L242_L243insNPC
insNPC - Mutant CD127
T244I
T244I - Mutant CD127
I356V
I356V - Mutant CD127

associated with severe combined immunodeficiency (SCID), T-cell acute lymphoblastic leukemia (T-ALL), and various autoimmune diseases.

1.6.1 CD127 in SCID

SCID is rare and fatal disease that causes diminished numbers of T-cells [37-39]. Infants with SCID clinically present with opportunistic infections, rash, diarrhea and failure to thrive [37]. Currently, there are two known types of SCID: SCID linked to chromosome X and autosomal recessive SCID [37-39]. X-linked SCID can be caused by truncation or nonsense mutations in the IL2R or JAK-3 genes [37-39]. Those with X-linked SCID have no T or NK cells, but normal levels of B cells [37-39]. Autosomal recessive SCID is caused by mutations in the IL7Rα (CD127) gene [37, 38, 40, 41]. Those with autosomal recessive SCID have no T-cells, but normal levels of B and NK cells [37]. Ten percent of all SCID patients examined present with autosomal recessive SCID [37]. One analysis of 22 patients with autosomal recessive SCID found that there were multiple mutations in the extracellular region of the IL7Rα gene [40, 42]. These mutations caused truncations or affected protein folding; leading to reduced IL-7Rα expression and function [40, 42]. Roifman *et al.* examined the lymphocytes from one group of patients that presented with autosomal recessive SCID and found that they all had a point mutation, P132S, in the extracellular domain of CD127 [41]. These patients were from an inbred family with consanguinity across five generations [41]. Roifman *et al.* used an *in vitro* cell line model to study the P132S mutation in CD127 and found that CD127 was still produced by the cells, but that IL-7 signaling was impaired [41]. Apart from the original paper by Roifman *et al.*, research into the P132S mutation is limited; therefore in this report I wanted to further examine the effects of this loss-of-function mutation on CD127 expression and signaling.

1.6.2 CD127 in T-ALL

T-cell acute lymphoblastic leukemia (T-ALL) is a common leukemia found in children and adults [38, 43]. *In vitro* and *in vivo* studies have shown that IL-7 contributes to the progression of T-ALL by increasing the proliferation and viability of lymphoblasts [44]. About 10% of T-ALL patients in multiple cohorts have somatic mutations in exon 6 of CD127 leading to constitutive signaling independent of IL-7 [45, 46]. These mutations introduce an unpaired cysteine into the transmembrane region of CD127 that cause two mutant CD127 subunits to homodimerize by forming a disulfide bridging between the cysteines [45, 46]. Zenetti *et al.* showed both in primary T-ALL cells and in multiple *in vitro* models that the insertion of an unpaired cysteine (insertion mutation: L242_L243insNPC) in CD127 causes hyper-activation of the JAK/STAT5 and PI3K pathways [45]. Considering that the effects of the L242_L243insNPC mutation have been well shown by Zenetti *et al.*, I used the mutation L242_L243insNPC to demonstrate a gain-of-function mutation in CD127 signaling.

1.6.3 CD127 in autoimmune diseases

In 2003, Tuetsch *et al.* were among the first to identify a genetic association between the CD127 gene and multiple sclerosis (MS) [41]. Since then multiple genome wide association studies (GWAS) have been conducted and found genetic associations for CD127 with other autoimmune diseases like rheumatoid arthritis (RA), type 1 diabetes (T1D), sarcoidosis and systemic lupus erythematosus (SLE).

The SNP, rs6897932, in exon 6 of the CD127 gene encodes for the T244I mutation in the transmembrane region of CD127 [48]. Increased risk for developing MS, RA, T1D, sarcoidosis and SLE has been associated with the T244I mutation, which is found at a

frequency of 0.7 in MS patients [37, 47, 48, 50-55]. Currently, there are two theories as to the effect of the T244I mutation. One theory is that T244I causes an increase in sCD127 transcripts by promoting alternative splicing mechanisms [37]. Gregory *et al.* showed in an *in vitro* model that T244I lead to a two fold increase in sCD127 transcripts [48]. The exact role of sCD127 in the context of autoimmunity is not fully understood. There is evidence that suggests sCD127 binds to IL-7 preventing T-cells from immediately consuming this limited cytokine and instead allows for a more limited but constant supply over time, thus potentiating IL-7 signal transduction [56]. This role for sCD127 is plausible in the context of autoimmunity. Another theory is that the T244I mutation in membrane bound CD127 directly causes enhanced signal transduction in T-cells [37]. Considering that this mutation occurs in the same area that the T-ALL gain-of-function mutations occur, this theory is also plausible [34]. It is also conceivable that both theories are correct with T244I enhancing IL-7 signaling from the membrane bound CD127 and increasing levels of soluble CD127.

The SNP, rs3194051, in exon 8 of the CD127 gene encodes for the I356V mutation in the cytoplasmic region [49]. The I356V polymorphism has been recognized as a risk factor for MS [49, 51]. There are currently no known theories as to how I356V may increase the risk for developing MS.

Since the effects of T244I and I356V in CD127 are not fully understood, in this report I set out to examine the effects these mutations have on CD127 expression, regulation and signaling to further enhance our knowledge of CD127 and its role in disease.

Hypothesis:

Disease specific mutations in CD127 result in aberrant signaling and/or receptor expression and/or receptor regulation.

Objectives:

1. To develop cell lines that stably express wild-type CD127, P132S mutated CD127, I356V mutated CD127, L242_L243insNPC mutated CD127 and T244I mutated CD127 proteins.
2. To examine the established mutant CD127 cell lines for altered expression of CD127 protein.
3. To examine the established mutant CD127 cell lines for altered CD127 regulation.
4. To examine the established mutant CD127 cell lines for altered CD127 signal transduction.

CHAPTER 2: MATERIALS AND METHODS

2.1 $CD8^+$ T-cell isolation

$CD8^+$ T-cells were isolated from heparinized blood of consenting healthy donors (Appendix I for consent form). Peripheral blood mononuclear cells (PBMC) were isolated from the blood using Ficoll-Paque density centrifugation. The pellet containing PBMCs was resuspended in 800µL of MACS buffer (5% BSA w/v, 2mM EDTA in sterile phosphate buffered saline (PBS), pH 7.4). $CD8^+$ T-cells were isolated using Miltenyi Biotec's human CD8 microbeads kit (Auburn, CA). Briefly, 1E8 PBMCs were incubated with 200µL of anti-CD8 antibody conjugated magnetic microbeads for 20 minutes at 4ºC. The cells were washed with PBS and centrifuged in a Megafuge 1.0 centrifuge (Heraeus Instruments, Inc.) at 1600rpm for 6 minutes. The cell pellet was resuspended in 2mL of MACS buffer and $CD8^+$ T-cells were separated from the PBMCs using the AutoMACS cell separator (Miltenyi Biotec, Inc.; Auburn, CA). Purified $CD8^+$ T-cells were washed with PBS, then counted using a hemocytometer and resuspended at 1E6 cells/mL in RPMI-10. RPMI-10 was composed of RPMI 1640 medium (Sigma-Aldrich Canada Co.; Oakville, ON) supplemented with 10% heat inactivated fetal bovine serum (HI FBS; Gibco; Carlsbad, CA), 100U/mL penicillin (Sigma-Aldrich Canada Co.; Oakville, ON), 100µg/mL streptomycin (Sigma-Aldrich Canada Co.; Oakville, ON) and 2g/L sodium bicarbonate (Sigma-Aldrich Canada Co.; Oakville, ON).

2.2 Cell culture

Four lymphoblastic cell lines, CCRF-CEM, A3, SupT1 and Jurkat E6.1 were obtained from the American Type Culture Collection (ATCC; Manassas, VA). All lymphoblastic cell lines were cultured in complete media, RPMI-10, at the density of 1E6 cells/mL.

The human kidney epithelial cell line, HEK293T, was obtained from ATCC and grown as an adherent monolayer in complete media, DMEM-10. DMEM-10 was composed of Dulbecco's Modified Eagles Medium (DMEM; HyClone Laboratories, Inc.; Logan, UT) supplemented with 10% HI FBS (Gibco), 100U/mL penicillin (Sigma-Aldrich Canada Co.), 100µg/mL streptomycin (Sigma-Aldrich Canada Co.) and 2g/L sodium bicarbonate (Sigma-Aldrich Canada Co.). HEK293T cells were used to produce lentiviruses.

All cells were maintained in a water jacketed humidified incubator (Forma™ Series II 3110; Thermo Scientific) at 37ºC and in 5% CO_2.

2.3 Development of cell lines that stably express WT or mutant CD127

To develop cell lines that expressed WT or mutant CD127 protein, I originally tried to transfect an eukaryotic expression plasmid, pCMV6-CD127 (Plasmid Clone # RC209687; OriGene USA; Rockville, MD) in Jurkat cells and use G418 sulfate (Wisent BioProducts; St-Bruno, QC) to select for positive clones. The plasmid pCMV6-CD127 (Appendix II.A for gene map) contains a CMV promoter upstream of the wild type CD127 cDNA. This promoter should drive constitutive expression of CD127 from the cDNA. This plasmid also contains a neomycin resistance gene allowing for selection of transfected cells by G418 sulfate. Positive clones were selected for using complete RPMI-10 media supplemented with 750µg/mL G418 sulfate (Appendix III for G418 sulfate kill curve). The transfection and selection approach (Appendix II.B) to making a cell line that stably expressed CD127 was unsuccessful. Several attempts were made but in each case clones failed to survive G418 selection. Hence, I shifted my approach towards a lentiviral system. Lentiviruses have been shown to provide higher transduction efficiency and be more efficient at genome integration compared to expression plasmid transfection approaches.

2.3.1 Lentiviral system

I opted to use a second generation lentiviral system originally developed by the lab of Didier Trono (École Polytechnique Fédérale de Lausanne, Switzerland), but modified to include either no gene of interest, wild type CD127 or mutant CD127 genes. The envelope vector, pMD2.G (Appendix IV.A for gene map; Addgene plasmid # 12259) and packaging vector, psPAX2 (Appendix IV.B for gene map; Addgene plasmid # 12260) were gifts from Dr. Didier Trono. The transfer vector, pWPI/hPLK2WT/Neo (Appendix IV.C for gene map; Addgene plasmid # 35385) was a gift from Dr. Anurag Tandon (University of Toronto, Canada). pWPI/hPLK2WT/Neo is a bicistronic plasmid that expresses the gene of interest, hPLK2WT, constitutively from an EF1-α promoter and simultaneously expresses the neomycin resistance gene from an internal ribosomal entry site (IRES). For the purposes of this project, pWPI/hPLK2WT/Neo plasmid was modified to incorporate no gene (MOCK), wild type CD127 gene (CD127WT) or one of four mutant CD127 genes (P132S, I356V, L242_L243insNPC, T244I) in place of hPLK2WT gene.

2.3.2 Production of transfer vector: pWPI/MOCK/Neo

To produce the empty transfer vector pWPI/MOCK/Neo, the pWPI/hPLK2WT/Neo vector was digested with BamHI to remove the hPLK2WT gene and then the vector backbone was re-ligated (Figure 4).

2.3.2.1 Restriction digestion of pWPI/hPLK2WT/Neo with BamHI

In a 100µL digestion reaction, I added 5µg of pWPI/hPLK2WT/Neo plasmid, 10µL of 10X NEBuffer3 (New England Biolabs, Inc.; Ipswich, MA.), 1µL of 100X BSA(New England Biolabs, Inc.; Ipswich, MA) and 7µL of BamHI (20U/µL; New England Biolabs,

Inc.; Ipswich, MA). The digestion reaction mixture was then incubated for 1 hour at 37°C.

2.3.2.2 Gel electrophoresis and isolation of pWPI/-/Neo backbone

I prepared a 0.7% agarose gel (Sigma-Aldrich Canada Co.; Oakville, ON) with 1X TAE buffer (40mM Tris-acetate, 1mM EDTA, pH 8.2-8.4) and 0.5µg/mL Ethidium Bromide (Sigma-Aldrich Canada Co.; Oakville, ON). I then loaded all of the BamHI double digested pWPI/hPLK2WT/Neo plasmid and ran 80V through the gel for 1 hour. Once the DNA fragments were separated, I exposed the gel to UV light for less than 45 seconds and excised the upper bands (~11400bp) corresponding to the pWPI/-/Neo backbone.

I isolated the digested DNA from the excised agarose using Macherey-Nagel's NucleoSpin® Gel and PCR Clean-up kit following the manufacturer's instructions. Purified DNA fragments were eluted in 30µL of elution buffer and quantified using a NanoDrop ND-1000 spectrometer (Nanodrop).

2.3.2.3 Self-ligation of pWPI/-/Neo vector backbone

The ligation reaction used Invitrogen's T4 DNA ligase kit (Carlsbad, CA) and was performed for 1 hour at 25°C.

The purified pWPI/-/Neo backbone from the BamHI double digestion was self-ligated. This ligation was performed in a 20µL reaction volume containing 50ng of the isolated pWPI/-/Neo backbone, 4µL of 5X T4 DNA ligase buffer (250mM Tris-HCl (pH 7.6), 50mM $MgCl_2$, 5mM ATP, 5mM DTT, 25% (w/v) polyethylene glycol-8000) and 1µL of T4 DNA ligase (1U/µL).

Once the ligation reaction was complete the mixture was diluted with H_2O to 70µL.

Figure 4: Sub-cloning strategy to produce the empty transfer vector: pWPI/MOCK/Neo

(1) pWPI/hPLK2WT/Neo was digested with BamHI to produce the hPLK2WT fragment and the vector backbone. (2) The digested plasmid was run on a 0.7% agarose gel and the upper band corresponding to the vector backbone was excised and purified. (3) Purified vector backbone was ligated using T4 DNA ligase to produce the plasmid, pWPI/MOCK/Neo.

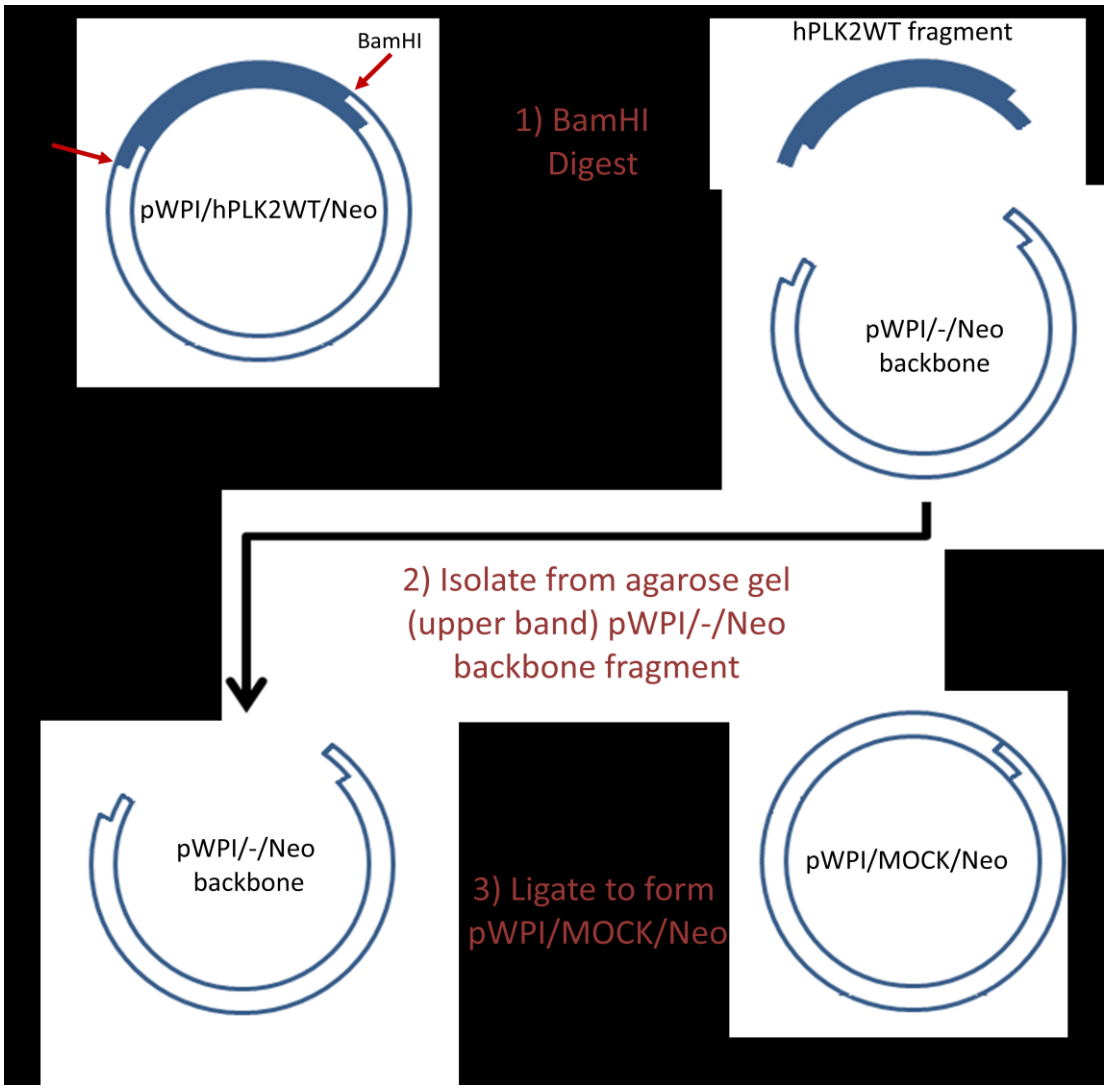
BamHI
pWPI/hPLK2WT/Neo
1) BamHI Digest
hPLK2WT fragment
pWPI/-/Neo backbone
2) Isolate from agarose gel (upper band) pWPI/-/Neo backbone fragment
pWPI/-/Neo backbone
3) Ligate to form pWPI/MOCK/Neo
pWPI/MOCK/Neo

2.3.2.4 Transformation of pWPI/MOCK/Neo into XL Gold Ultracompetent bacteria

XL-Gold Ultracompetent (Agilent Technologies; Santa Clara, CA) bacteria were gently thawed on ice. XL-Gold Ultracompetent bacteria is a unique strain of *E.coli* that was specifically developed for enhanced transformation efficiency of large plasmids (>10Kbp). To each 100µL aliquot of XL-Gold Ultracompetent cells, I added 2µL of β-mercaptoethanol mix (Agilent Technologies; Santa Clara, CA). Aliquots were then mixed by tapping and chilled on ice for 10 minutes.

I added 40µL of the diluted ligation mixture containing pWPI/MOCK/Neo into one aliquot of XL-Gold cells. Bacteria and DNA mixtures were gently mixed and chilled on ice for 30 minutes. Aliquots were then heat shocked at 42°C for 30 seconds and then chilled again on ice for 2 minutes. Next, 500µL of pre-warmed Miller's Luria Broth (LB; Invitrogen, Inc.; Carlsbad, CA) was added to the transformation mixture and incubated at 37°C in a shaking incubator (225rpm) for 1 hour. Following this incubation and under aseptic conditions, 250µL of transformed bacteria were spread onto an Agar-LB plate (Wisent BioProducts; St-Bruno, QC) containing 200µg/mL of Ampicillin (Wisent BioProducts; St-Bruno, QC). The plate was then incubated at 37°C for 24 hours.

2.3.3 Production of transfer vector: pWPI/CD127WT/Neo

To produce the transfer vector containing the wild type CD127 gene, pWPI/CD127WT/Neo, I isolated the insert fragment, CD127 cDNA, from pCMV6-CD127 and the vector backbone from pWPI/hPLK2WT/Neo vector and then ligated the insert into the vector fragment (Figure 5).

2.3.3.1 Restriction digestion of pWPI/hPLK2WT/Neo and pCMV6-CD127 with XmaI

In two individual digestion reactions, I digested purified pWPI/hPLK2WT/Neo and pCMV6-CD127 with XmaI (New England Biolabs, Inc.; Ipswich, MA) for 16 hours at 37°C. Each 100µL digestion reaction contained the following: 5µg of pWPI/hPLK2WT/Neo plasmid or 5µg of pCMV6-CD127 plasmid, 10µL of 10X Cutsmart buffer (New England Biolabs, Inc.; Ipswich, MA) and 7µL of XmaI (10U/µL; New England Biolabs, Inc.; Ipswich, MA). Following the 16 hour digestions, the XmaI enzyme was deactivated by incubating the reactions at 65°C for 20 minutes.

After XmaI deactivation, 5µL of calf intestinal alkaline phosphatase (CIP; New England Biolabs, Inc.; Ipswich, MA) was added to the pWPI/hPLK2WT/Neo digestion reaction and incubated at 37°C for 1 hour. The CIP treatment prevents the re-circularization of the linearized plasmids by dephosphorylating the 5' and 3' ends produced by restriction enzyme digestions.

2.3.3.2 Restriction digestion of XmaI linearized pWPI/hPLK2WT/Neo with BamHI

In the digestion reaction containing CIP treated, XmaI linearized pWPI/hPLK2WT/Neo plasmid; I added 7µL of BamHI (20U/µL; New England Biolabs, Inc.) and incubated the digestion reaction for 1 hour at 37°C.

2.3.3.3 Restriction digestion of XmaI linearized pCMV6-CD127 with BglII

In the digestion reaction containing XmaI linearized pCMV6-CD127 plasmid; I added 10µL of salt buffer I (30mM Tris-HCl, 100mM NaCl) and 7µL of BglII (10U/µL; New England Biolabs, Inc.) and incubated the digestion reaction for 1 hour at 37°C.

2.3.3.4 Gel electrophoresis and isolation of pWPI/-/Neo backbone and CD127 fragment

I prepared a 0.7% agarose gel, as described above, and loaded all of the XmaI/ BamHI double digested pWPI/hPLK2WT/Neo and all of the XmaI/BglII double digested pCMV6-CD127. I then ran 80V through the gel for 1 hour. Once the DNA bands were separated I exposed the gel to UV light and I excised the upper band (~11400 bp) corresponding to the pWPI/-/Neo backbone and the lower band (~1500bp) corresponding to the wild type CD127 cDNA fragment.

I then used Macherey-Nagel's NucleoSpin® Gel and PCR Clean-up kit to isolate the digested DNA from the excised agarose, as described above. DNA was again quantified using a NanoDrop ND-1000 spectrometer (Nanodrop).

2.3.3.5 Ligation of CD127 fragment with the pWPI/-/Neo vector backbone

Invitrogen's T4 DNA ligase kit (Carlsbad, CA) was used to ligate the CD127 fragment to the vector backbone. The ligation was performed at 25°C for 1 hour.

The 20µL ligation reaction contained a molar ratio of 2:1 for DNA insert to vector backbone and was performed as described above. Once the ligation was completed, the ligation reaction was diluted with H_2O to a final volume of 70µL.

2.3.3.6 Transformation of pWPI/CD127WT/Neo into XL Gold Ultracompetent bacteria

An aliquot of XL Gold Ultracompetent (Agilent Technologies) bacteria was prepared using the method described above. The aliquot was transformed with 40µL of diluted ligation reaction containing pWPI/CD127WT/Neo plasmid, following the transformation method described above.

Figure 5: Sub-cloning strategy to produce the transfer vector: pWPI/CD127WT/Neo

(1) pWPI/hPLK2WT/Neo was first digested with XmaI, then BamHI to produce the hPLK2WT fragment and the pWPI/-/Neo backbone. (2) pCMV6-CD127 was first digested with XmaI, then BglII to produce the CD127 cDNA fragment and the pCMV6 backbone. (3) Double digested pWPI/hPLK2WT/Neo was run on a 0.7% agarose gel; the upper band corresponding to the pWPI/-/Neo backbone was excised and purified. (4) Double digested pCMV6-CD127 was run on a 0.7% agarose gel; the lower band corresponding to the CD127 cDNA fragment was excised and purified. (5) Purified pWPI/-/Neo backbone was ligated to the purified CD127 cDNA fragment using T4 DNA ligase to produce the plasmid pWPI/CD127WT/Neo.

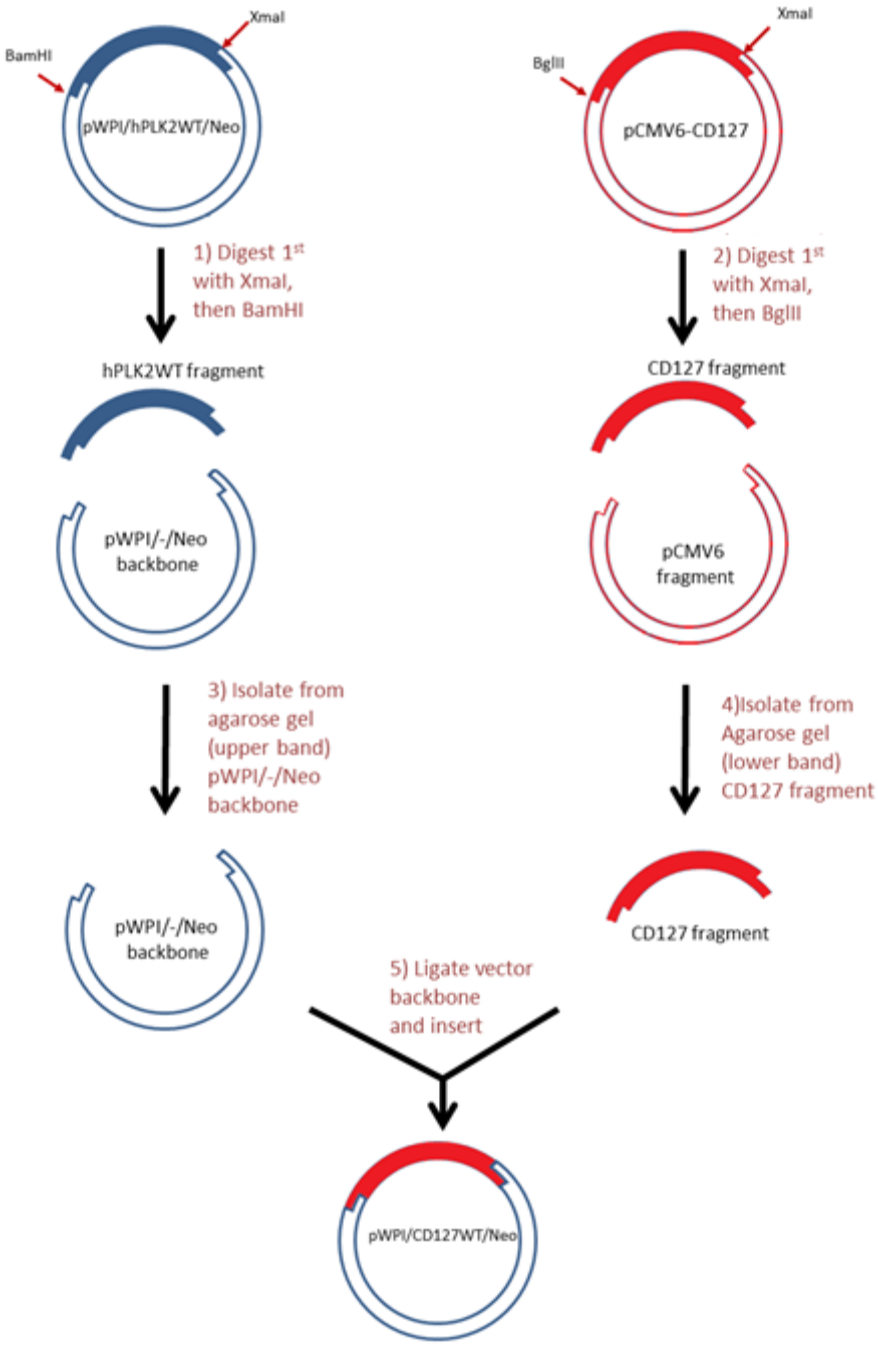
XmaI
BamHI
pWPI/hPLK2WT/Neo
1) Digest 1st with XmaI, then BamHI
hPLK2WT fragment
pWPI/-/Neo backbone
3) Isolate from agarose gel (upper band) pWPI/-/Neo backbone
pWPI/-/Neo backbone
XmaI
BglII
pCMV6-CD127
2) Digest 1st with XmaI, then BglII
CD127 fragment
pCMV6 fragment
4)Isolate from Agarose gel (lower band) CD127 fragment
CD127 fragment
5) Ligate vector backbone and insert
pWPI/CD127WT/Neo

2.3.4 Production of the four CD127 mutants in pWPI/CD127WT/Neo transfer vectors

2.3.4.1 Site directed mutagenesis (SDM) to create four CD127 mutants

To produce lentiviral transfer vectors that encode for mutant CD127 genes (P132S, I356V, L242_L243insNPC & T244I), we utilized the QuikChange II XL SDM Kit (Agilent Technologies; Santa Clara, CA) and custom primers (Invitrogen, Inc.; Grand Island, NY).

The custom primers (Table 1) were designed using Agilent Technologies' custom primer online software. To create each of the four mutations in CD127 the software designed forward and reverse primers that are complementary to the template vector with either the inserted nucleotides or nucleotide substitutions in the middle of the primers.

Each SDM reaction utilized a high fidelity DNA polymerase, PfuUltra, which extends the DNA strand from the mutagenic primers around the vector template (Figure 6). The SDM reactions were prepared as follows: 15ng of pWPI/CD127WT/Neo plasmid, 125ng of forward primer, 125ng of reverse primer, 1µL of dNTP mix, 5µL of 10X reaction buffer, 3µL of QuikSolution, 1µL of PfuUltra (2.5 U/µL) and ddH_2O to bring the final volume to 50µL.

The SDM reaction mixtures were first incubated for 1 minute at 95°C to denature the DNA template and activate the polymerase. SDM reactions then underwent 18 cycles of PCR amplification, as follows: 95°C for 50 seconds, 60°C for 50 seconds and 68°C for 13 minutes. After thermal cycling, final extension was done at 68°C for 7 minutes.

Once the PCR amplification was completed, 1µL of DpnI (10 U/µL) was added to each SDM reaction. DpnI treated reactions were incubated at 37°C for 1 hour. The parental template, pWPI/CD127WT/Neo, is a methylated plasmid since it was isolated from XL-Gold Ultracompetent bacteria, a dam+ strain of *E.coli.* The addition of DpnI results in

Table 1: Primer sequences used in QuikChange II XL SDM kit to produce four different mutants of CD127 in the pWPI/CD127WT/Neo plasmid

Mutation achieved in CD127 protein	Primer Name	Primer Sequence
P132S	P132S-FWD	5'-CTATAGTTAAACCTGAGGCTTCTTTTGACCTGAGTGTCATC -3'
	P132S-REV	5'-GATGACACTCAGGTCAAAAGAAGCCTCAGGTTTAACTATAG -3'
I356V	I356V-FWD	5'-CCATCTGAGGATGTAGTCGTCACTCCAGAAAGCTTTG -3'
	I356V-REV	5'-CAAAGCTTTCTGGAGTGACGACTACATCCTCAGATGG -3'
L242_L243 insNPC	insNPC-FWD	5'-GGGAGATGGATCCTATCTTAAACCCTTGTCTAACCATCAGCATTTTGAG -3'
	insNPC-REV	5'-CTCAAAATGCTGATGGTTAGACAAGGGTTTAAGATAGGATCCATCTCCC -3'
T244I	T244I-FWD	5'-GGGGAGATGGATCCTATCTTACTAATCATCAGCATTTTGA -3'
	T244I-REV	5'-TCAAAATGCTGATGATTAGTAAGATAGGATCCATCTCCCC -3'

*Primer sequences highlighted RED are either substituted or inserted nucleotides

Figure 6: Cloning strategy to produce CD127 mutants in the transfer vector: pWPI/CD127WT/Neo

(1) Forward (purple) and reverse (green) primers are designed to be complementary to the pWPI/CD127WT/Neo plasmid. Each primer incorporates a mutation (orange) in the middle. (2) The primers, parental plasmid and DNA polymerase (PfuUltra) are mix together and thermal cycled. (3) Each amplification cycle produces an unmethylated copy plasmid (green and purple), with the mutations incorporated. (4) The methylated parental plasmid is then digested by DpnI, while the mutant copies remain intact.

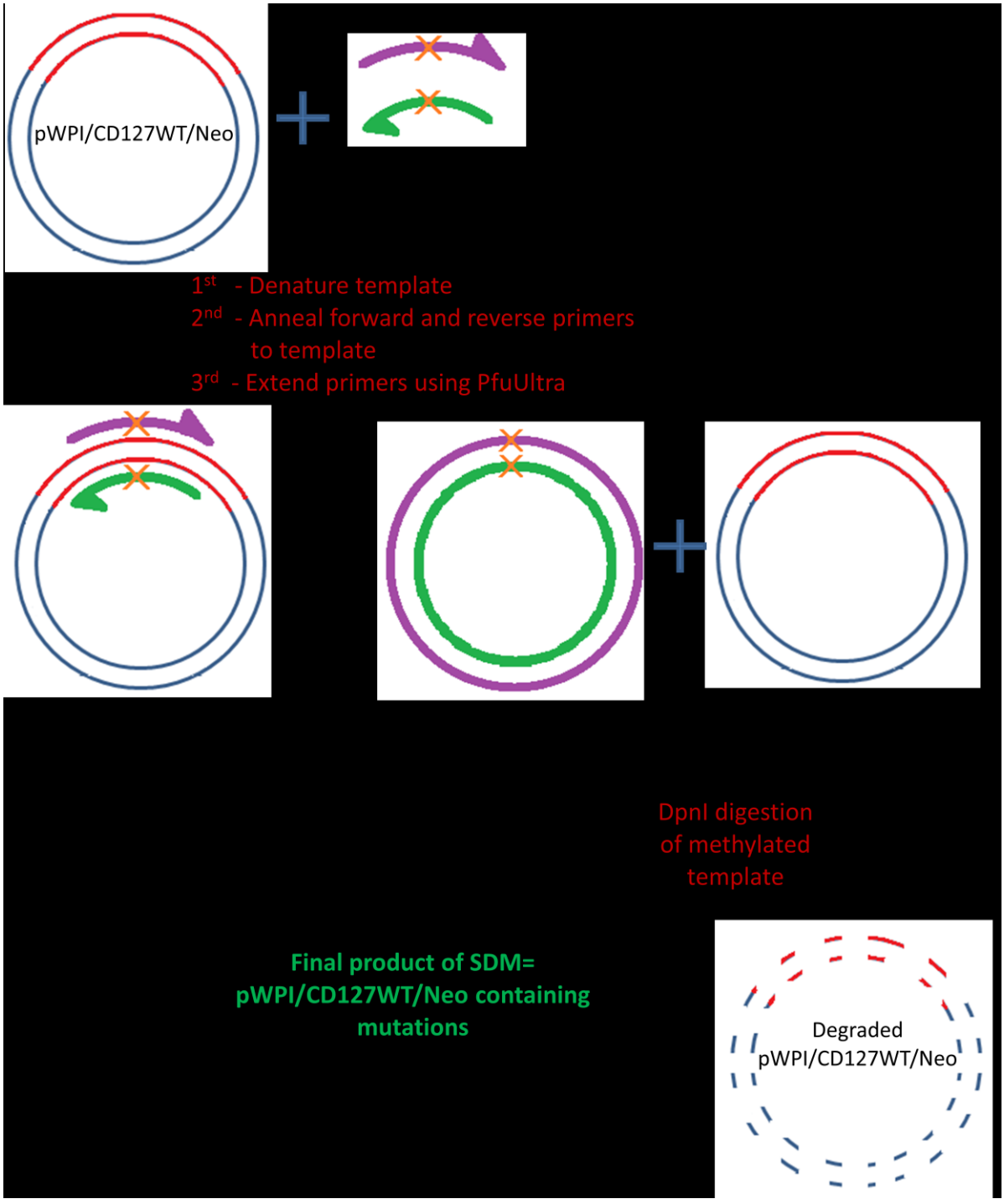
pWPI/CD127WT/Neo
1st - Denature template
2nd - Anneal forward and reverse primers to template
3rd - Extend primers using PfuUltra
DpnI digestion of methylated template
Final product of SDM= pWPI/CD127WT/Neo containing mutations
Degraded pWPI/CD127WT/Neo

digestion of the methylated template plasmid leaving the unmethylated mutated copy intact.

2.3.4.2 Transformation of the four CD127 mutants

Four aliquots of XL-Gold Ultracompetent (Agilent Technologies) bacteria were prepared using the method described above. Each aliquot was transformed with 40µL from one of the four SDM products using the method described above.

2.3.5 Amplification of positive bacterial colonies and isolation of plasmids

Per plate, a single colony was isolated and expanded in 5mL of LB supplemented with 100µg/mL of Ampicillin at 37°C in a shaking incubator (225rpm). When the LB media became turbid (~16 hours of incubation), plasmids were isolated and purified using Qiagen's HiSpeed® Plasmid Maxi Kit in accordance with the manufacturer's instructions. To confirm that the pWPI/MOCK/Neo and pWPI/CD127WT/Neo plasmids were isolated, I performed a BamHI digestion, as described above. Gel electrophoresis was performed and lane profiles were examined.

2.3.6 DNA sequencing to confirm the wild type CD127 cDNA was incorporated into the open reading frame of pWPI/-/Neo and to confirm the four mutations of CD127

Isolated pWPI/CD127WT/Neo, pWPI/P132S/Neo, pWPI/I356V/Neo, pWPI/L242_L243insNPC/Neo and pWPI/T244I/Neo plasmids were verified using capillary-based Sanger DNA sequencing at the StemCore facility of the Ottawa Hospital Research Institute (OHRI). Sequencing utilized a forward primer (5'-ATC ACG AGA CTA GCC TCG AGG-3') upstream of CD127 gene and the m13 reverse primer (5'-TCA CAC AGG AAA CAG CTA TGA C-3') downstream of CD127 gene in the plasmids.

2.3.7 Production and harvesting of lentiviruses

2.3.7.1 Transfection of HEK293T cells with envelope, packaging and transfer vectors

HEK293T cells were grown in 15cm tissue culture plates to 60-70% confluency. The medium was then aspirated and replaced with 12mL of serum free DMEM in preparation for transfection. Each plate was co-transfected with envelope vector pMD2.G, packaging vector psPAX2, and one of the six transfer vectors (pWPI/MOCK/Neo, pWPI/CD127WT/Neo, pWPI/P132S/Neo, pWPI/I356V/Neo, pWPI/L242_L243insNPC/Neo or pWPI/T244I/Neo). Each plate was transfected with 7140ng of total DNA. In six separate microtubes, 446.25ng of pMD2.G, 2231.25ng of psPAX2 and 4462.50ng of vector construct (different vector per microtube) were combined. I then diluted each DNA mixture by bringing the final volumes to 300µL with serum free DMEM. In another six separate microtubes, I added 50µL of FuGENE®6 transfection reagent (Roche Applied Science, Inc.) to 250µL aliquots of serum free DMEM, pre-warmed to 37°C, and allowed the mixture to incubate at room temperature for 5 minutes. After the 5 minute incubation, I slowly added each 300µL DNA mixture to an aliquot of 300µL of diluted FuGENE®6 transfection reagent. The DNA/FuGENE®6 mixtures were then incubated at room temperature for 20 minutes. The 600µL DNA/FuGENE®6 mixture was then added drop-wise and slowly onto the HEK293T cells. After the addition of the DNA/FuGENE®6 mixture, I gently rocked the plates and then incubated them for 6 hours at 37°C. Finally, 12mL of DMEM-10 was added to each plate and the plates were incubated at 37°C for 48 hours to allow production of Lentiviruses.

2.3.7.2 Detection of lentiviruses

After 48 hours, each plate has produced a different lentivirus (MOCK, CD127WT, P132S, I356V, insNPC and T244I). Lenti-X™GoStix™ (Clontech Laboratories, Inc.; Mountain View, CA) was used to confirm that lentiviruses were present in the media and that the concentration was at least 5E5 infectious units of virus/mL of media. Lenti-X™GoStix™ is a quick, hand held, visual test stick that detects the presence of lentiviral p24 from a 20µL sample of media. When there were at least 5E5 infectious units of virus/mL, the lentivirus was harvested.

2.3.7.3 Harvesting the six different lentiviruses produced

The cells from each plate were scraped off and collected with the supernatants into 50mL tubes. The tubes were centrifuged in a Megafuge 1.0 at 1600rpm for 6 minutes to pellet the cells, while lentiviruses remained in the supernatant. The supernatants from each tube were then passed through a 0.45µm polyethersulfone membrane (PES) filter (UltiDent Scientific, Inc.; St. Laurent, QB) to remove any remaining cellular debris. Filtered supernatants were then centrifuged, in a Beckman Coulter Avanti™J-25I ultracentrifuge, at 24,000rpm for 90 minutes at 4°C. The supernatants were decanted and the pellets containing the lentiviruses were resuspended in 200µL of PBS.

2.3.8 Lentiviral transduction and selection of Jurkat cells that stably express wild type or mutant CD127

2.3.8.1 Coating of 6-well plate with RetroNectin® for lentiviral transduction

RetroNectin® (Takara Bio, Inc.; Otsu, Shiga, Japan) is a recombinant human fibronectin fragment that is composed of three functional domains: cell-binding domain,

heparin-binding domain and CS-1 domain. The heparin-binding domain located in the middle of the fibronectin fragment binds to the lentivirus, while the cell-binding and CS-1 domains flank either side of the heparin-binding domain and bind to the target cell. The binding of the fibronectin fragment to the target cell brings the lentivirus in close proximity to the target cell, thus leading to increased infection and gene transduction.

Each well in a 6-well plate was coated with 2mL of RetroNectin® in PBS (20µg/mL). The 6-well plate was incubated at room temperature for 2 hours to allow for the RetroNectin® to coat the plastic fully. After 2 hours, the excess RetroNectin® solution was removed. Wells were then coated with 2.5mL of 2% (w/v) BSA in PBS, for 30 minutes. The 2% BSA in PBS was removed and the wells were washed twice with 2mL of PBS. After the final wash, the wells were fully coated and ready for lentiviral transduction.

2.3.8.2 Lentiviral transduction of Jurkat cells

In each well of the RetroNectin® coated 6-well plate, 1.48mL of serum free RPMI 1640 was added. Per well, I then added 20µL of lentivirus concentrate, with each well containing a different lentivirus. Lentiviruses were incubated in the wells for 4 hours at 37°C. Next, I added 2E6 Jurkat cells per well and centrifuged the 6-well plate at 1600rpm for 6 minutes to bring the Jurkat cells down to the bottom of the plate. This plate was then incubated at 37°C for 48 hours. At the end of this time, 1mL of RPMI-10 was added to each well and the cells were incubated for another 48 hours.

2.3.8.3 Selection of transduced Jurkat cells

Four days post infection, transduced Jurkat cells from each well were transferred into sterile 15mL tubes. The Jurkat cells were centrifuged at 1600rpm for 6 minutes and the

supernatants were discarded. Cell pellets were washed with PBS twice. Finally, the Jurkat cells were resuspended at the density of 1E6 cells/mL in RPMI-10 supplemented with 750µg/mL of G418 sulfate and placed into the wells of a new 6-well plate. Over a 20 day period, six different Jurkat cell lines expressing only the neomycin resistance gene, wild type CD127 or one of the four mutated CD127 proteins were selected. The new cell lines stably express only neomycin resistance (MOCK), wild type CD127 (CD127WT), CD127 with the P132S point mutation (P132S), CD127 with the I356V point mutation (I356V), CD127 with the L242_L243insNPC insertion mutation (insNPC) or CD127 with the T244I point mutation (T244I).

2.4 Western blot analysis

Cell pellets (2E6 cells per sample) were lysed for 45 minutes on ice in modified NP-40 lysis buffer (50mM Tris-HCl, pH7.5, 150mM NaCl, 1% (v/v) NP-40, 0.5% (w/v) Sodium Deoxycholate) supplemented with 1X HALT™ Protease and Phosphatase inhibitor (Pierce Biotechnology; Rockford, IL). Whole cell lysates were centrifuged at 17,000g for 10 minutes to remove cellular debris. After clearing the cell lysates, I added 12µL of the lysate to 6µL of New England Biolabs' 3X SDS Sample Loading Buffer (187.5mM Tris-HCl , pH 6.8), 6% (w/v) SDS, 30% glycerol, 0.03% (w/v) phenol red) supplemented with 5% (v/v) β-mercaptoethanol (Sigma-Aldrich Canada Co.; Oakville, ON). Samples were heated at 90°C for 10 minutes, then cooled on ice for 2 minutes. Cell proteins were then resolved on a 10% SDS-polyacrylamide gel with a 5% stacking gel. Gel electrophoresis was carried out using a Mini-PROTEAN Tetra Cell apparatus (Bio-Rad; Hercules, CA). Samples were run using the following protocol: 85V for 25 minutes, 125V for 90 minutes and held at 20V until transferred.

After electrophoresis, the gel was gently washed in ddH2O and then equilibrated for 10 minutes in 1X Transfer Buffer (50mM Tris-Base, 96mM Glycine and 20% (v/v) methanol). An 0.45µm Immobilon®-P polyvinylidene fluoride (PVDF) membrane (EMD Millipore Corporation; Billerica, MA) was first activated in 100% methanol for 5 minutes and then equilibrated in 1X Transfer Buffer for 10 minutes. After the equilibration, the proteins from the gel were transferred onto the PVDF membrane using a Mini Trans-Blot® Electrophoretic Transfer Cell (Bio-Rad; Hercules, CA) run at 100V for 60 minutes in 1X Transfer Buffer.

Following the protein transfer, the blot was blocked overnight at 4°C on an orbital shaker using 3% dried non-fat milk dissolved in 1X Tris-Buffered Saline (20mM Tris-HCl, pH 7.6, 137mM NaCl) supplemented with 0.5% Tween-20 (TBST). After the blocking step, the blot was washed for 5 minutes on an orbital shaker at room temperature, three times, with 1X TBST.

Western blots were incubated overnight at 4°C, with agitation, with primary antibodies diluted in 2% dried non-fat milk dissolved in 1X TBST. The following primary antibodies were used: 1:1000 dilution of polyclonal rabbit anti-STAT5 (9363; Cell Signaling Technology, Inc.; Danvers, MA); 1:1000 dilution of polyclonal rabbit anti-phospho-STAT5 (9351; Cell Signaling Technology, Inc.; Danvers, MA); 1:1000 dilution of polyclonal goat anti-human CD127 (AF-306-PB; R&D Systems, Inc.; Minneapolis, MN); 1:500 dilution of polyclonal rabbit anti-DDK (TA100023; OriGene USA; Rockville, MD); and 1:1000 dilution of polyclonal rabbit anti-β-actin (Poly6221; Biolegend; San Diego, CA).

Following the primary antibody incubation, western blots were washed for 10 minutes in 1X TBST, three times, with constant agitation. Then the blots were incubated for

1 hour, at room temperature, with constant agitation with secondary antibody diluted 1:1000 in 2% dried non-fat milk dissolved in 1X TBST. For blots incubated in rabbit primary antibodies, I used polyclonal goat anti-rabbit IgG secondary antibody conjugated with horseradish peroxidase (HRP) (HAF008; R&D Systems, Inc.; Minneapolis, MN). For blots incubated in goat primary antibodies, I used polyclonal donkey anti-goat IgG secondary antibody conjugated with HRP (HAF109; R&D Systems, Inc.; Minneapolis, MN).

Following the secondary incubation, western blots were washed three times in 1X TBST for 10 minutes with constant agitation. Bio-Rad's Clarity™ Western ECL substrate kit was used to visualize labeled proteins by chemiluminescence. This kit contains luminol/enhancer and peroxide solutions that were mixed in equal parts to form the ECL substrate solution. Western blots were then evenly coated with ECL substrate solution and chemiluminescent bands were detected from the blots using FluorChem HD2 Imager (Alpha Innotech) and AlphaView SA image analysis software (Protein Simple; San Jose, CA).

2.5 Flow cytometry

2.5.1 Surface CD132 and CD127

Cells were labeled for 20 minutes in the dark at room temperature with 4µL/1E5 cells of mouse anti-CD132-PE monoclonal antibody (clone AG184; BD Pharmingen; Mississauga, ON) or mouse anti-CD127-PE monoclonal antibody (clone R34.34; Immunotech Beckman Coulter; Marseille, France).

2.5.2 Alternative staining protocols for surface CD127

A) Cells were labeled for 20 minutes in the dark at room temperature with 1µL/2E5 cells of mouse anti-CD127-PE monoclonal antibody (clone hIL-7R-M21; BD Pharmingen, Marseille, France).

B) Cells were resuspended in 5% BSA in PBS, labeled for 30 minutes in the dark at room temperature with 2µL/1.5E5 cells of mouse anti-CD127 monoclonal antibody (clone 40131; R&D Systems, Inc.; Minneapolis, MN). Cells were then centrifuged at 1600rpm for 6 minutes, the supernatant was discarded and the cell pellet was resuspended in 5% normal goat serum (NGS; Sigma-Aldrich Canada, Co.; Oakville, ON) in PBS. The cells were then labeled for 30 minutes at room temperature in the dark with 2uL of goat anti-mouse IgG1 secondary antibody conjugated with Alexa Fluor® 555 (Cat # A-21422; Molecular Probes, Inc.; Eugene, OR). Cells were then washed and resuspended in 100µL of PBS. Staining for secondary control was done following the same procedure except no primary antibody was used.

C) Cells were resuspended in 5% BSA in PBS, labeled for 30 minutes in the dark at room temperature with 2µL/1.5E5 cells of goat anti-CD127 polyclonal antibody (AF-306-PB; R&D Systems, Inc.; Minneapolis, MN). Cells were then centrifuged at 1600rpm for 6 minutes, the supernatant was discarded and the cell pellet was resuspended in 5% normal donkey serum (NDS; Sigma-Aldrich Canada, Co.; Oakville, ON) in PBS. Then the cells were labeled for 30 minutes at room temperature in the dark with 2uL of donkey anti-goat IgG secondary antibody conjugated with Alexa Fluor® 647 (Cat# A-21447; Molecular Probes, Inc.; Eugene, OR). Cells were then washed and resuspended in 100µL of PBS. Staining for secondary control was done following the same procedure except no primary

antibody was used.

2.5.3 Intracellular staining protocol for CD127

Cells were fixed and permeabilized using Invitrogen's FIX & PERM® Cell Fixation and Permeabilization Kit. In brief, 1E5 cells were centrifuged at 1600rpm for 6 minutes, after which supernatants were discarded and the cell pellet was resuspended in 150µL of Fixation Buffer (Cat# GAS001S100; Life Technologies, Corp.; Frederick, MD) for 10 minutes at room temperature. Cells were centrifuged and fixation buffer was removed; cells were next resuspended in 150µL of Permeabilization Buffer (Cat# GAS002S-100; Life Technologies, Corp.; Frederick, MD) for 10 minutes at room temperature. Fixed and permeabilized cells were then incubated for 30 minutes at room temperature with 2µL/1.5E5 cells of goat anti-CD127 polyclonal antibody (AF-306-PB; R&D Systems, Inc.; Minneapolis, MN). Following this, the cells were centrifuged and the cell pellet was resuspended in 5% NGS in PBS and incubated for 10 minutes at room temperature. The cells were then labeled for 30 minutes at room temperature in the dark with 2uL of donkey anti-goat IgG secondary antibody conjugated with Alexa Fluor® 647 (Cat# A-21447; Molecular Probes, Inc.; Eugene, OR). The cells were then washed and resuspended in 100µL of PBS. Staining for secondary control was done following the same procedure except no primary antibody was used.

2.5.4 pSTAT5 staining protocol

Per condition, 5E6 cells were incubated in media alone or media containing IL-7 (10ng/mL) or IFNα (125ng/mL) for 15 minutes. The cells were then centrifuged and supernatants were decanted. Cell pellets were resuspended in 750µL of 2% Para

formaldehyde (PFA) in PBS and incubated for 10 minutes at room temperature in the dark. Then, 3mL of 1% BSA in PBS was added and the cells were centrifuged at 1600rpm for 6 minutes. The cell pellets were resuspended in 500µL of ice cold methanol and incubated for 10 minutes at 4ºC. Then cells were washed twice in 3mL of 1% BSA in PBS. Finally, cell pellets were resuspended in 100µL of 1% BSA in PBS followed by the addition of 5µL of mouse anti - pSTAT5 (pY694) - Alexa Fluor® 488 (clone 47/Stat5 (pY694); BD Pharmingen; Mississauga, ON) and incubated for 25 minutes at room temperature in the dark. After staining, cells were washed with 3mL of 1% BSA in PBS, centrifuged and resuspended in 200µL of 2% PFA in PBS.

2.5.5 Acquisition and analysis for flow cytometry

All flow cytometry on stained cells was performed on a Beckman Coulter Cytomics FC-500 flow cytometer instrument. Cells were gated based on forward and side scatter and 10,000 events were collected per condition. Flow cytometry data were analyzed using FCS Express 3 software (De Novo; Glendale, CA).

2.6 Comparing levels of transcripts encoding soluble CD127 versus total CD127 in cell lines expressing WT or mutant CD127

2.6.1 Total RNA isolation

Total RNA was isolated from each of the six cell lines produced using the RNAqueous®-4PCR Total RNA Isolation Kit from Ambion (Austin, TX) according to the manufacturer's instructions. In brief, 1E7 cells from each of the six cell lines were lysed with 500µL of Lysis/Binding solution and lysates were passed over silica filters. Total RNA was eluted from the filters in two consecutive steps using a total of 70µL (35µL + 35µL) of

elution buffer that was pre-warmed to 70°C. Total RNA was then quantified using a NanoDrop ND-1000 (Nanodrop) spectrometer. Elution buffer was used as a blank reference. cDNA was synthesized after total RNA was isolated and excess RNA was stored at -80°C. Five individual total RNA isolations were done for each cell line.

2.6.2 cDNA synthesis

cDNA was synthesized using the iScript™ cDNA synthesis kit (Bio-Rad; Hercules, CA) according to the manufacturer's instructions. In brief, each reaction contained 1µL of iScript reverse transcriptase, 4µL of 5X iScript reaction mix, and 1µg of isolated RNA in 15µL of nuclease-free water. Reaction samples were first incubated for 5 minutes at 25°C to allow binding of random hexamer primers to the RNA, followed by an incubation for 30 minutes at 42°C to allow for reverse transcription, and a final incubation for 5 minutes at 85°C to inactivate the reverse transcriptase. cDNA was diluted 1:20 with nuclease free water and either used in real time PCR reactions or stored at -20°C.

2.6.3 Real-Time PCR

Real time (RT) PCR was performed to quantify the relative amounts of soluble and total CD127 isoform transcripts produced by CD127WT, P132S, I356V, insNPC and T244I Jurkat cell lines. Mock transduced Jurkat cells were used as controls. To quantify the relative amounts of soluble CD127 isoform, RT-PCR was performed on isolated cDNA using soluble CD127 (exon 5/7 - FWD) and (exon 8 - REV) primers (Table 2). To quantify the relative amounts of both soluble and trans-membrane isoforms (Total CD127), RT-PCR was performed on isolated cDNA using total CD127 (exon 4/5 - FWD) and (exon 5 - REV) primers (Table 2). Ribosomal protein S18 (RPS18) was quantified using RPS18 (exon 2/3 -

FWD) and (exon 3 - REV) primers (Table 2). Primers were made to order by Invitrogen, Inc. (Grand Island, NY) and were resuspended in nuclease-free water to a concentration of 500nM.

The iQ™ SYBR® Green Supermix from Bio-Rad (Hercules, CA) was used to perform the RT-PCR according to the manufacturer's instructions. Briefly, each 20µL reaction contained 10µL of 2X iQ™ SYBR® Green Supermix, 5µL of 1:20 diluted cDNA, 2.5µL of forward primer (500nM) and 2.5µL of reverse primer (500nM). RT-PCR reactions were performed using Bio-Rad's CFX Connect™ Real-Time PCR Detection System (Hercules, CA). Samples were first incubated for 3 minutes at 95°C to activate the hot-start iTaq DNA polymerase in the supermix and denature the cDNA. Following this initial incubation, the reactions underwent 50 cycles of amplification. Each cycle of amplification contained three steps: 30 seconds at 95°C to denature DNA secondary structures, 20 seconds at 57°C for primer annealing to cDNA template and 20 seconds at 72°C for DNA polymerization. At the end of each cycle, fluorescence was measured. Melt-curve analysis was performed once the samples had undergone 50 cycles of amplification by measuring fluorescence for 5 seconds as the temperature increased from 65°C to 95°C, in 0.5°C increments. Melt-curve analysis was used to confirm that a single specific amplicon was produced. Standard curves were performed, in parallel with the RT-PCR analysis for soluble CD127, total CD127 and RPS18 transcripts, using the cDNA pooled from all six cell lines. Pooled cDNA was used at dilutions of 1:5, 1:40, 1:320 and 1:260. All RT-PCR reactions were performed in triplicate.

Table 2: Primers used in real time PCR experiments to quantify the relative amounts of total CD127, soluble CD127 and RPS18 transcripts.

Primer Name	Primer Sequence
Total CD127(exon 4/5 - FWD)	5'- ATG GAC GCA TGT GAA TTT ATC -3'
Total CD127(exon 5 - REV)	5'- TTA TTG ATC TCT GGA GTT CTG AAG
Soluble CD127(exon 5/7 - FWD)	5'- TAG CTC AGG ATT AAG CCT AT -3'
Soluble CD127(exon 8 - REV)	5'- CTG GAG TGA TGA CTA CAT C -3'
RPS18(exon 2/3 - FWD)	5'- CTG CCA TTA AGG GTG TGG -3'
RPS18(exon 3 - REV)	5'- TCC ATC CTT TAC ATC CTT CTG -3'

2.6.3.1 Analysis of RT-PCR data

For each gene analyzed by RT-PCR, the CFX Connect software (Bio-Rad; Hercules, CA) calculated the mean Ct value by averaging triplicate readings (Ct values). Using the mean Ct, I then determined the fold change (ΔΔCt) of soluble CD127 or total CD127 relative to the expression of reference gene, RPS18, for each of the six cell lines. The calculation of fold change (ΔΔCt) contains a correction for endogenous soluble or total CD127 transcripts in the Jurkat cell (mean Ct from MOCK). The equation used to calculate ΔΔCt is shown below:

$$\Delta\Delta Ct = \frac{2^{(Mean\ Ct\ of\ Target\ gene\ from\ MOCK - Mean\ Ct\ of\ Target\ gene\ from\ Cell\ Line)}}{2^{(Mean\ Ct\ of\ RPS18\ from\ MOCK - Mean\ Ct\ of\ RPS18\ from\ Cell\ Line)}}$$

We then normalized the relative expression of soluble CD127 to the relative expression of total CD127 for each cell line (see equation below).

$$\Delta\Delta Ct\ of\ soluble\ CD127\ nomralized\ to\ total\ CD127 = \frac{\Delta\Delta Ct\ of\ soluble\ CD127}{\Delta\Delta Ct\ of\ total\ CD127}$$

The above calculations were repeated on four other RT-PCR analyses done on cDNA isolated from the six cell lines. Thus each cell line had five calculated values for ΔΔCt of soluble CD127 normalized to ΔΔCt of total CD127. For each cell line, these values were averaged and the standard error mean (SEM) was calculated.

CHAPTER 3: RESULTS

3.1 Development of an *in vitro* model to study the effect that disease specific mutations have on CD127 expression, regulation and signal transduction

In light of the importance that CD127 has in T-cell biology, I sought to develop an *in vitro* T-cell model to study and observe the effects that disease specific mutations have on CD127. To develop this T-cell model I began by looking at four lymphoblastic cell lines: A3, CEM, Jurkat and SupT1. In choosing which cell line to use for my model, I developed a set of specific criteria. The chosen cell line must have high endogenous surface levels of CD132 and low endogenous surface levels of CD127; be susceptible to G418 sulfate mediated death; must have endogenous STAT5; must be easily cultured; and must not be responsive to IL-7 in its untransduced state.

3.1.1 All four lymphoblastic cell lines expressed high surface levels of endogenous CD132

Our lab has previously shown that $CD8^+$ T-cells isolated from healthy individuals express high surface levels of endogenous CD132 and CD127; as such I used $CD8^+$ T-cells as a reference for high surface expression of CD132 and CD127 [19]. To determine the expression levels of CD132 in the four cell lines, I stained the cell surface with phycoerythrin (PE) conjugated anti-CD132 antibodies and analyzed the expression by flow cytometry. Figure 7 shows four flow histograms each comparing one of the lymphoblastic cell lines to $CD8^+$ T-cells. These histograms indicate that all four lymphoblastic cell lines examined express high surface levels of endogenous CD132 relative to $CD8^+$ T-cells.

Figure 7: A3, CEM, Jurkat and SupT1 cell lines express high surface levels of endogenous CD132 relative to primary human $CD8^+$ T-cells.

Four histograms are presented each comparing one of the four lymphoblastic cell lines (A3, CEM, Jurkat and SupT1) to $CD8^+$ T-cells. All cells were stained with PE conjugated anti-CD132 antibodies. Cells were gated on a live cell population based on forward and side scatter. CD132 expression was observed in the FL2 channel. Flow analysis was done using FCS Express 3.

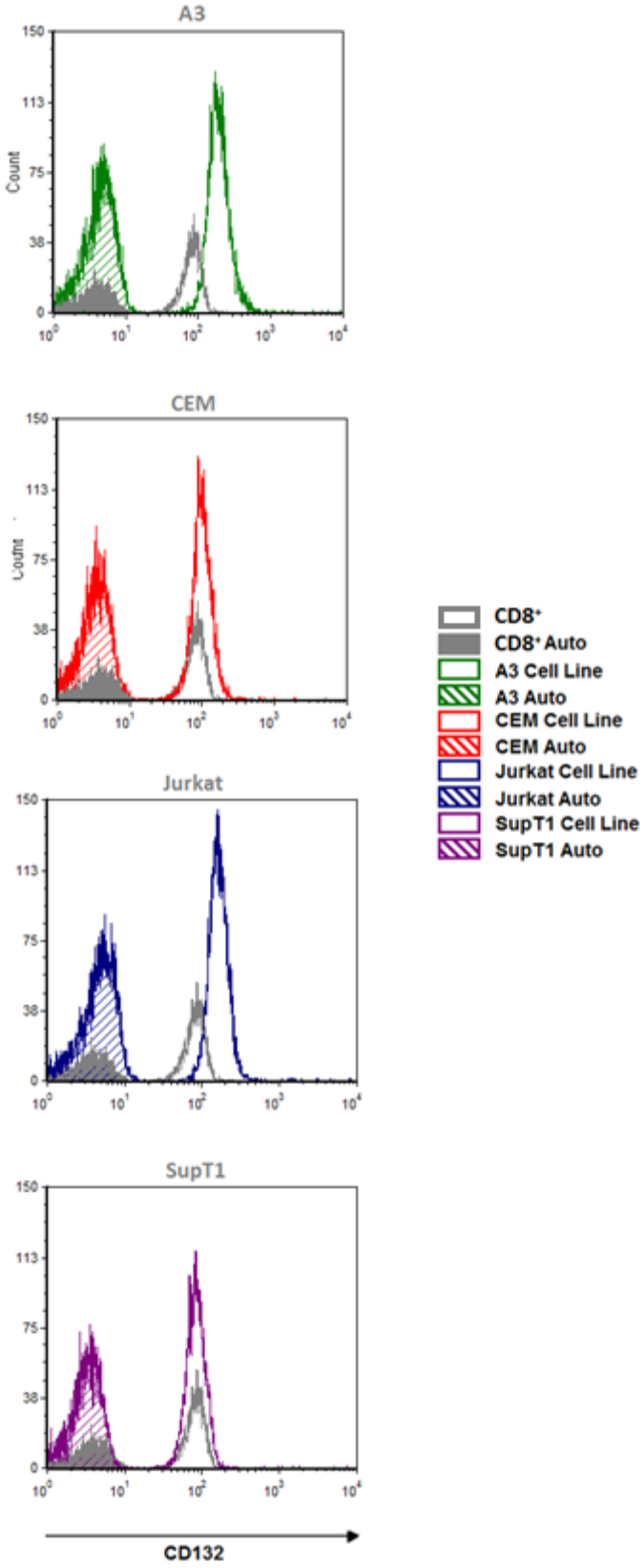
A3
CEM
Jurkat
SupT1
Count
150
113
75
38
0
10^0
10^1
10^2
10^3
10^4
CD8+
CD8+ Auto
A3 Cell Line
A3 Auto
CEM Cell Line
CEM Auto
Jurkat Cell Line
Jurkat Auto
SupT1 Cell Line
SupT1 Auto
CD132

3.1.2 A3, CEM and Jurkat cells expressed low surface levels of endogenous CD127

As mentioned above, primary human $CD8^+$ T-cells express high levels of CD127, thus these cells were used as a reference for high endogenous expression of CD127. To determine the expression levels of CD127 in the four cell lines, I stained the cell surface with PE conjugated anti-CD127 antibodies and analyzed the expression by flow cytometry. Figure 8 shows that A3, CEM and Jurkat cells express low surface levels of endogenous CD127 compared to $CD8^+$ T-cells. SupT1 cells express high levels of CD127, as such this cell line was unsuitable for my model since I wanted to introduce the expression wild type or mutant CD127 protein into the cell line.

3.1.3 A3 cells were unsuitable for the T-cell model because they are resistant to G418 sulfate mediated cell death

I then conducted a literature review on A3, CEM and Jurkat cell lines. I found that of these three cell lines, A3 cells are a derivative of Jurkat cells that already contained the neomycin resistance gene [57]. Considering that I wanted to introduce the CD127 gene using a lentivirus and select for cells that expressed CD127 by G418 sulfate, A3 cells were determined unsuitable for my purposes.

3.1.4 CEM and Jurkat cell lines expressed endogenous STAT5

Since one of the main objectives of the project was to determine how mutations in CD127 affect cell signaling; I decided to use STAT5 phosphorylation as my main signaling output and therefore required a cell line that expressed endogenous STAT5. Figure 9 shows by western blot that Jurkat and CEM cells express endogenous STAT5. In this western blot, primary $CD8^+$ T-cells were used as a positive control for STAT5 expression.

Figure 8: A3, CEM and Jurkat cells have the lowest surface expression of endogenous CD127 relative to primary human $CD8^+$ T-cells.

(A) Four histograms are presented each comparing one of the four lymphoblastic cell lines (A3, CEM, Jurkat and SupT1) to $CD8^+$ T-cells. All cells were stained with PE conjugated anti-CD127 antibodies. Cells were gated on the live cell population based on forward and side scatter. CD127 expression was observed in the FL2 channel (B) Analysis of the flow histograms using FCS Express 3 shows that A3, CEM, and Jurkat cells have low surface expression (mean fluorescence intensity; MFI) of CD127.

A

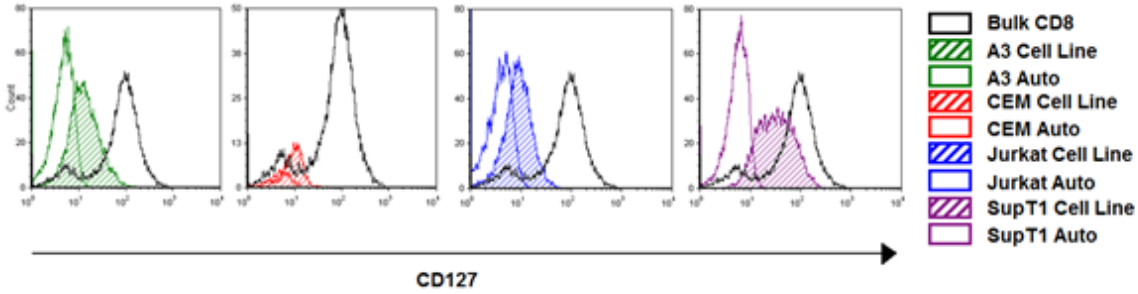
Bulk CD8
A3 Cell Line
A3 Auto
CEM Cell Line
CEM Auto
Jurkat Cell Line
Jurkat Auto
SupT1 Cell Line
SupT1 Auto
CD127

B

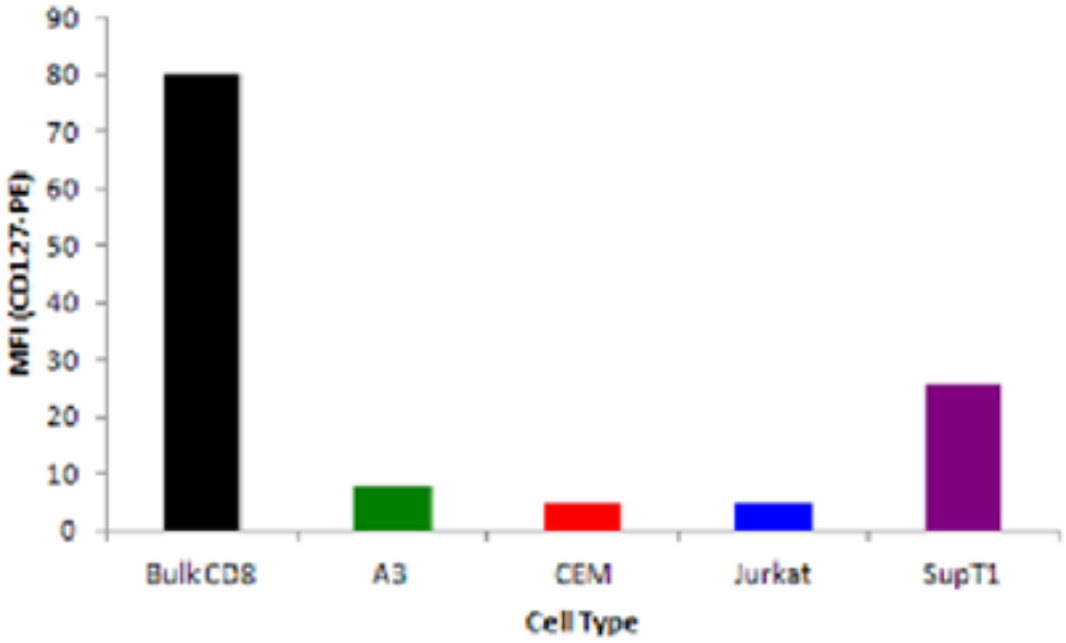
90
80
70
60
50
40
30
20
10
0
MFI (CD127-PE)
Bulk CD8
A3
CEM
Jurkat
SupT1
Cell Type

Figure 9: STAT5 is endogenously expressed in both Jurkat and CEM cell lines.

Primary human $CD8^+$ T-cells, CEM and Jurkat cells were lysed and run on a 10% SDS-PAGE gel. Following transfer, the blot was probed for STAT5 and β-actin. $CD8^+$ T-cells were used a positive control for STAT5 expression. Western blot is representative of n=2.

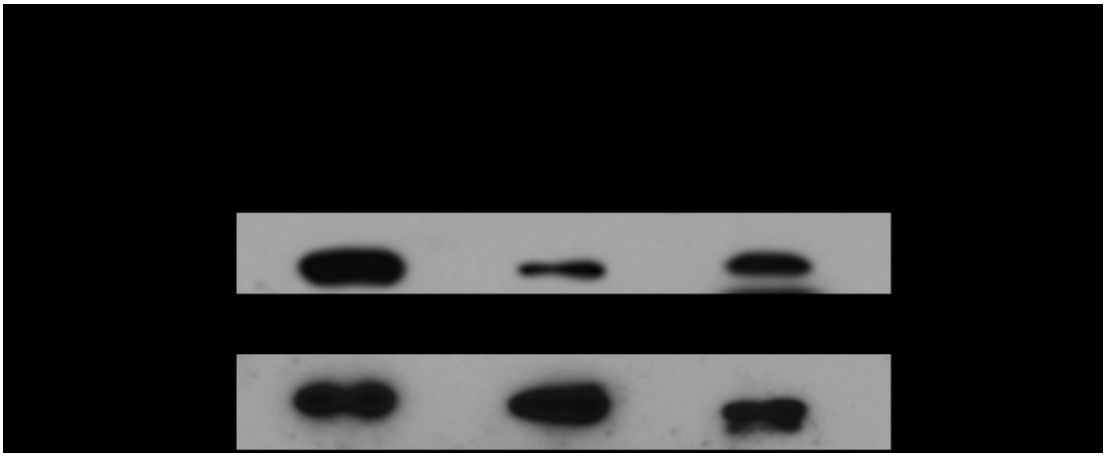

3.1.5 CEM cells are unsuitable for the T-cell model because they were difficult to culture and readily died

While culturing both Jurkat and CEM cell lines I found that the CEM cell line was difficult to culture. I observed that the CEM cell line population doubled much more slowly compared to Jurkat cells by counting the number of cells in a hemocytometer. Additionally, while culturing cells I observed more cell death using trypan blue dye in the CEM cell line compared to Jurkat cell line. To ensure that these observations on the CEM cell line were not due to a single bad batch of cells, I cultured three additional batches of CEM cells and observed similar results. Based on all the observations, I determined that the CEM cell line would not be suitable for my cell line model.

3.1.6 Parental Jurkat cells are unresponsive to IL-7 stimulation

Since I want to use my T-cell model to study the effects that CD127 mutations have on IL-7 mediated signaling, I wanted to ensure that the parental Jurkat cell line did not respond to IL-7. Any signaling affects due to CD127 mutations could be masked by signaling from the endogenous CD127 protein on Jurkat cells. Thus I stimulated the Jurkat cells with 10ng/mL of IL-7 for 15 minutes, lysed the cells and performed a western blot for phospho-STAT5 (figure 10).

In this western blot I used primary human $CD8^+$ T-cells as a positive control for pSTAT5 expression in response to IL-7. The western blot in figure 10 shows that parental untransduced Jurkat cells do not phosphorylate STAT5, in response to IL-7.

Figure 10: Jurkat cells do not phosphorylate STAT5 in response to IL-7 (10ng/mL).

Jurkat and primary human $CD8^+$ T-cells were incubated in media or media plus IL-7 (10ng/mL) for 15 minutes. Cells were pelleted, lysed and run on a 10% SDS-PAGE gel. Following transfer, the blot was probed for pSTAT5, STAT5, and β-actin. $CD8^+$ T-cells were used as a positive control for phosphorylation of STAT5 in response to IL-7. Western blot is representative of n=2.

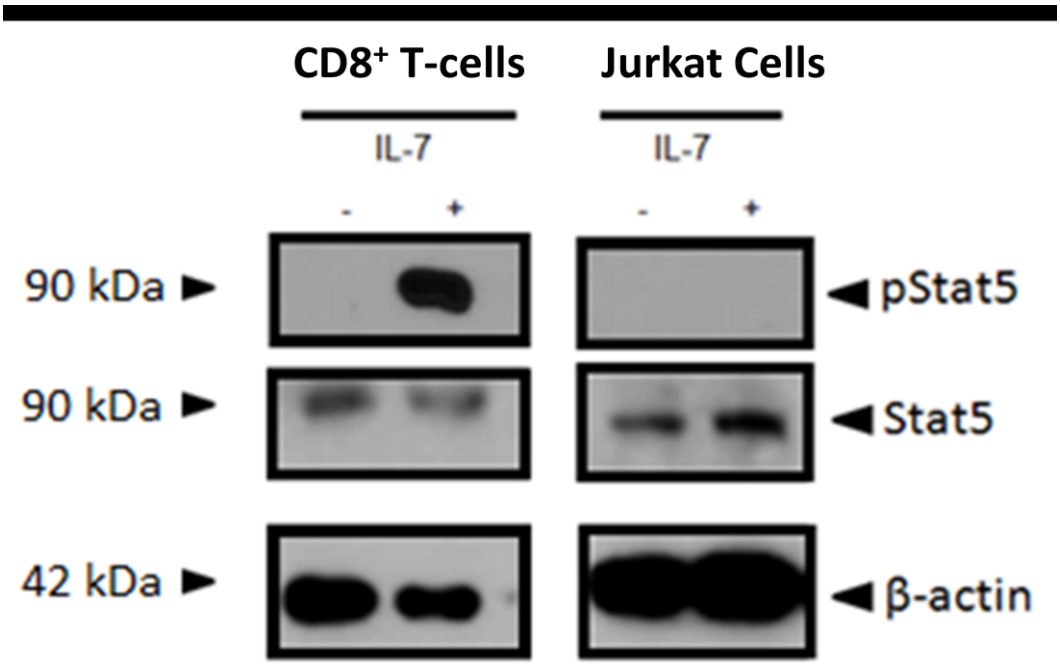
CD8+ T-cells
Jurkat Cells
IL-7
IL-7
-
+
-
+
90 kDa
pStat5
90 kDa
Stat5
42 kDa
β-actin

3.1.7 Transducing Jurkat cells with WT or mutant CD127 genes to develop the T-cell models

Based on all the observations, I determined that Jurkat cells would be a good choice to build my T-cell model. The next step was to stably introduce expression of wild type CD127 or mutant CD127 (P132S, I356V, L242_L243insNPC and T244I) into Jurkat cells. To accomplish this, I made six lentiviruses that each had the neomycin resistance gene and lacked an insert (MOCK), or contained wild type CD127 (CD127WT) or mutant CD127 (P132S, I356V, L242_L243insNPC (also known as insNPC) and T244I). Cultured Jurkat cells were split into six batches and each batch was transduced with one of the six lentiviruses. Transduced cells were then selected using 750µg/mL of G418 sulfate (Appendix III for G418 sulfate kill curve). After 20 days of culturing the transduced cells under selective conditions, the T-cell models each expressing one of the four disease specific mutations in CD127 or wild type CD127 were established.

3.1.8 Jurkat cells transduced with WT or mutant CD127 genes produced CD127 proteins

To confirm that these cell lines expressed wild type or mutant CD127 protein from the transduced CD127 genes, I performed a western blot probing for CD127 and DDK on lysates from the established cell lines (figure 11). In the established cell lines, CD127 expressed from the transduced CD127 genes also has a DDK tag on the C-terminus, as such a western blot probing for DDK would indicate that the cell line is producing the wild type or mutant CD127 protein based on the transduced gene.

The western blot probing for CD127 showed that the parental, MOCK, CD127WT, P132S, I356V, insNPC, and T244I Jurkat cell lines produced CD127 protein (figure 11).

The CD127-Fc chimera has the same molecular weight as full length CD127 protein and anti-CD127 western antibodies are shown to bind to it; as such I used the CD127-Fc chimera as a positive control for CD127 [33]. The blot probing for DDK showed that the CD127WT, P132S, I356V, insNPC, and T244I Jurkat cell lines produce a DKK tagged protein that is the same size, ~75kDa, as CD127 protein (figure 11).

In the anti-CD127 blot, there are two distinct bands for CD127 protein from the lysates of CD127WT, P132S, I356V, insNPC and T244I cell lines (figure 11). While in the parental and MOCK Jurkat cell lines, there is only the single higher band. Here I observed that the CD127 bands in the lanes of untransduced and MOCK transduced Jurkat cell lysates are much lighter in density then the bands in the lanes of the wild type and mutant CD127 transduced cell line lysates (figure 11). In the anti-DDK blot, the same two distinct bands observed from the anti-CD127 blot are observed for DDK tagged CD127 in lanes containing the lysates of CD127WT, I356V, insNPC and T244I cell lines (figure 11). Interestingly, only the lower band for DDK tagged CD127 in the P132S cell line is observed. The parental and MOCK Jurkat cell lines had no bands present for DDK tagged CD127.

Together these blots in figure 11 suggest that the CD127WT, P132S, I356V, insNPC and T244I Jurkat cell lines produce the wild type or respective mutant CD127 protein from the transduced genes.

Figure 11: Transduced Jurkat cell lines stably express wild type CD127 and mutant CD127 genes.

Western blots were performed on cell lysates from MOCK, CD127WT, P132S, T244I, I356V, L242_L243insNPC transduced Jurkat cell lines and parental untransduced Jurkat cells. Upper panel is a western blot probing for CD127 using a polyclonal anti-CD127 antibody. CD127-Fc Chimera (5ng) is used as a positive control. Lower panel is a western blot probing for the DDK tag on the C-terminus of CD127 using a polyclonal anti-DDK antibody. Western blots are representative of n=4

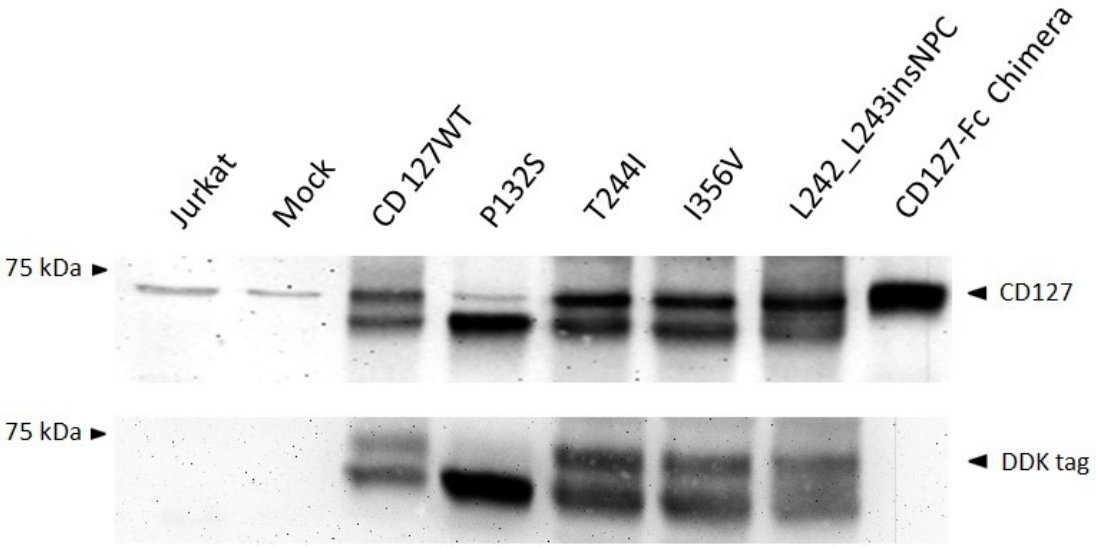
Jurkat
Mock
CD 127WT
P132S
T244I
I356V
L242_L243insNPC
CD127-Fc Chimera
75 kDa
CD127
75 kDa
DDK tag

3.2 CD127 protein expression in Jurkat cells transduced with wild type or mutant CD127 genes

3.2.1 CD127 protein with the I356V, L242_L243insNPC and T244I mutations are detected on the surface of the established cell lines

To determine if the CD127 proteins expressed from the transduced genes are expressed on the cell surface, I stained the MOCK, CD127WT, P132S, I356V, insNPC and T244I Jurkat cell lines with PE conjugated anti-CD127 antibody (clone R34.34). The MOCK cell line expresses only low levels of endogenous CD127 and by setting the voltages on the flow cytometer such that the expression of CD127 on the MOCK cell line was $CD127^{low}$, I could observe differences in the surface expression of CD127 protein in the WT and mutant cell lines.

Flow histograms indicate that CD127 surface expression can be detected on the CD127WT, I356V, insNPC and T244I Jurkat cell lines (figure 12.A). The level of surface expression of CD127 in all the cell lines except P132S is about 3-fold higher ($p<0.05$) compared to the expression level of endogenous CD127 on the MOCK cell line (figure 12.B). CD127 expression levels on the mutant cell lines I356V, insNPC and T244I are relatively the same as the CD127 expression levels on the CD127WT cell line (figure 12.B).

While I could detect surface expression of CD127 on the CD127WT, I356V, insNPC and T244I Jurkat cell lines, I could not detect surface CD127 on the P132S Jurkat cell line above the endogenous CD127 levels expressed on the MOCK cell line (figure 12.B).

Figure 12: CD127WT, I356V, L242_L243insNPC and T244I transduced Jurkat cells have significantly higher surface expression of CD127 relative to the MOCK vector transduced Jurkat cell line.

The MOCK, CD127WT, P132S, I356V, insNPC and T244I cell lines were stained with PE conjugated anti-CD127 (clone R34.34). Voltage was set such that CD127 expression in the MOCK cell line was $CD127^{low}$. (A) Representative flow histograms of CD127 surface expression of n=9. (B) Bar graph showing mean MFI of surface CD127 of n=9. Error bars are +/- SEM. $p<0.0001$ as measured by One-way ANOVA. Dunnett's multiple comparison post-test compares WT and mutant CD127 cell lines to Mock, * $p<0.05$ and ns is $p>0.05$. Differences between CD127 expression of I356V, insNPC and T244I cell lines to the CD127 expression in CD127WT were not significant ($p>0.05$).

A

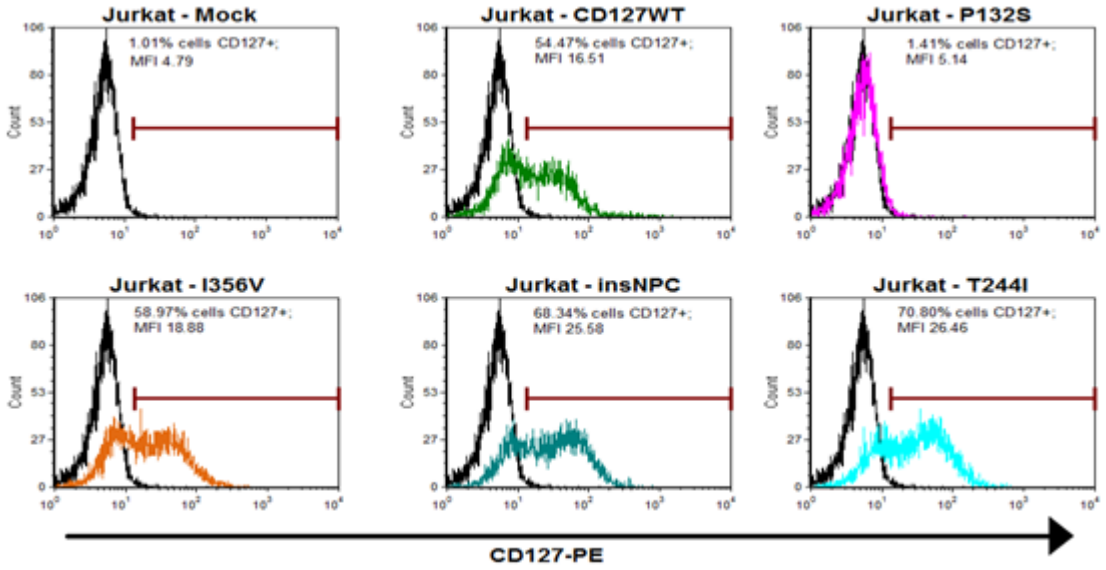
Jurkat - Mock
1.01% cells CD127+;
MFI 4.79
Jurkat - CD127WT
54.47% cells CD127+;
MFI 16.51
Jurkat - P132S
1.41% cells CD127+;
MFI 5.14
Jurkat - I356V
58.97% cells CD127+;
MFI 18.88
Jurkat - insNPC
68.34% cells CD127+;
MFI 25.58
Jurkat - T244I
70.80% cells CD127+;
MFI 26.46
Count
CD127-PE

B

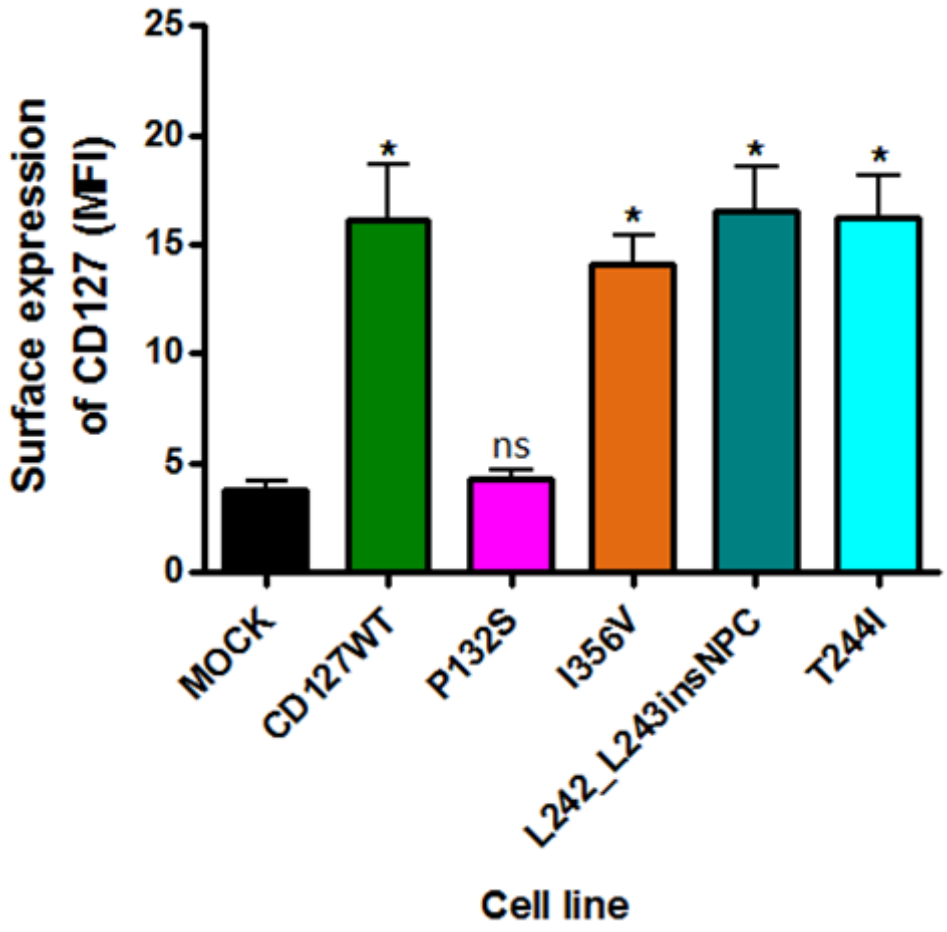
Surface expression of CD127 (MFI)
25
20
15
10
5
0
*
ns
*
*
*
MOCK
CD127WT
P132S
I356V
L242_L243insNPC
T244I
Cell line

3.2.2 CD127 containing the P132S mutation cannot be detected by flow cytometry on the cell surface

Considering that the P132S mutation, which is located in the extracellular domain of CD127, may cause conformational changes in this region of the protein, it is possible the monoclonal antibody (clone R34.34) used for flow cytometry was not able to recognize its epitope on P132S mutated CD127. Thus I surface stained MOCK, P132S, and CD127WT Jurkat cell lines with two other monoclonal anti-CD127 antibodies (clones hIL-7R-M21 and 40131) and the same polyclonal anti-CD127 antibody used in our anti-CD127 western blot, from figure 11.

Figure 13 shows that surface CD127 protein can be detected on the CD127WT cell line using any of the three monoclonal antibodies and the polyclonal antibody. Unlike the CD127WT cell line, surface CD127 expression could not be detected for the P132S cell line above the endogenous levels expressed on the MOCK cell line (figure 13).

3.2.3 P132S mutated CD127 cannot be detected intracellularly by flow cytometry

Since I could not detect CD127 protein on the surface of the P132S cell line, I considered that perhaps CD127 protein remains intracellular and is not expressed on the surface. To test this, I fixed and permeabilized MOCK, P132S and CD127WT cell lines, then stained these cells with polyclonal anti-CD127 antibody and performed flow cytometry. Figure 14 shows that CD127 is not detected intracellularly nor on the surface of the P132S - Jurkat cells. While in the CD127WT cell line, CD127 protein is detected on the surface and intracellularly (figure 14).

In the flow cytometry experiments where I used two-step staining techniques to detect surface or intracellular CD127 protein, I also performed a secondary antibody

Figure 13: P132S mutant CD127 cannot be detected on the surface of cells by three different monoclonal anti-CD127 antibodies or by a polyclonal anti-CD127 antibody.

MOCK, CD127WT and P132S Jurkat cells were surface stained using PE conjugated monoclonal anti-CD127 antibody (clone R34.34 or hIL-7R-M21) or two-step stained using monoclonal anti-CD127 antibody (clone 40131) with goat anti-mouse IgG1 antibody conjugated with Alexa Fluor 555 or polyclonal anti-CD127 antibody with donkey anti-goat IgG antibody conjugated with Alexa Fluor 647. Where two step staining was used, a secondary antibody control was done to ensure that data reflects specific binding to CD127. Voltage was set such that CD127 expression on the MOCK cell line was $CD127^{low}$. The CD127WT cell line was used as a positive control for CD127 expression. Grey shaded area in histograms represents the auto-fluorescence of unstained MOCK cell line.

A

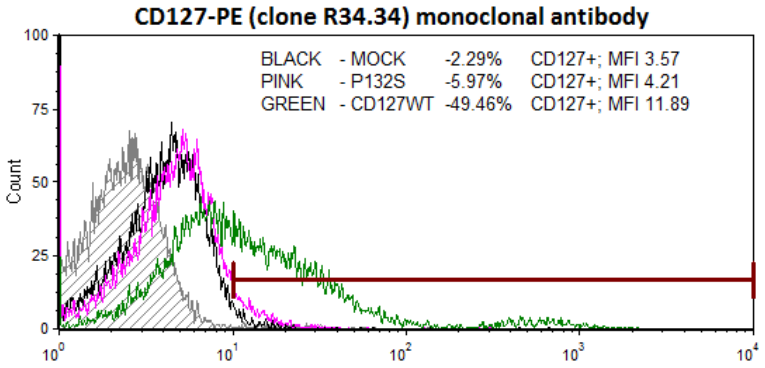
CD127-PE (clone R34.34) monoclonal antibody
BLACK - MOCK -2.29% CD127+; MFI 3.57
PINK - P132S -5.97% CD127+; MFI 4.21
GREEN - CD127WT -49.46% CD127+; MFI 11.89
Count

B

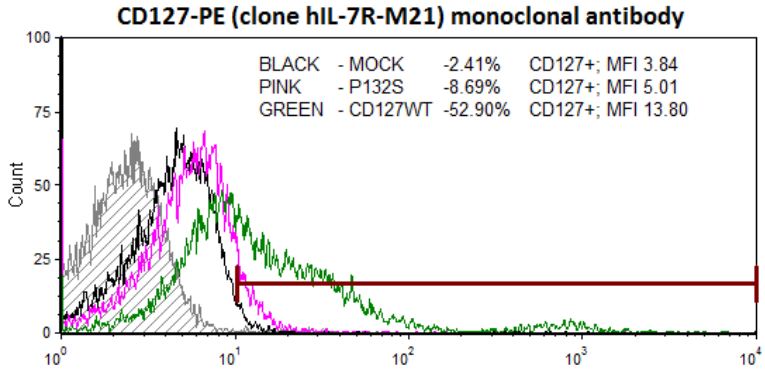
CD127-PE (clone hIL-7R-M21) monoclonal antibody
BLACK - MOCK -2.41% CD127+; MFI 3.84
PINK - P132S -8.69% CD127+; MFI 5.01
GREEN - CD127WT -52.90% CD127+; MFI 13.80
Count

C

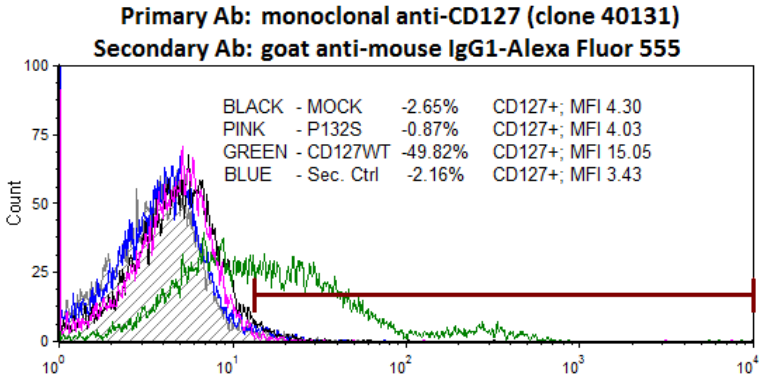
Primary Ab: monoclonal anti-CD127 (clone 40131)
Secondary Ab: goat anti-mouse IgG1-Alexa Fluor 555
BLACK - MOCK -2.65% CD127+; MFI 4.30
PINK - P132S -0.87% CD127+; MFI 4.03
GREEN - CD127WT -49.82% CD127+; MFI 15.05
BLUE - Sec. Ctrl -2.16% CD127+; MFI 3.43
Count

D

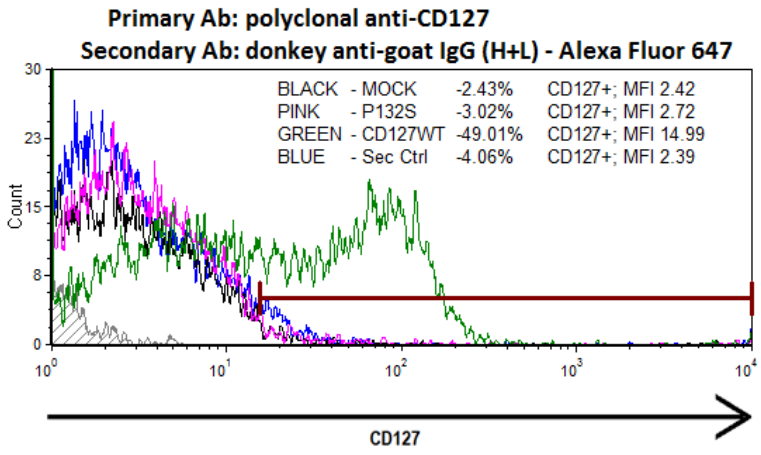
Primary Ab: polyclonal anti-CD127
Secondary Ab: donkey anti-goat IgG (H+L) - Alexa Fluor 647
BLACK - MOCK -2.43% CD127+; MFI 2.42
PINK - P132S -3.02% CD127+; MFI 2.72
GREEN - CD127WT -49.01% CD127+; MFI 14.99
BLUE - Sec Ctrl -4.06% CD127+; MFI 2.39
Count
CD127

Figure 14: Intracellular CD127 cannot be detected in the P132S - Jurkat cell line.

Two step staining using a polyclonal anti-CD127 antibody with donkey anti-goat IgG conjugated with Alexa Fluor 647 was performed on the MOCK, CD127WT and P132S Jurkat cell lines. Secondary antibody control was done to ensure that data reflects specific binding to CD127. Voltage was set such that CD127 expression on the MOCK cell line was $CD127^{low}$. The CD127WT cell line was used as a positive control for CD127 expression on the surface and intracellularly. Grey shaded area in histograms represents the auto-fluorescence of unstained MOCK cell line.

A

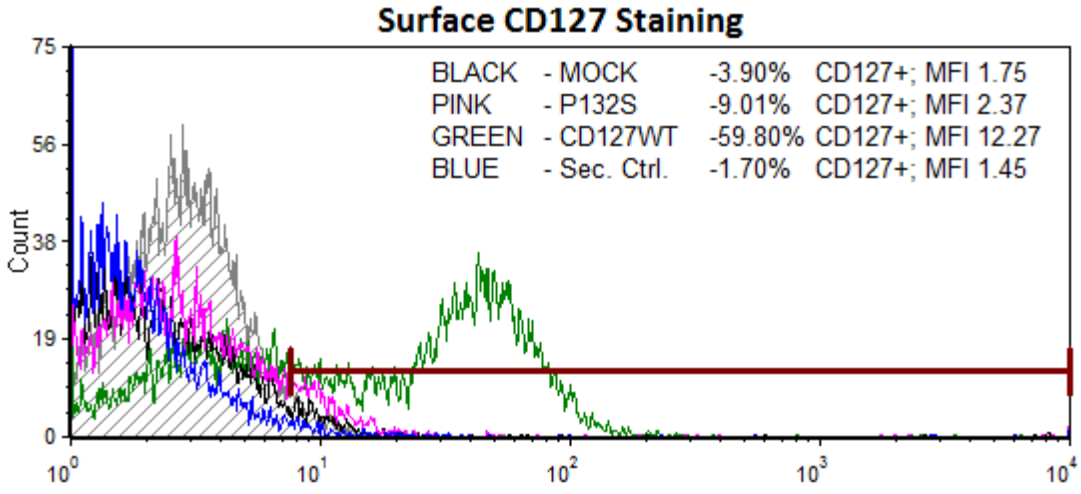
Surface CD127 Staining
BLACK - MOCK -3.90% CD127+; MFI 1.75
PINK - P132S -9.01% CD127+; MFI 2.37
GREEN - CD127WT -59.80% CD127+; MFI 12.27
BLUE - Sec. Ctrl. -1.70% CD127+; MFI 1.45
Count
75
56
38
19
0
10^0
10^1
10^2
10^3
10^4

B

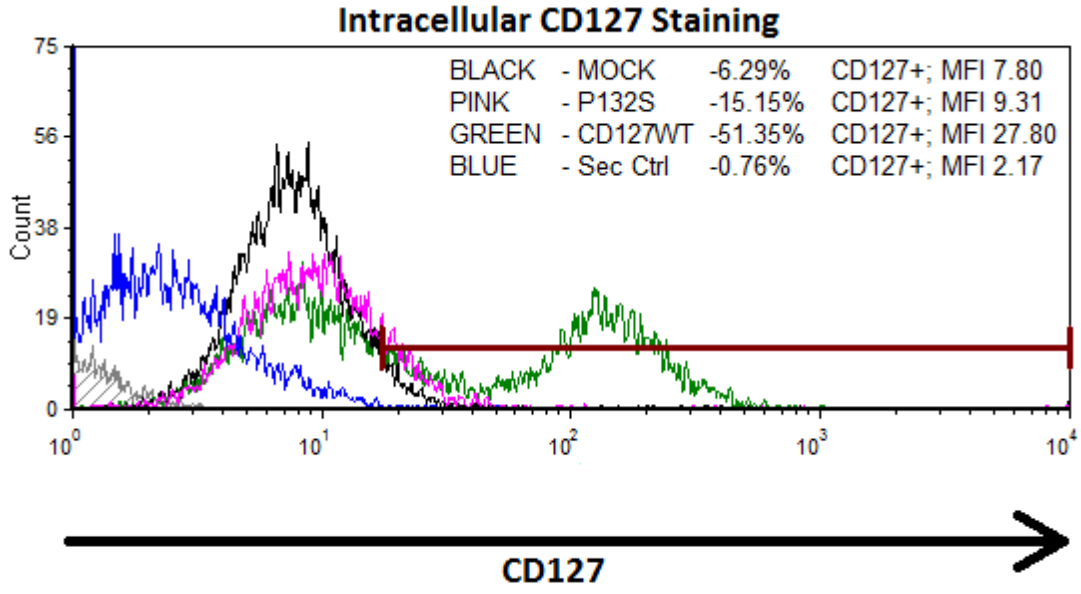
Intracellular CD127 Staining
BLACK - MOCK -6.29% CD127+; MFI 7.80
PINK - P132S -15.15% CD127+; MFI 9.31
GREEN - CD127WT -51.35% CD127+; MFI 27.80
BLUE - Sec Ctrl -0.76% CD127+; MFI 2.17
Count
75
56
38
19
0
10^0
10^1
10^2
10^3
10^4
CD127

control. This control was used to ensure that the observed data represents the specific interaction between the anti-CD127 antibody and CD127 proteins; and not the interaction of the secondary anti-IgG antibody and CD127 proteins or other cellular proteins.

3.3 Examining the established mutant cell lines for CD127 transcripts

3.3.1 The four mutant CD127 cell lines show no significant fold differences in the transcript levels of soluble CD127 (sCD127) compared to the CD127WT cell line.

As mentioned in the introduction, Gregory *et al.* showed in their own *in vitro* model a two fold increase in transcripts encoding the soluble isoform of CD127 in cells carrying the T244I mutation compared to the wild type CD127 gene [48]. As such I was curious whether I would see a similar result in my *in vitro* T-cell model.

We know that full length membrane bound CD127 is translated from mRNA that spans exons 1 to 8. Soluble CD127 protein is transcribed from mRNA that spans exons 1 to 8, but skips exon 6 as a result of alternative splicing. Our lab has previously been able to detect both the soluble and membrane bound isoforms of CD127 transcripts in primary human $CD8^+$ T-cells using RT-PCR [58]. To detect the soluble isoform of CD127 mRNA, we previously used a forward primer that spans the exon 5/7 boundary and a reverse primer in exon 8. The forward primer spanning the exon 5/7 boundary is complementary to the end of exon 5 and the beginning of exon 7, and is used to specifically detect transcripts that skipped exon 6. To detect total CD127 transcripts (soluble and membrane bound isoforms), we previously used a forward primer that spans the exon 4/5 boundary and a reverse primer in exon 5. To detect transcripts encoding total and soluble CD127 isoforms in the established cell lines, I used these same primer combinations (Table 2).

In my T-cell models, I cloned the wild type and mutant CD127 cDNA into the lentiviruses used to transduce Jurkat cells. While I recognize that the cDNA is solely composed of exons, there is still the possibility that splicing can occur because there are 5' and 3' splice site sequences (Appendix V for splice site predictions in CD127 cDNA) in the exons before and after exon 6.

Here I performed RT-PCR analysis on the MOCK, CD127WT and the four mutant cell lines and measured the amount of transcripts encoding soluble and total CD127. From each cell line, I also measured the transcript levels of RPS18 as a reference gene. I then normalized the transcript levels encoding soluble and total CD127 to the transcript level of RPS18 for each cell line. Using the normalized transcript levels of soluble and total CD127, I then calculated the relative expression of transcripts encoding soluble and total CD127 from each cell line to the relative expression of transcripts encoding soluble and total CD127 in the MOCK cell line. The MOCK cell line only contains endogenous CD127 transcripts, thus the calculated relative expression of transcripts encoding soluble and total CD127 represents the mRNA expression levels of the exogenous CD127 transduced into the cell lines and not the endogenous CD127 mRNA.

Interestingly, I was able to detect transcripts encoding the soluble CD127 isoform in the wild type and mutant CD127 cell lines (Figure 15A). The relative mRNA expression for the soluble CD127 isoform was lower than that of the total CD127 isoform in the wild type and all the mutant CD127 cell lines (figure 15A). However within each cell line there was no statistical difference between the relative expression of soluble CD127 mRNA and total CD127 mRNA (figure 15A). When normalizing relative expression of transcripts encoding soluble CD127 to the relative expression of transcripts encoding total CD127 (figure 15B), I

noticed that the relative level of soluble CD127 mRNA in the CD127WT, P132S, I356V and insNPC cell lines were roughly the same at around 50%. The relative level of soluble CD127 mRNA in the T244I cell line was higher than the other cell lines at roughly 70% (figure 15B). One way ANOVA statistical analysis of the normalized relative expression transcripts encoding soluble CD127 between the cell lines revealed no significance differences (figure 15B). Post-test analysis comparing the normalized relative expression of transcripts encoding soluble CD127 in the CD127WT cell line to each mutant CD127 cell line showed no significant differences (figure 15B). Based on these results, I did not see the same effect as Gregory *et al.* saw with regards to the T244I mutation [48].

3.4 Surface CD127 down-regulation is altered in the I356V, insNPC and T244I cell lines compared to the down-regulation in the CD127WT cell line

3.4.1 Surface CD127 is down-regulated in the CD127WT, I356V, insNPC and T244I cell lines in response to IL-7.

We know that in healthy primary human $CD8^+$ T-cells, surface CD127 protein is down regulated in response to IL-7 in a dose and time dependent manner [34]. The down-regulation of CD127 in response to IL-7 is one of cell's regulatory mechanisms that ensures IL-7 signaling is not constitutive [34, 35]. In this study, I wanted to know whether surface CD127 would be down-regulated in the CD127WT cell line in response to IL-7 and if the IL-7 response is dose and time dependent. I also wanted to know if the disease specific mutations would affect the down-regulation of CD127 in response to IL-7. To this end, I cultured the CD127WT, I356V, insNPC and T244I cell lines in media alone or media plus 1ng/mL, 10ng/mL or 25ng/mL of IL-7. Cells were then stained with PE conjugated anti-CD127 (clone R34.34) antibodies. Live cells were gated based on forward and side scatter

Figure 15: The four mutant CD127 cell lines have no significant differences in the relative mRNA expression levels of soluble CD127 (sCD127) compared to the CD127WT cell line.

Real-time PCR was performed on MOCK, CD127WT, P132S, I356V, insNPC and T244I Jurkat cell lines to determine the mRNA transcript levels encoding total CD127 and soluble CD127. The transcript levels of total and soluble CD127 were normalized to RPS18 reference gene expression. Relative mRNA expression level for total and soluble CD127 was calculated using the ΔΔCt method. Bar graph (A) shows the relative mRNA expression levels for soluble and total CD127 for each cell line. There is no statistical difference between the relative expression of soluble and total CD127 mRNA within each cell line, as measured by t tests (ns>0.05). Bar graph (B) shows the relative mRNA expression levels encoding soluble CD127 normalized to relative mRNA expression levels of total CD127 for each cell line. One way ANOVA analysis revealed no significant differences between the different cell lines in soluble CD127 transcript levels. Dunnett's post-test comparison determined no significant differences between CD127WT and each mutant (ns>0.5). Bars in graphs (A) and (B) represent pooled data from five individual experiments (n=5) and error bars show +/- SEM.

A

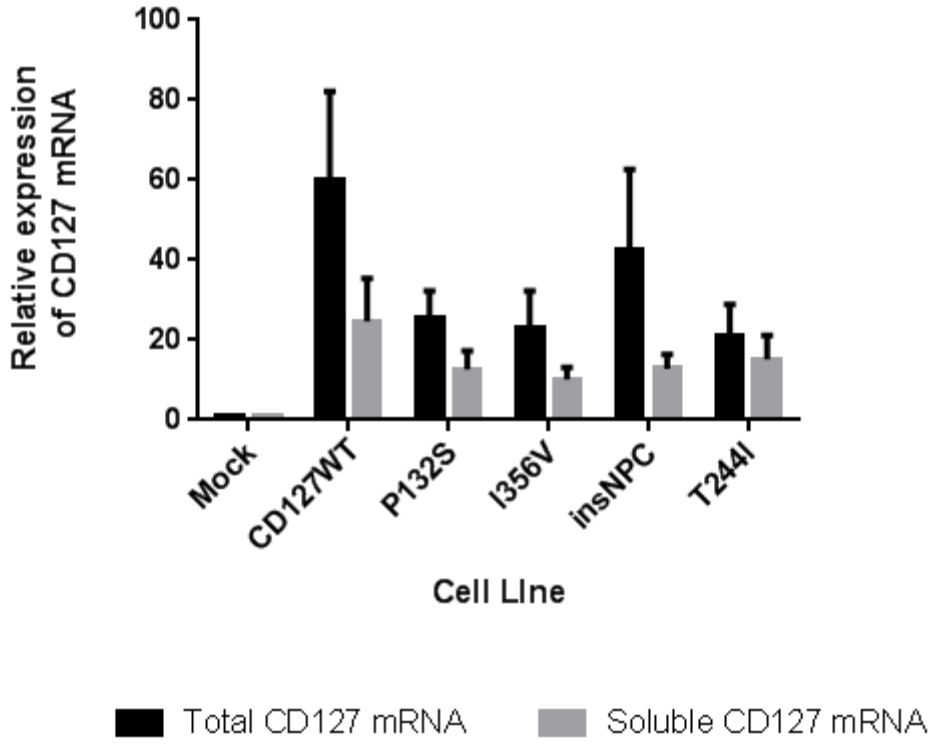
Relative expression of CD127 mRNA
100
80
60
40
20
0
Mock
CD127WT
P132S
I356V
insNPC
T244I
Cell LIne
Total CD127 mRNA
Soluble CD127 mRNA

B

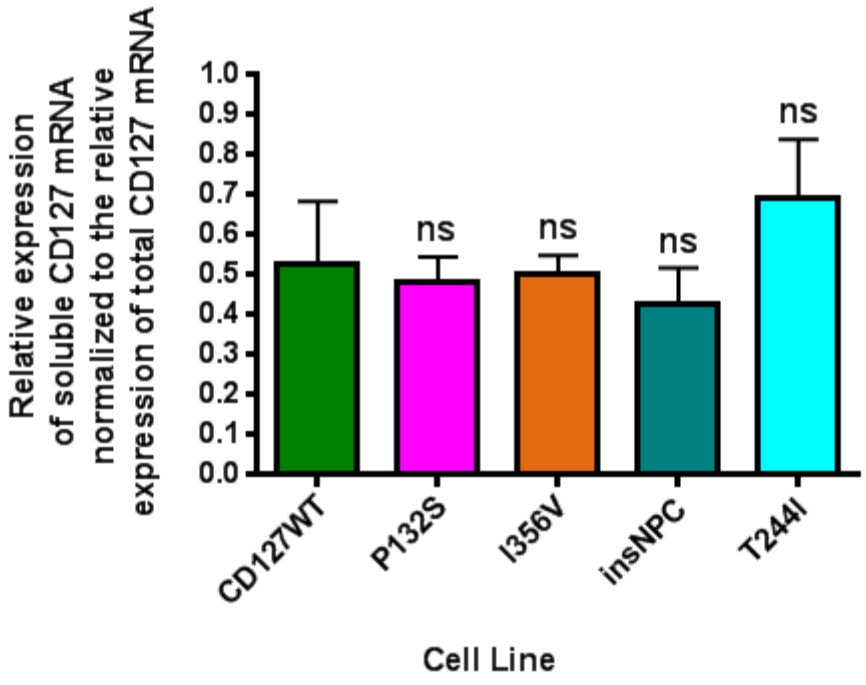
Relative expression of soluble CD127 mRNA normalized to the relative expression of total CD127 mRNA
1.0
0.9
0.8
0.7
0.6
0.5
0.4
0.3
0.2
0.1
0.0
ns
ns
ns
ns
CD127WT
P132S
I356V
insNPC
T244I
Cell Line

and examined by flow cytometry for the expression of CD127 (MFI) at 0, 3, 12 and 24 hours after IL-7 stimulation. CD127 expression (MFI) on IL-7 stimulated cells was normalized to the CD127 expression (MFI) on cells in media alone at each time point. In this experiment I did not examine the effects on P132S because I could not detect CD127 on the surface of this cell line by flow cytometry.

In figure 16A, CD127 expression on the CD127WT cell line is down-regulated in response to IL-7. CD127WT cells stimulated with 1ng/mL of IL-7 down-regulated CD127 by ~10% from basal levels at 3 hours; 12 hours after stimulation these cells down-regulated CD127 by ~20% from basal levels; by 24 hours the expression level of CD127 returned to basal levels (~100%). CD127WT cells stimulated with 10 and 25ng/mL of IL-7 down-regulated CD127 expression by ~30% from basal levels at 3 hours and the CD127 expression remained at this level up to 12 hours. Between 12 and 24 hours the expression of CD127 in CD127WT cells stimulated with 10ng/mL of IL-7 returned to basal levels (~100%) and the expression of CD127 in CD127WT cells stimulated with 25ng/mL of IL-7 only increased by ~10% (~20% below basal levels). Based on these results, in the CD127WT cell line, CD127 down-regulation is dose and time dependent.

In figure 16 B and C, CD127 expression on the I356V and insNPC cell lines is down-regulated in response to IL-7. Interestingly, at low IL-7 concentrations (1ng/mL) the expression of CD127 on I356V and insNPC cell lines is not affected. However, when I356V and insNPC cells are stimulated with 10ng/mL or 25ng/mL of IL-7, CD127 expression is down-regulated by ~20% from basal levels at 3 hours (figure 16B and C). Between 3 to 24 hours post IL-7 (10 and 25ng/mL) stimulation there is a steady slow increase in CD127 expression. At 24 hours, for both I356V and insNPC cell lines stimulated with IL-7 (10 and

25ng/mL), the CD127 expression has increased by ~10% (~10% below basal levels). Compared to the CD127 down-regulation seen in CD127WT cells, these two mutant CD127 proteins remain on the cell surface to a greater degree when stimulated with a low IL-7 concentration (1ng/mL). When stimulated with higher IL-7 concentrations (10 and 25ng/mL) the mutant CD127 proteins are down-regulated, but to a lesser degree than in CD127WT cells. The CD127 down-regulation that does occur in the I356V and insNPC cell lines is not sustained as long as the down-regulation of wild type CD127 in the CD127WT cell line.

In figure 16D, CD127 expression on the T244I cell line is down-regulated in response to IL-7. The CD127 down-regulation in T244I cells is similar to the down regulation observed in the I356V and insNPC cell lines. T244I cells stimulated with 1ng/mL of IL-7 down-regulated CD127 by ~10% from basal levels at 3 hours; between 3 and 12 hours the CD127 expression returns to basal levels and remains at this level. At higher IL-7 concentrations (10 and 25ng/mL) the down-regulation of CD127 in the T244I cell line is very similar to the CD127 down-regulation observed in I356V and insNPC cell lines. T244I cells stimulated with 10ng/mL of IL-7 down-regulated CD127 by ~25% from basal levels at 3 hours; between 3 and 24 hours the CD127 expression slowly and steadily returns to basal levels. T244I cells stimulated with 25ng/mL of IL-7 down-regulated CD127 by ~30% from basal levels at 3 hours; between 3 and 12 hours CD127 expression remain the same between ~70-75% of the basal level; and between 12 and 24 hours CD127 expression slowly rises to ~80% of the basal level. In comparing the CD127 down-regulation in T244I cells with CD127WT cells, I noticed that in the T244I cell line stimulated with low IL-7 concentrations (1ng/mL) CD127 surface protein was down-regulated to a lesser degree than

Figure 16: CD127 is down-regulated on the surface of the CD127WT, I356V, insNPC and T244I cell lines in a dose and time dependent manner.

CD127WT, I356V, insNPC and T244I cells were cultured in media alone or media plus IL-7 at ng/mL, 10ng/mL or 25ng/mL. Prior to stimulation and at 3, 12 and 24 hours following stimulation, an aliquot of these cells were stained with PE conjugated anti-CD127 (clone R34.34) antibodies and CD127 expression (MFI) was examined by flow cytometry. The dose and time curves for (A) CD127WT, (B) I356C, (C) insNPC and (D) T244I cell lines shows the mean MFI normalized to the MFI of media controls at each time point for each concentration. The mean is of n=4 experiments with +/- SEM.

A

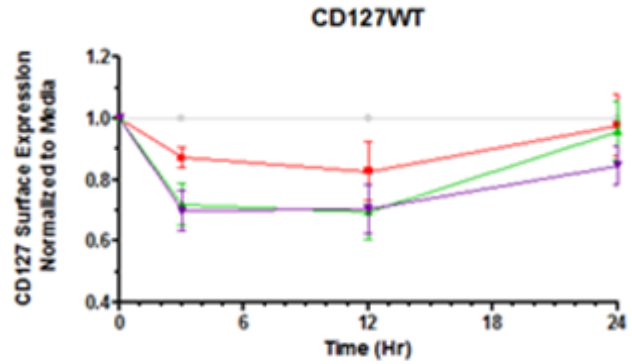
CD127WT
CD127 Surface Expression Normalized to Media
1.2
1.0
0.8
0.6
0.4
0
6
12
18
24
Time (Hr)

B

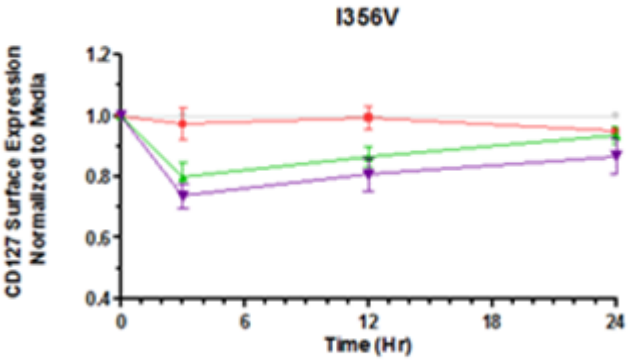
I356V
CD127 Surface Expression Normalized to Media
1.2
1.0
0.8
0.6
0.4
0
6
12
18
24
Time (Hr)

C

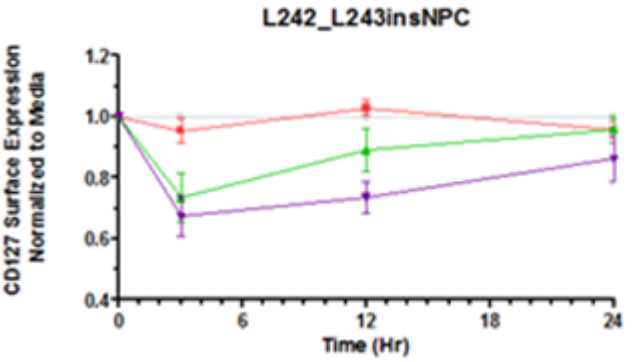
L242_L243insNPC
CD127 Surface Expression Normalized to Media
1.2
1.0
0.8
0.6
0.4
0
6
12
18
24
Time (Hr)

D

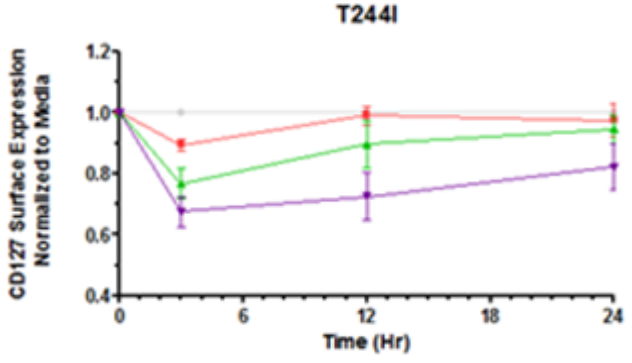
T244I
CD127 Surface Expression Normalized to Media
1.2
1.0
0.8
0.6
0.4
0
6
12
18
24
Time (Hr)

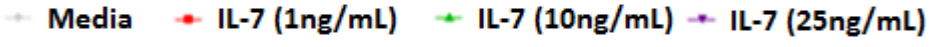
Media
IL-7 (1ng/mL)
IL-7 (10ng/mL)
IL-7 (25ng/mL)

in the CD127WT cell line. At high IL-7 concentration (25ng/mL), CD127 down-regulation in the T244I cell line is very similar to the down-regulation seen in the CD127WT cell line.

3.5 Examining the established mutant cell lines for altered IL-7 signal transduction

3.5.1 In IL-7 stimulated cell lines, pSTAT5 cannot be detected above background signal

As mentioned above, I wanted to see if the disease associated mutations in CD127 would result in altered signal transduction. To measure altered signal transduction, I decided to examine the phosphorylation level of STAT5. This measure of signal transduction has been used in multiple cell lines and in primary T-cells. To measure pSTAT5 levels, I cultured the MOCK, CD127WT, P132S, I356V, insNPC and T244I Jurkat cell lines for 15 minutes in complete media alone, complete media plus IL-7 (10ng/mL), or complete media plus IFNα (125ng/mL) as a positive control. After culturing the cells in various conditions, I fixed and permeabilized the cells and then stained the cells with Alexa Fluor® 488 conjugated anti-phospho-STAT5 antibodies. These cells were then examined using flow cytometry to detect changes in pSTAT5 expression levels.

Our lab has previously detected IL-7 signal transduction by measuring the level of pSTAT5 in primary human $CD8^+$ T-cells stimulated with 10ng/mL of IL-7 [10, 13]. As such, I felt that this concentration of IL-7 would be appropriate to stimulate the cell lines in order to observe signal transduction. As shown above, 10ng/mL of IL-7 was also able to down-regulate surface CD127expression in the CD127WT, I356V, insNPC and T244I cell lines suggesting that the cell lines were responsive to IL-7 at this concentration.

IFNα has also been shown to cause signal transduction in Jurkat cells resulting in phosphorylation of STAT5 [59]. As such, I decided to stimulate the cell lines with IFNα (125ng/mL) as a positive control for pSTAT5 expression.

Figure 17 shows that in all six cell lines IFNα stimulation caused only a slight increase in pSTAT5 expression above the media control. In all six cells line stimulated with IL-7 (10ng/mL) there was no increase in pSTAT5 expression levels above media control. This suggests that in these cell lines, pSTAT5 expression is already high and IL-7 stimulation cannot increase the expression of pSTAT5 above basal levels.

Figure 17: pSTAT5 cannot be detected above background in the CD127 expressing cell lines when stimulated with IL-7 (10ng/mL).

MOCK, CD127WT, P132S, I346V, insNPC and T244I Jurkat cell lines were cultured in RPMI-10. The cell lines were stimulated with IFNα (125ng/mL) or IL-7 (10ng/mL) for 15 minutes. Cells were also left in media alone as a control. Cells were then fixed, permeabilized and stained with anti-pSTAT5 antibody conjugated to Alexa Fluor 488. Cells were analyzed for pSTAT5 expression using flow cytometry. Voltages were set on cells in media alone and shifts in pSTAT5 represent increases in pSTAT5 expression above basal levels of pSTAT5. IFNα was used as a positive control for inducing pSTAT5 expression in Jurkat cells.

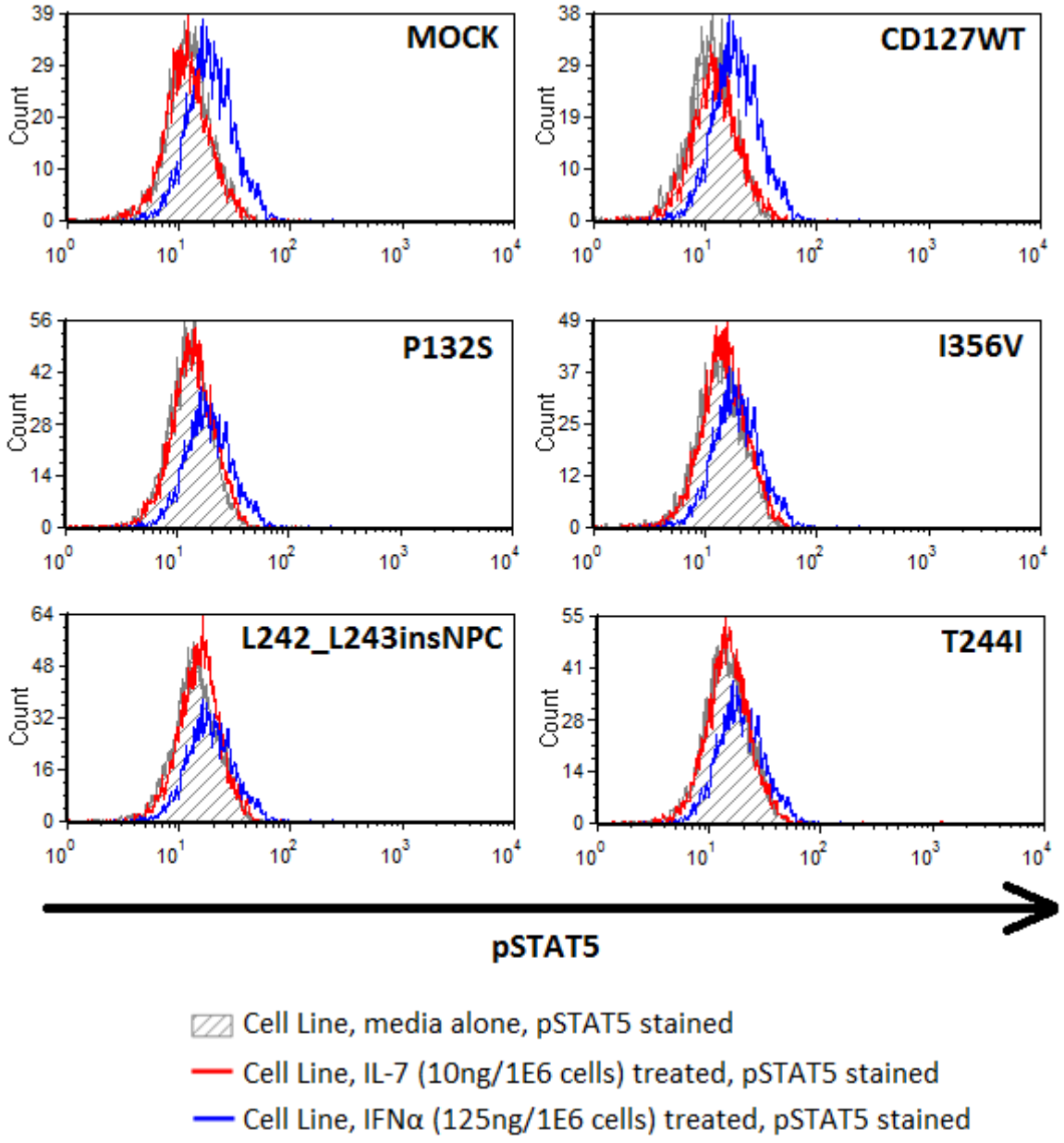
MOCK
CD127WT
P132S
I356V
L242_L243insNPC
T244I
Count
pSTAT5
Cell Line, media alone, pSTAT5 stained
Cell Line, IL-7 (10ng/1E6 cells) treated, pSTAT5 stained
Cell Line, IFNα (125ng/1E6 cells) treated, pSTAT5 stained

CHAPTER 4: DISCUSSION

4.1 Development of an *in vitro* model to study the effect that disease specific mutations have on CD127 expression, regulation and signal transduction

To address the hypothesis of whether disease associated mutations in CD127 cause aberrant IL-7 signaling and CD127 expression and regulation, I developed *in vitro* T-cell models using Jurkat cells and introduced the express of wild type CD127, or CD127 carrying the following mutations: P132S, I356V, L242_L243insNPC and T244I.

The cell line chosen as the basis for this model had to satisfy a set of criteria. The cell line had to express high endogenous levels of surface CD132, so that the complete IL7R could form with the introduced wild type or mutant CD127 protein. From the four lymphoblastic cell lines (A3, CEM, Jurkat and SupT1) examined, my data show that all four cell lines express levels of CD132 that were comparable to the high surface expression seen on primary human $CD8^+$ T-cells. Next, the cell line had to express low endogenous levels of surface CD127, thereby allowing us to study the expression and regulation of the introduced wild type or mutant CD127 protein with little interference from endogenous CD127 protein. From the four cell lines examined, my data show that SupT1 cells express high levels of CD127 (MFI ~25) compared to the other three cells lines which express low levels of endogenous CD127 (MFI less than 10). Patel *et al.* made similar observations and found that SupT1 cells expressed high levels of endogenous CD127, while Jurkat cells expressed low levels of endogenous CD127 [62]. Due to the high expression level of CD127 on SupT1 cells, these cells were deemed inappropriate for the T-cell model. Next, I reviewed the available literature for CEM, Jurkat and A3 cells to determine if these cells were susceptible to G418 mediated cell death. The susceptibility to G418 sulfate was essential because G418 sulfate was to be used in selecting cells that stably expressed wild type or

mutant CD127 protein. From the literature available I learned that A3 cells are a derivative of the Jurkat cell line that are susceptible to Fas mediated cell death [57]. The A3 cell line was isolated using G418 sulfate selection, as such A3 cells are resistant to G418 sulfate mediated cell death [57]. Jurkat and CEM cells contain no neomycin resistance gene [64]. Based on this information, I continued to examine the Jurkat and CEM cell lines. Next, the cell line had to have endogenous STAT5. Previous studies in primary human $CD8^+$ T-cells have measured changes in the level of phosphorylated STAT5 as a means of studying IL-7 signaling [10, 13, 34]. My data show that both CEM and Jurkat cells both express endogenous STAT5. Thus both of these cell lines could potentially be used in my T-cell model. Since I was to going to be developing six stable cell lines and selecting for them using G418 sulfate, I wanted the cell line in my model to be easy to culture and for the cell population to double quickly, thus allowing for rapid expression of induced proteins and faster selection of stable cell. Qualitative observations I made while culturing the cell lines indicated that CEM cells were difficult to culture and doubled slowly, as such I decided not to use them in my model. Thus from the four lymphoblastic cell lines examined, Jurkat cells were determined to be the best option for my T-cell model. My data also indicated that Jurkat cells did not phosphorylate STAT5 in response to IL-7. Our lab has previously, used 10ng/mL of IL-7 to observe phosphorylation of STAT5 in T-cells; as such I decided that this concentration would be appropriate to observe signaling effects in Jurkat cells [10]. The lack of response to IL-7 was most probably due to the fact that Jurkat cells expressed such low levels of CD127 that the complete IL7R could not be formed and hence there was no signal transduction. The lack of response to IL-7 was also determined to be of benefit because there would presumably be no endogenous STAT5 signaling that would mask or skew the

potential signaling affects that could be observed in the IL-7 stimulated cell lines that expressed wild type or mutant CD127 protein. While the observation above indicates that Jurkat cells do not phosphorylate STAT5 in response to IL-7, there is evidence that STAT5 can be phosphorylated in Jurkat cells when stimulated with other reagents like IFNα or Gas6 [59, 65]. Other cellular components of the IL-7 signaling pathway like JAK-1 and JAK-3 were previously found in Jurkat cells [66, 67]. Together this all suggests that Jurkat cells engineered to express wild type or mutant CD127 protein could potentially form the IL7R in response to IL-7 and transduce a signal that could be measured by STAT5 phosphorylation.

After choosing to build my T-cell models using Jurkat cells, my next step was to introduce the expression of CD127 or mutant CD127 proteins into these cells. Originally, I tried to transfect Jurkat cells using a eukaryotic expression vector, pCMV6-CD127, which contained wild type CD127 cDNA. The expression of CD127 was constitutively driven from a CMV promoter on the pCMV6-CD127 plasmid. This plasmid also contained the neomycin resistance gene that could be used to select for transfected cells using G418 sulfate. As shown in appendix II.C, when using this approach, the expression of surface CD127 protein was modestly increased in Jurkat cells over the endogenous surface CD127 level. Expression of the introduced CD127 and/or neomycin resistance genes was also transient, as a stable cell line that expressed wild type CD127 could not be selected in Jurkat cells using complete media supplemented with G418 sulfate. This transfection and selection approach may have failed because the neomycin resistance gene may not have integrated into the genome of Jurkat cells. It is also possible that no part of the plasmid integrated into the genome and that the transient expression of CD127 protein observed was translated from the plasmid itself.

In view of the many issues and lack of success in the transfection and selection approach using the pCMV6-CD127 vector, I proceeded to use a lentiviral system to introduce the expression of wild type or mutant CD127 genes in Jurkat cells. Transduction and integration of a gene of interest using a lentivirus is known to be more efficient than the transfection and selection approach. Alves *et al.* have previously used a lentivirus to produce a Jurkat cell line that stably expressed wild type CD127; this reaffirms that the lentiviral system would be a good option for inducing expression of wild type or mutant CD127 in Jurkat cells [68]. The lentiviral system that I used was a 2nd generation system that included an envelope, packaging and transfer vector. The transfer vector originally obtained from Dr. Anurag Tandon, pWPI/hPLK2WT/Neo, contained the wild type human polo-like kinase 2 (hPLK2WT) gene downstream of an elongation factor-1 alpha (EF-1α) promoter. The EF-1α promoter drives constitutive expression of the gene of interest. Studies comparing EF-1α to the CMV promoter have found the EF-1α promoter is better suited to producing cell lines that stably expressed the gene of interest over a long period of time because as time progresses the activity of the CMV promoter becomes silenced [69]. The EF-1α promoter was also found to induce expression of the gene of interest with greater efficiency than the CMV promoter [69]. The transfer vector also has an internal ribosomal entry site (IRES) element from an encephalomycocarditis virus (EMCV) downstream of the gene of interest. The IRES allows for the translation of the neomycin resistance gene simultaneously from the same transcript as the gene of interest, thus ensuring selected cells express the gene under study [70]. As such, I rationalized that cells transduced with the CD127 gene from this transfer vector would produce high levels of exogenous CD127, the expression would be

sustained long term and the cells expressing CD127 could also be selected using G418 sulfate.

In making my lentiviruses, I successfully removed the hPLK2WT gene from pWPI/hPLK2WT/Neo to make the mock transfer vector, pWPI/MOCK/Neo; and incorporated the wild type CD127 cDNA in place of the hPLK2WT fragment to make the transfer vector, pWPI/CD127WT/Neo. The cloning techniques I used were optimized by Zhang *et al.* [71]. The four mutant CD127 transfer vectors (pWPI/P132S/Neo, pWPI/I356V/Neo, pWPI/L242_L243insNPC/Neo and PWPI/T244I/Neo) were successfully made using an SDM kit to make point mutations or insert nucleotides into the CD127 gene of the pWPI/CD127WT/Neo plasmid. Six different lentiviruses were then made using these transfer vectors and the envelope and packaging vector. The Lenti-X^{TM} GoStix^{TM} from Clontech, Inc. were used to visually confirm that lentivirus were made and that at least 5E5 infectious units of virus were present per mL of media. Jurkat cells were infected with concentrated lentiviruses and the cells that stably expressed the wild type or mutant CD127 proteins were selected using G418 sulfate.

The stable cell lines were examined for expression of CD127 by western blot. Figure 11 shows that the untransduced, mock, wild type and mutant CD127 cell lines all produced CD127 protein. The CD127 protein detected was of the same size as the recombinant human CD127-Fc chimera, which had a molecular mass ~75kDa. The exogenous wild type and mutant CD127 proteins expressed in the stable cell lines also contain a DDK-tag on the C-terminus of the protein; thus allowing us to only detect the exogenous CD127 by western blot. The blot probing for DDK-tagged proteins in figure 11 shows that the wild type and mutant cell lines do produce the exogenous CD127 protein, while there are no observable

bands in the lanes from untransduced and mock transduced Jurkat cells, as was expected since these cell lines were not transduced with a DDK tagged CD127 gene. Together this suggests that the stable cell lines were successfully established using the lentiviral approach. In the anti-DDK blot, the lack of bands in the lanes containing lysates from untransduced and mock transduced Jurkat cells indicates that the faint bands seen in these lanes from the anti-CD127 probed blot represent endogenous CD127 protein. In the anti-DDK probed blot, two bands are observed at around 75kDa from the lanes containing lysates from Jurkat cells transduced with wild type, I356V, L242_L243insNPC and T244I mutated CD127. The observed double bands could possibly be due to differences in the extent of glycosylation; where the upper band is glycosylated and the lower band is unglycosylated or less glycosylated. Multiple bands due to glycosylation differences in CD127 have been previously reported in cell lines transfected with murine CD127 [4]. Alternatively, the double bands observed could represent membrane and soluble isoforms of CD127, where the upper band is membrane bound CD127 protein while the lower band is soluble CD127 protein. Interestingly, in the anti-DKK probed blot there is only the lower band in the lane containing lysates from Jurkat cells transduced with P132S mutated CD127. This lower band could mean that P132S mutated CD127 is not glycosylated or is mostly of the soluble CD127 isoform. Considering that this mutation is in the extracellular region, it may be affecting the six glycosylation sites in the extracellular region from becoming glycosylated post-translationally [28]. Roifman *et al.* also observed the same band pattern for P132S and wild type CD127 protein as found here [41].

4.2 Wild type and CD127 proteins containing the I356V, L242 L243insNPC and T244I mutations are all expressed on the cell surface while P132S could not be detected by flow cytometry

Once I established that the wild type and the four mutant CD127 cell lines produce CD127 protein, I next wanted to know whether CD127 surface expression was altered by the mutations. My flow data in figure 12 suggest that the I356V, L242_L243insNPC and T244I mutated CD127 proteins are expressed on the surface of the cell and that these mutants are expressed at relatively the same level as wild type CD127 protein.

Interestingly, I could not detect P132S mutated CD127 on the cell surface above background endogenous CD127. This mutation may be causing conformational changes to the CD127 extracellular domain [28]. As such monoclonal antibodies may not be able to detect the epitope on the P132S mutated CD127. Alternatively, this mutation may also be causing CD127 not to be expressed on the surface and remain intracellular or become degraded due to structural instability. To test whether the protein is intracellular, I performed an intracellular and surface stain on the CD127WT and P132S cell lines using the same polyclonal anti-CD127 used in the western blot analysis. The data show that in the CD127WT cell line, CD127 protein can be detected using the polyclonal anti-CD127 both on the surface and intracellularly; however the P132S mutated CD127 protein cannot be detect either on the surface or intracellularly (figure 13 and 14). P132S mutated CD127 was also not detect using two other monoclonal anti-CD127 antibodies (figure 13). The fact that the P132S mutated CD127 could be detected by the polyclonal antibody by western blot but not by flow cytometry suggests that in the unreduced, non-denatured native state, the P132S mutated CD127 is conformationally altered in such a manner that the epitope which anti-

CD127 monoclonal and polyclonal antibodies binds to is hidden or that the binding to the epitope is prevented. While P132S mutated CD127 is most likely conformationally altered, the question still remains whether the P132S mutated CD127 protein is expressed on the surface or not. One possible experiment to answer this question would be to biotin label the surface of the cell and isolate all surface proteins, and then run the western blot probing for CD127 on the isolated biotin labeled surface proteins and the remaining non labeled proteins. This western blot would show whether P132S mutated CD127 is expressed on the surface or intracellularly. Interestingly, Roifman *et al.* did not examine whether P132S mutated CD127 is expressed on the surface; instead they showed that radioisotope labeled IL-7 binds at very low levels to cells with the P132S mutated CD127 protein compared to cells that express wild type CD127 protein [41]. Roifman *et al.* interpretation of their data was that the P132S mutation is causing reduced binding affinity of IL-7 to CD127 [41]. Since they did not confirm the surface expression of P132S mutated CD127 protein, I feel that Roifman *et al.* interpretations on the effect of the P132S mutation in CD127 to be unjustified and that the proposed western would either support or refute their interpretation.

4.3 CD127 cell lines express mRNA transcripts encoding the full length and soluble CD127 isoforms and there is no difference in the relative level of the transcript encoding soluble CD127 between the mutants and wild type CD127

There have been reports that the T244I mutation increases the incidence of alternative splicing during transcription of the CD127 gene. These reports indicate that the T244I mutation causes a two-fold increase in the level of transcripts encoding soluble CD127 compared to membrane bound CD127 [48, 56, 72]. As such, I was curious as to whether I would observe similar results in my T-cell model. A significant limitation to

addressing that question here is that cell lines contain the cDNA of wild type or mutant CD127 and as such there are no introns present within the CD127 trans-gene. Thus the traditional view of alternative splicing occurring between donor and acceptor site in the introns does not occur. Nevertheless, I proceeded to examine the relative expression of transcripts encoding soluble CD127 and total CD127 (figure 15A) using the previously established forward and reverse primers (Table 2) for sCD127 and total CD127 transcripts. The reason I proceeded to examine the transcript levels considering the limitations of my T-cell models was because an analysis of the CD127 cDNA revealed donor and acceptor splice sequences in the exons (Appendix V), which suggests splicing could still occur. There is also evidence in literature that shows that alternative splicing can occur in mRNA transcribed from cDNA that is retroviral transduced into cell lines [61, 73]. Interestingly, I found that all the cell lines examined produced transcripts encoding soluble CD127 (figure 15A), suggesting that alternative splicing is occurring within the transcribed pre-mRNA from the CD127 cDNA. My data also suggest that there is no significant difference in the level of soluble CD127 transcripts in each mutant CD127 expressing cell line compared to the wild type CD127 expressing cell line. However, due to the limitations of my T-cell model I acknowledge that these results may not represent the alternative splicing observed in nature and thus may not be biologically significant. While I did not see the same two-fold increase in soluble CD127 in the T244I cell line compared to the CD127WT cell line, as Gregory *et al.* have seen, this does not mean that their data is wrong or misinterpreted. In fact, there is other evidence that suggests that the T244I mutation increases the level of soluble CD127 protein [56, 60, 72, 74].

4.4 Surface CD127 protein is down-regulated on the CD127WT cell line when stimulated with IL-7

Next, I was interested in determining whether any of the mutations in CD127 resulted in altered cell surface expression in response to IL-7 stimulation. To investigate this, cells expressing wild type CD127, I356V, L242_L243insNPC and T244I CD127 proteins were stimulated with 1, 10 and 25ng/mL of IL-7 and changes in CD127 expression were examined at time zero and at 3, 12 and 24 hours post stimulation. Here I did not study the down-regulation of P132S-CD127 because I was not able to detect surface expression of this protein by flow cytometry.

My data suggest that in the CD127WT cell line, CD127 expression is down-regulated in a dose and time dependent manner. The down-regulation of CD127 expression was maximal when cells were stimulated with 10ng/mL of IL-7 (figure 16A). CD127WT cells stimulated with 1ng/mL of IL-7 reached the maximal down-regulation by 12 hours and the surface CD127 returned to normal levels by 24 hours. CD127WT cells stimulated with 10 and 25ng/mL of IL-7 reached the maximal down-regulation by 3 hours and this down-regulation was sustained up to 12 hours. Between 12 and 24 hours, the CD127 expression levels increased back or close to the basal level (figure 16A). This initial dose response seen at early time point is comparable to what was observed in primary human $CD8^+$ T-cells [34].

Our lab has previously shown that in primary human $CD8^+$ T-cells stimulated with IL-7, surface CD127 protein is down-regulated from the surface and then degraded, and that transcription of CD127 mRNA is also independently down-regulated [34]. The degradation of CD127 was shown to be dependent on JAK phosphorylating Y449 and marking the internalized CD127 protein for proteosomal degradation [34]. The transcriptional down-

regulation of CD127 mRNA together with the degradation of surface CD127 protein is the reason the expression of CD127 does not return to basal levels after IL-7 stimulation in primary human $CD8^+$ T-cells [34]. While in this experiment I am able to observe the down-regulation of surface CD127 in response to IL-7, I am not able to determine whether CD127 is degraded. While the surface CD127 that is down-regulated may be degraded, the increase back to basal levels observed at 24 hours may be do the constitutive production of CD127 that is driven by transcription from the EF-1α promoter. On the other hand, if the down-regulated surface CD127 is not degraded, the increase back to basal levels could also be partly due to CD127 returning to the cell surface over time if it has not been phosphorylated in the Jurkat cells. One experiment to check if the down-regulated CD127 is degraded would be to treat the CD127WT cell line with a protein synthesis inhibitor, cycloheximide (CHX), and stimulate the cells with IL-7; then lyse the cell 24 hours later and run a western blot probing for CD127. Cycloheximide should prevent new CD127 from being produced and if the CD127 is degraded after IL-7 stimulation you should see less CD127 on the western blot. One way to make this T-cell model better suited to studying CD127 down-regulation in response to IL-7 would be to replace the EF-1α promoter with the wild type IL-7 promoter found in T-cells; thereby restoring the mechanism that down-regulates CD127 transcription.

4.5 Surface CD127 protein is down-regulated on I356V, insNPC and T244I cell lines when stimulated with high doses (>10ng/mL) of IL-7

With regards to the down-regulation of surface CD127 observed in the I356V, insNPC and T244I cell lines, I find it very interesting that at the low IL-7 concentration (1ng/mL) the cells do not down-regulate CD127 to the same extent as seen in the CD127WT cell line. The very small level of CD127 down-regulation that does occur when the mutant

cell lines were stimulated with 1ng/mL of IL-7 is very short lived. Interestingly, high doses of IL-7 (10 and 25ng/mL) are required to observe down-regulation of surface CD127 in these cell lines. Together this suggests that there is a threshold level of IL-7 needed to induce down-regulation on CD127 and that these mutations are increasing the threshold.

Our lab has previously shown that the threshold level of IL-7 needed to down-regulate surface CD127 on primary human $CD8^+$ T-cells was 100pg/mL of IL-7 [34]. Since the binding affinity between IL-7 and the receptor is very strong (K_d=40pM), then very few molecules of IL-7 may be needed to come in contact with the IL7R before one molecule remains bound and down-stream effects can be observed [1]. Conversely, if these mutations are altering the structure of the CD127, then the binding affinity of CD127 to IL-7 may also be lowered. If the affinity is lowered then more molecules of IL-7 would be required to come in contact with the receptor before any downstream effects could be observed; hence a higher threshold of IL-7 needed to induce down-regulation of surface CD127. In future experiments, we can use radioisotope labeled IL-7 to measure the differences in binding affinity between IL-7 and the wild type CD127 or the mutant CD127 proteins. This experiment would help confirm the hypothesis that binding affinities are affected by the mutations. This experiment would also provide evidence to the correlation that lower binding affinity means more IL-7 is required to induce down-regulation. While in these mutant cell lines, a high level of IL-7 is needed to induce down-regulation of CD127, it still remains possible that at low doses (1ng/mL) of IL-7 the cell is signaling. In primary $CD8^+$ T-cells stimulated with 1ng/mL of IL-7, our lab has previously observed increases in cell proliferation, STAT5 phosphorylation and Bcl-2 levels [10]. Since CD127 remains on the cell surface of these mutant CD127 cell lines after IL-7 stimulation (1ng/mL) it is possible

that IL-7 signaling could be prolonged or even constitutive; leading to greater proliferation and anti-apoptotic affects. To show that this is the case, future experiments will require the wild type and mutant CD127 cell lines to be stimulated with 1ng/mL of IL-7 then examined for IL-7 signaling by measuring pSTAT5 levels over time. If the mutant CD127 cell lines induce phosphorylation of STAT5 and maintain the pSTAT5 level over time and the surface expression is not down-regulated, while the wild type CD127 cell line only temporarily induces pSTAT5 expression and down-regulates CD127 from the surface we could then conclude that mutations to CD127 cause constitutive or prolonged IL-7 signaling in response to low doses.

4.6 The established cell lines had high basal levels of pSTAT5 and thus IL-7 signaling could not be measured by flow cytometry

To examine the effects that these CD127 mutations have on IL-7 signaling, I stimulated the cells with IL-7 (10ng/mL) and examined them by flow cytometry for altered pSTAT5 expression (figure 17). I also treated the cells with IFNα (125ng/mL), which has also been reported to induce pSTAT5 expression in Jurkat cells (figure 17).

The results in this experiment were inconclusive because there was a high level of pSTAT5 expression in the all of the established cell lines cultured in media alone (figure 17). The affect IL-7 has on inducing pSTAT5 expression could not be observed above the background level; while IFNα only modestly increased pSTAT5 expression above background (figure 17). In this experiment it is possible that something in the serum of the media caused the cells to phosphorylate STAT5. In future experiments, the cell lines could be first cultured for a few hours in serum free media to reset all the signaling pathways and sync the cell population.

The result in figure 17 is interesting because my original examination of pSTAT5 levels in the untransduced Jurkat cell line (figure 10) indicated that Jurkat cells incubated with media alone or with media supplemented with IL-7 do not phosphorylate STAT5. It is quite possible that the process of transducing trans-genes into Jurkat cells has altered the cell in such a manner that STAT5 is constitutively phosphorylated or phosphorylated to a greater degree than previous basal levels. Alternatively, the addition of G418 sulfate in the media may be causing the cells to phosphorylate STAT5 via an unknown mechanism. As mentioned above, in future experiments the cells could be cultured in serum free and G418 sulfate free media before measuring pSTAT5 levels. To determine whether the transduction of trans-genes into the Jurkat cells is causing higher basal levels of pSTAT5 in future experiments an untransduced Jurkat cells should also be examined as a control.

Alternatively, if pSTAT5 cannot be measured changes in Bcl-2 expression could be examined. Since Bcl-2 expression is a down-stream effect of IL-7 signaling, we could infer how signaling is affected by these mutations, by measuring the differences in Bcl-2 expression. I would not advise measuring proliferative changes because the mutant CD127 cell lines are already proliferating at an accelerated rate and so differences in proliferation caused by aberrant IL-7 signaling would be masked. To determine how the CD127 mutations affect IL-7 signaling we could also measure the phosphorylation of JAK in response to IL-7.

Since we could not measure CD127 signaling in response to IL-7, I would not make any conclusions as to whether the P132S mutation results in reduced IL-7 signaling or whether the T244I and I356V mutations result in constitutive or enhanced signaling. The

L242_L243insNPC mutation in CD127 has been well shown to cause constitutive, IL-7 independent signaling in multiple models [45, 46].

CHAPTER 5: CONCLUSION

One of my main objectives in this project was to develop an *in vitro* T-cell model that expressed wild type or one of four disease associated mutant CD127 proteins. To this end, I was successful in developing five stable cell lines expressing wild type CD127, P132S mutated CD127, I356V, L242_L243insNPC and T244I mutated CD127 proteins.

In examining these cell line, I have found that these cells produce these mutant CD127 proteins. I have been able to detect all the mutant CD127 proteins on the surface of the cells except for P132S CD127. An additional experiment is required to determine whether P132S CD127 is expressed on the surface; this experiment is essential for us to understand how the P132S mutation leads to the SCID phenotype.

Several researchers have suggested that the T244I mutation results in increased sCD127 protein and that this increase in sCD127 results in the IL-7 signaling being potentiated leading to autoimmunity. The fact that T244I mutated CD127 is highly expressed on the cell surface is notable because it allows for the possibility that the T244I mutated membrane bound CD127 protein may cause enhanced IL-7 signaling similar to the constitutive signaling observed in T-ALL cells with the L242_L243insNPC mutation in CD127.

Although, there are limitations with my T-cell model that prevent me from examining CD127 regulation at the transcriptional level, I was able to observe some interesting surface CD127 down-regulation affects in the I356V, insNPC and T244I cell lines. The data from these experiments suggested that leukemia and autoimmune associated mutations may reduce the effect of IL-7 in down-regulating surface CD127. I would speculate that the sustained expression of CD127 in the I356V, insNPC and T244I cell lines stimulated with IL-7 could contribute to enhanced or constitutive IL-7 signaling.

Unfourtunately, I was not able to successful study the effect these mutations have on signaling. Future experiments I have suggested may be used to explore any signaling affects these mutations may cause. These future experiments would be very useful in confirming that the sustained CD127 expression on the IL-7 stimulated I356V, insNPC and T244I cell lines does lead to enhanced signaling.

In studying these four disease specific mutations, my hope was to provide additional insights into how these CD127 mutations affect receptor expression, regulation and signaling; and by gathering these insights our knowledge of these diseases may be expanded. To this end, I have contributed some new information as to the effect these mutations have on CD127, identified areas of our knowledge that are lacking and possibly misinterpreted, and developed a *in vitro* system that could be used to further advance our knowledge as to how the P132S, I356V, L242_L243insNPC and T244I mutations in CD127 affect T-cell biology.

REFERENCES

1. Jiang, Q., et al. (2006). Cell biology of IL-7, a key lymphotrophin. *Cytokine & Growth Factors Reviews, 16*: 513-533

2. Tal, N., et al. (2013). Interleukin 7 and thymic stromal lymphopoietin: from immunity to leukemia. *Cell. Mol. Life Sci., 71*(3): 365-378

3. Alpdogan, O., et al. (2005). IL-7 and IL-15: therapeutic cytokines for immunodeficiency. *TRENDS in Immunol., 26*(1): 56-64

4. Goodwin, R.G., et al. (1990). Cloning of the Human and Murine Interleukin-7 Receptors: Demonstration of a Soluble Form and Homology to a New Receptor Superfamily. *Cell, 60*: 941-951

5. Alves, N.L., et al. (2006). Common γ chain cytokines: Dissidence in the details. *Immunology Letters, 108*: 113-120

6. Peschon, J.J., et al. (1994). Early Lymphocyte Expansion Is Severely Impaired in Interleukin 7 Receptor-deficient Mice. *J. Exp. Med., 180*: 1955-1960

7. Iwanami, N., et al. (2011). Genetic Evidence for an Evolutionary Conserved Role of IL-7 Signaling in T Cell Development of Zebrafish. *J. Immunol., 186*: 1-7

8. Chaiken, I.M., & Williams, W.V. (1996). Identifying structure-function relationships in four-helix bundle cytokines: towards *de novo* mimetics design. *TIBTECH Rev., 14*: 369-375

9. Fry, T.J., et al. (2001). A potential role for interleukin-7 in T-cell homeostasis. *Blood, 97*(10): 2983-2990

10. Crawley, A.M., et al. (2013). Jak/STAT and PI3K signaling pathways have both common and distinct roles in IL-7-mediated activities in human $CD8^+$ T cells. *J. Leukocyte Biol., 95*: 117-127

11. Welch, P.A., et al. (1989). Human IL-7: A Novel T Cell Growth Factor. *J. Immunol., 143*(11): 3562-3567

12. Armitage, R.J., et al. (1990). Regulation of Human T Cell Proliferation by IL-7. *J. Immunol., 144*(3): 938-941

13. Faller, E., et al. (2009). IL-7 and the HIV Tat protein act synergistically to down-regulate CD127 expression on CD8 T cells. *International Immunol., 21*(3): 203-216

14. Soares, M.V., et al. (1998). IL-7-dependent extrathymic expansion of CD45RA + T cells enables preservation of a naive repertoire. *J. Immunol., 161*(11): 5909-5917

15. Hernandez-Caselles, T., et al. (1995). Interleukin-7 Rescues Human Activated T Lymphocytes from Apoptosis Induced by Glucocorticoesteroids and Regulates bcl-2 and CD25 Expression. *Human Immunol., 43*: 181-189

16. Mullbacher, A., & Kos, F.J. (1992). Induction of primary anti-viral cytotoxic T cells by *in vitro* stimulation with short synthetic peptide and interleukin-7. *Eur. J. Immunol., 22*: 3183-3185

17. Smyth, M.J., et al. (1991). IL-& Regulation of Cytotoxic Lymphocytes: Pore-Forming Protein Gene Expression, Interferon-γ Production, and Cytotoxicity of Human Peripheral Blood Lymphocyte Subsets. *Cell. Immunol., 138*: 390-403

18. Jicha, D.L., Mulé, J.J., & Rosenberg, S.A. (1991). Interleukin 7 Generates Antitumor Cytotoxic T Lymphocytes against Murine Sarcomas with Efficacy in Cellular Adoptive Immunotheraphy. *J. Exp. Med., 174*: 1511-1515

19. Faller, E., et al. (2006). Interleukin-7 Receptor Expression on CD8 T-cells Is Downregulated by the HIV Tat Protein. *J. Acquir. Immune Defic. Syndr., 43*(3): 257-269

20. Cheng, L.E., et al. (2002). Enhancing signaling through the IL-2 receptor in $CD8^+$ T cells regulated by antigen recognition results in preferential proliferation and expansion of responding $CD8^+$ T cells rather than promotion of cell death. *Proc Natl Acad Sci U S A., 99*(5): 3003-3006

21. Mazzucchelli, R., & Durum, S.K. (2007). Interleukin-7 receptor expression: intelligent design. *Nat. Rev. Immunol., 7*: 144-154

22. Fry, T.J., & Mackall, C.L. (2005). The Many Faces of IL-7: From Lymphopoiesis to Peripheral T Cell Maintenance. *J. Immunol., 174*: 6571-6576

23. Bradley, L.M., et al. (2005). IL-7: maintaining T-cell memory and achieving homeostasis. *TRENDS in Immunol., 26*(3): 172-176

24. Boudil, A., et al. (2015). IL-7 coordinates proliferation, differentiation and *Tcra* recombination during thymocyte β-selection. *Nat. Immunol., 16*: 397-405

25. Pleiman, C.M., et al. (1991). Organization of the Murine and Human Interleukin-7 Receptor Genes: Two mRNAs Generated by Differential Splicing and Presence of Type I-Interferon-Inducible Promoter. *Mol. Cell. Biol., 11*(6): 3052-3059

26. Rose, T., et al. (2009). Identification and Biochemical Characterization of Human Plasma Soluble IL-7R: Lower Concentrations in HIV-1-Infected Patients. *J. Immun., 182*: 7389-7397

27. Walsh, S.T.R. (2010). A Biosensor Study Indicating That Entropy, Electrostatics, and Receptor Glycosylation Drive the Binding Interaction between Interleukin-7 and its Receptor. *Biochemistry, 49*(40): 8766-8778

28. McElroy, C.A., et al. (2009). Structural and Biophysical Studies of the Human IL-7/IL-7Rα Complex. *Structure, 17*(1): 54-65

29. Haan, C., et al. (2006). Jaks and cytokine receptors - An intimate relationship. *Biochemical Pharmacology, 72*:1538-1546

30. Sharfe, N., et al. (1995). JAK3 Protein Tyrosine Kinase Mediates Interleukin-7 - Induced Activation of Phosphatidylinositol-3' Kinase. *Blood, 86*(6): 2077-2085

31. Cuevas, B.D., et al. (2001). Tyrosine Phosphorylation of p85 Relieves Its Inhibitory Activity on Phosphatidylinositol 3-Kinase. *J. Bio. Chem., 276*(29): 27455-27461

32. McElroy, C.A., et al. (2012). Structural reorganization of the interleukin-7 signaling complex. *Proc Natl Acad Sci U S A., 109*(7): 2503-2508

33. Faller, E.M., et al. (2010). Soluble HIV Tat protein removes the IL-7 receptor alpha-chain from the surface of resting CD8 T cells and targets it for degradation. *J. Immunol., 185*(5): 2854-2866

34. Ghazawi, F.M., et al. (2013). IL-7 downregulates IL-7Rα expression in human CD8 T cells by two independent mechanisms. *Immunol., Cell Biol., 91*: 149-158

35. Ghazawi, F.M. (2013). Understanding the mechanisms by which interleukin (IL)-7 down-regulates expression of the IL-7 receptor alpha-chain (CD127) in human CD8 T cells. *PhD Thesis, University of Ottawa.*

36. MacPherson, P.A., et al. (2001). Interleukin-7 receptor expression on CD8(+) T cells is reduced in HIV infection and partially restored with effective antiretroviral therapy. *J. Acquir. Immune Defic. Syndr., 28*(5): 454-457

37. Mazzucchelli, R.I., et al. (2012). The human IL-7 receptor gene: Deletions, polymorphisms and mutations. *Seminars in Immunol., 24*: 225-230

38. Lundstrom, W., et al. (2012). IL-7 in Human Health and Disease. *Semin. Immunol., 24*(3): 218-224

39. Noguchi, M., et al. (1993). Interleukin-2 Receptor γ Chain Mutation Results in X-linked Severe Combined Immunodeficiency in Humans. *Cell, 73*: 147-157

40. Puel, A., et al. (1998). Defective IL7R expression in $T^{-}B^{+}NK^{+}$ severe combined immunodeficiency. *Nature Genetics, 20*: 394-397

41. Roifman, C.M., et al. (2000). A partial deficiency of interleukin-7Rα is sufficient to abrogate T-cell development and cause severe combined immunodeficiency. *Blood, 96*(8): 2803-2807

42. Buckley, R.H., et al. (1997). Human severe combined immunodeficiency: Genetics, phenotypic, and functional diversity in one hundred eight infants. *J. Pediatrics, 130*(3): 378-387

43. Kim, M.S., et al. (2013). Somatic mutation of IL7R exon 6 in acute leukemias and solid cancers. *Human Patholohy, 44*: 551-555

44. Silva, A., et al. (2011). IL-7 Contributes to the Progression of Human T-cell Acute Lymphoblastic Leukemias. *Cancer Res., 71*(14): 4780-4789.

45. Zenatti, P.P., et al. (2011). Oncogenic IL7R gain-of-function mutations in childhood T-cell acute lymphoblastic leukemia. *Nature Genetics, 43*(10): 932-939

46. Shochat, C., et al. (2011). Gain-of-function mutations in interleukin-7 receptor-α (IL7R) in childhood acute lymphoblastic leukemias. *J. Exp. Med., 208*(5): 901-908

47. Teutsch, S.M., et al. (2003). Identification of 11 novel and common single nucleotide polymorphisms in the interleukin-7 receptor-α gene and their associations with multiple sclerosis. *Eur. J. Human Genetics, 11*: 509-515

48. Gregory, S.G., et al. (2007). Interleukin 7 receptor α chain (IL7R) shows allelic and functional association with multiple sclerosis. *Nat. Genetics, 39*(9): 1083-1091

49. Zhang, Z., et al. (2005). Two gene encoding immune-regulatory molecules (LAG3 and IL7R) confer susceptibility to multiple sclerosis. *Gene and Immunity, 6*: 145-152

50. Broux, B., et al. (2010). Haplotype 4 of the multiple sclerosis-associated interleukin-7 receptor alpha gene influences the frequency of recent thymic emigrants. *Genes and Immunity, 11*: 326-333

51. Lundmark, F., et al, (2007). Variation in interleukin 7 receptor α chain (IL7R) influences risk of multiple sclerosis. *Nat. Genetics, 39*(9): 1108-1113

52. Zhang, R., et al. (2011). Association between the IL7R T244I polymorphism and multiple sclerosis: a meta-analysis. *Mol. Biol. Rep., 38*: 5079-5084

53. Booth, D.R., et al. (2005). Gene expression and genotyping studies implicate the interleukin 7 receptor in the pathogenesis of primary progressive multiple sclerosis. *J. Mol. Med., 83*: 822-830

54. Wang, X.S., et al. (2013). Interleukin-7 Receptor Single Nucleotide Polymorphism rs6897932 (C/T) and the Susceptibility to Systemic Lupus Erythematosus. *Inflammation, 37*(2): 1-6

55. Todd, J.A., et al. (2007). Robust associations of four new chromosome regions from genome-wide analyses of type 1 diabetes. *Nat. Genet., 39*(7): 857-864

56. Lundstrom, W., et al. (2013). Soluble IL7Rα potentiates IL-7 bioactivity and promotes autoimmunity. *Proc Natl Acad Sci U S A., 110*(19): E1761-E1770

57. Characteristics of A3 cells. (2014). ATCC website. <http://www.atcc.org/products/all/CRL-2570.aspx#characteristics>

58. Juzer, K. (2009). Transcriptional regulation of the CD127 gene in primary human CD8 T-cells. *M.Sc Thesis, University of Ottawa*

59. Osmond, R.I.W., et al. (2010). Development of cell-based assays for cytokine receptor signaling, using an AlphaScreen SureFire assay format. *Analytical Biochemistry, 403*: 94-101

60. Evsyukova, I., et al. (2012). Cleavage and polyadenylation specificity factor 1 (CPSF1) regulates alternative splicing of interleukin 7 receptor (IL7R) exon 6. *RNA, 19*(1): 103-115

61. Cmejlova, J., et al. (2003). Impact of splice-site mutations of the human MDR1 cDNA on its stability and expression following retroviral gene transfer. *Gene Therapy, 10*: 1061-1065

62. Patel, E. S., & Chang, L-J. (2012). Synergistic effects of interleukin-7 and pre-TCR signaling in human T cell development. *J. Biol. Chem., 287*(40):33826-33835

63. Characteristics of Jurkat E6.1 cells. (2014). ATCC website. < https://www.atcc.org/products/all/TIB-152.aspx?slp=1#characteristics>

64. Information sheets on cell lines deposited to NIH AIDS Reagent program. <https://www.aidsreagent.org/catalog_download_files/003_cell_lines.pdf>

65. Brandao, L. N., et al. (2013). Inhibition of MerTK increases chemosensitivity and decreases oncogenic potential in T-cell acute lymphoblastic leukemia. *Blood Cancer Journal, 3*(e101): 1-9

66. So, E-Y., et al. (2007). Ras/Erk pathway positively regulates Jak1/STAT6 activity and IL-4 gene expression in Jurkat cells. *Molecular Immunol., 44*(13): 3416-3426

67. Jahn, T., et al. (2007). Direct interaction between Kit and the interleukin-7 receptor. *Blood, 110*(6): 1840-1847

68. Alves, N.L., et al. (2008). Differential Regulation of Human IL-7 Receptor α Expression by IL-7 and TCR signaling. *Journal of Immunol., 108*(8): 501-5210

69. Teschendorf, C., et al. (2002). Comparison of the EF-1 alpha and the CMV promoter for engineering stable tumor cell lines using recombinant adeno-associated virus. *Anticancer Res., 22*(6A): 3325-3330

70. Martinez-Salas, E. (1999). Internal ribosome entry site biology and its use in expression vectors. *Current Opinion in Biotechnology, 10*: 458-464

71. Zhang, G., et al. (2012). Quantitative assessment on the cloning efficiencies of lentiviral transfer vectors with a unique clone site. *Scientific Reports, 2*(415): 1-8

72. Rane, L., et al. (2010). Alternative splicing of interleukin-7 (IL-7) and its interleukin-7 receptor alpha (IL-7Rα) in pheripheral blood from patients with multiple sclerosis (MS). *Journal of Neuroimmunology, 222*: 82-86

73. Online tool to predict splice site acceptor and donors <http://spliceport.cbcb.umd.edu/>

74. Kreft, K. L., et al. (2012). Decreased systemic IL-7 and soluble IL-7Rα in multiple sclerosis patients. *Genes and Immunity, 13*: 587-592

APPENDIX

I. Ethics approval and consent form from the Ottawa Hospital Research Ethics Board

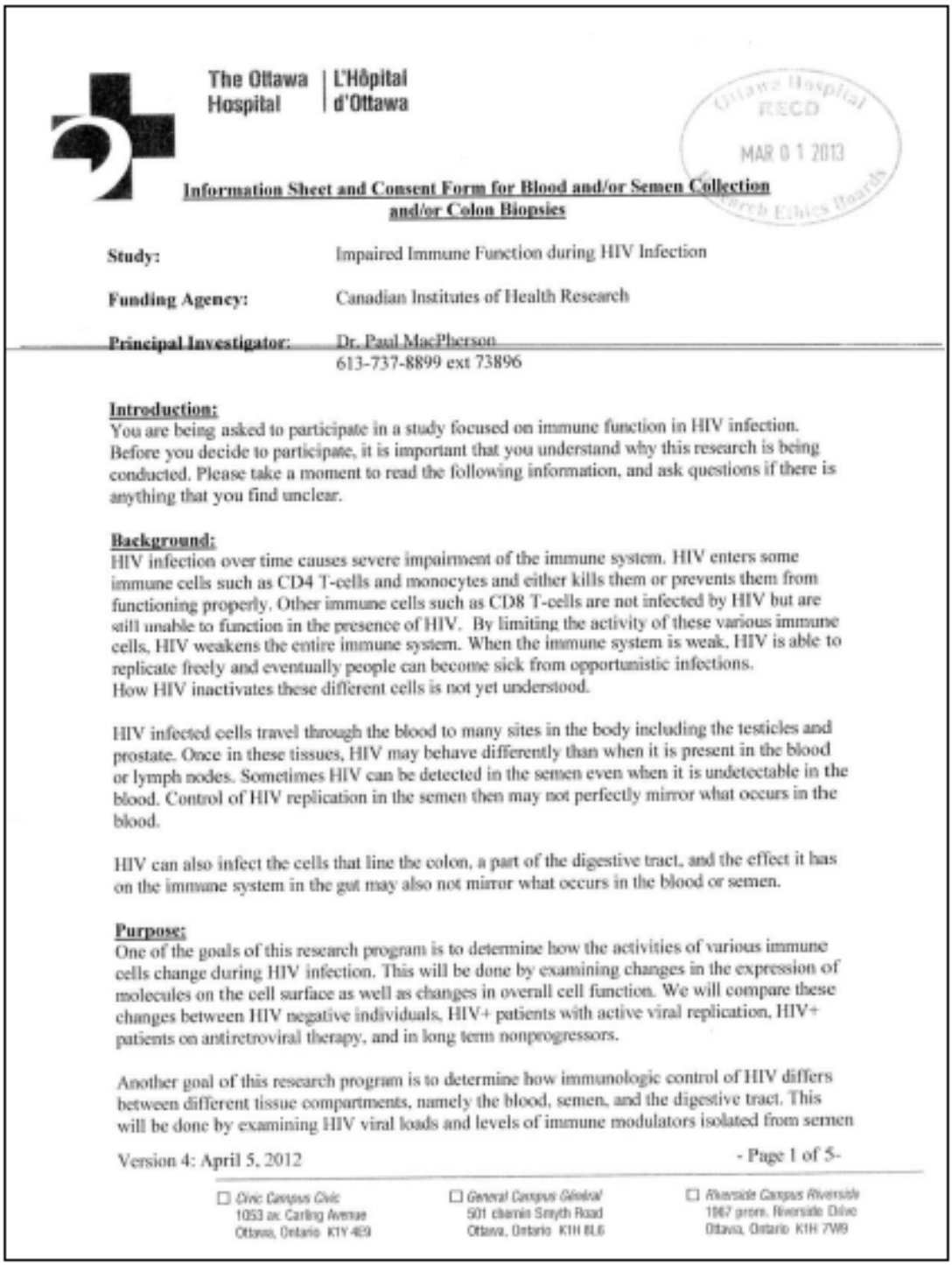

The Ottawa Hospital | L'Hôpital d'Ottawa

Ottawa Hospital RECD MAR 0 1 2013 Research Ethics Boards

Information Sheet and Consent Form for Blood and/or Semen Collection and/or Colon Biopsies

Study: Impaired Immune Function during HIV Infection

Funding Agency: Canadian Institutes of Health Research

Principal Investigator: Dr. Paul MacPherson
613-737-8899 ext 73896

Introduction:
You are being asked to participate in a study focused on immune function in HIV infection. Before you decide to participate, it is important that you understand why this research is being conducted. Please take a moment to read the following information, and ask questions if there is anything that you find unclear.

Background:
HIV infection over time causes severe impairment of the immune system. HIV enters some immune cells such as CD4 T-cells and monocytes and either kills them or prevents them from functioning properly. Other immune cells such as CD8 T-cells are not infected by HIV but are still unable to function in the presence of HIV. By limiting the activity of these various immune cells, HIV weakens the entire immune system. When the immune system is weak, HIV is able to replicate freely and eventually people can become sick from opportunistic infections. How HIV inactivates these different cells is not yet understood.

HIV infected cells travel through the blood to many sites in the body including the testicles and prostate. Once in these tissues, HIV may behave differently than when it is present in the blood or lymph nodes. Sometimes HIV can be detected in the semen even when it is undetectable in the blood. Control of HIV replication in the semen then may not perfectly mirror what occurs in the blood.

HIV can also infect the cells that line the colon, a part of the digestive tract, and the effect it has on the immune system in the gut may also not mirror what occurs in the blood or semen.

Purpose:
One of the goals of this research program is to determine how the activities of various immune cells change during HIV infection. This will be done by examining changes in the expression of molecules on the cell surface as well as changes in overall cell function. We will compare these changes between HIV negative individuals, HIV+ patients with active viral replication, HIV+ patients on antiretroviral therapy, and in long term nonprogressors.

Another goal of this research program is to determine how immunologic control of HIV differs between different tissue compartments, namely the blood, semen, and the digestive tract. This will be done by examining HIV viral loads and levels of immune modulators isolated from semen

Version 4: April 5, 2012 - Page 1 of 5-

☐ Civic Campus Civic
1053 av. Carling Avenue
Ottawa, Ontario K1Y 4E9

☐ General Campus Général
501 chemin Smyth Road
Ottawa, Ontario K1H 8L6

☐ Riverside Campus Riverside
1967 prom. Riverside Drive
Ottawa, Ontario K1H 7W9

or gut. Cells of the immune system involved in controlling HIV replication may also be isolated from semen or gut in order to examine their functional abilities.

Study Procedures:
Participants will be typically asked to provide a sample of either blood **or** semen **or** gut tissue. Participants who provide semen or gut samples may be also asked to provide blood.

Blood Samples:
Participants will be asked to donate samples of blood ranging from 10 ml, less than 1 tablespoon ~~(one tube) to a maximum of 200ml, approximately 14 tablespoon (less than one half the volume~~ drawn by Canadian Blood Services for routine blood donation; one unit = 500ml, approximately 33 tablespoon). White cells will be isolated from the blood and analyzed in the laboratory for changes in the expression of different molecules, and for immune activity. Serum may also be examined for molecules which regulate the activity of the immune cells.

Semen Samples:
Participants may be asked to donate semen samples. Sterile containers will be provided. Samples will be collected privately by the participant but must be delivered to the clinic within two hours.

Gut Samples:
During your colonoscopy procedure small biopsies of the colon wall will be performed in order to gather gut-associated lymphoid tissue. Approximately 30 tissue biopsies will be obtained, each consisting of about 0.3mm of tissue (9 mm total).

Duration:
Your participation will be complete once the blood and/or semen and/or gut tissue sample is obtained.

Risks:

Blood Samples:
The risks of participating in this study are those associated with routine blood drawing and may include minor pain at the site where blood is drawn and minimal bruising. Some people may experience temporary lightheadedness after drawing blood. If this occurs, you may be asked to rest in the clinic for a short period of time until the lightheadedness passes.

Semen Samples:
There are no risks associated with semen donation. Semen samples will only be used to determine HIV viral loads and for immunologic studies. Under no circumstances will the semen be available to achieve fertilization under any conditions.

Gut Samples:
During the procedure, you may feel pressure in the rectum similar to the sensation you feel with the urge to have a bowel movement. You may also feel a small amount of cramping in your abdomen as well. The most serious risk of the procedure is perforation, poking a hole in the

lining of the intestine, but it is extremely uncommon, occurring once out of every 10,000 procedures. If this occurs the attending physician will be responsible for treatment. Some bleeding will likely occur at the point where the biopsies were done. If you should experience severe discomfort during colon mucosa biopsy the procedure will be stopped immediately; you will be seen by the physician and the research nurse will monitor you until you are ready to go home.

Due to the possible bleeding following the procedure, the risk of transmitting HIV after the biopsy procedure may be increased.

Benefits:
Participation in this study will provide no direct benefits to you. It will, however, help to advance our understanding of how HIV inactivates the immune system and may lead to new strategies for the developement of immune based therapies to control HIV replication.

Voluntary Participation and Withdrawal:
You are under no obligation to participate in this study. If you choose to participate, you may change your mind at any time without providing a reason. You should inform the study doctor/study staff if you decide to withdraw so that your sample may be destroyed. You are not waiving your legal rights by agreeing to take part. Whether you choose to participate or not will have absolutely no effect on the medical care you receive, now or in the future.

Confidentiality:
All personal health information will be kept confidential, unless release is required by law. Representatives of the Ottawa Hospital Research Ethics Board, as well as the Ottawa Hospital Research Institute, may review your original medical records under the supervision of Dr. MacPherson's staff for audit purposes.

You will not be identifiable in any publications or presentations resulting from this study. No identifying information will leave the Ottawa Hospital.

The link between your name and the independent study number will only be accessible by Dr. MacPherson and/or his staff. The link and study files will be stored separately and securely. Both files will be kept for a period of 15 years after the study has been completed. All paper records will be stored in a locked file and/or office. All electronic records will be stored and protected by a user password, again only accessible by Dr. MacPherson and/or his staff. At the end of the retention period, all paper records will be disposed of in confidential waste or shredded, and all electronic records will be deleted.

Your chart will be used only to obtain CD4 counts, viral loads, and overall health status. Data will be compiled using a code. Your name will not be used and will not be known to laboratory personnel. The results of this study may be presented at meetings or in publications. Your identity will not be disclosed at any time in any of these presentations or publications.

Questions About The Study:

If during the course of this study you have questions concerning the study, you may contact the principle investigator Dr Paul MacPherson at 613-737-8899 ext 73896.

The Ottawa Hospital Research Ethics Board has approved this study. This committee considers the ethical aspects of all research projects involving people. If you have any questions about your rights with regard to participating in a research study, you may contact the Chair of the Ottawa Hospital Research Ethics Board at 613-798-5555, extension 14902. Do not sign the consent form unless you have had a chance to ask questions and have received satisfactory answers to all you questions. By signing the consent form you are not waiving your legal rights.

The Ottawa Hospital | L'Hôpital d'Ottawa

Consent Form
Impaired Immune Function during HIV Infection

Consent to Participate in Research

I understand that I am being asked to participate in a research study about immune function in HIV infection. This study has been explained to me.

I have read this, 5-page Participant Information Sheet and Consent Form (or have had this document read to me). All my questions have been answered to my satisfaction. If I decide at a later stage in the study that I would like to withdraw my consent, I may do so at any time.

I voluntarily agree to participate in this study and will provide a:

Please Initial:

_____Blood Sample

_____Semen Sample

_____Gut Sample

A copy of the signed Information Sheet and/or Consent Form will be provided to me.

Signatures

_____
Participant's Name (Please Print)

_____ _____
Participant's Signature Date

Investigator Statement (or Person Explaining the Consent)

I have carefully explained to the research participant the nature of the above research study. To the best of my knowledge, the research participant signing this consent form understands the nature, demands, risks and benefits involved in participating in this study. I acknowledge my responsibility for the care and well being of the above research participant, to respect the rights and wishes of the research participant, and to conduct the study according to applicable Good Clinical Practice guidelines and regulations.

_____
Name of Investigator/Delegate (Please Print)

_____ _____
Signature of Investigator/Delegate Date

Valid until MAR 2 8 2014

☐ *Civic Campus Civic*
1053 av. Carling Avenue
Ottawa, Ontario K1Y 4E9

☐ *General Campus Général*
501 chemin Smyth Road
Ottawa, Ontario K1H 8L6

☐ *Riverside Campus Riverside*
1967 prom. Riverside Drive
Ottawa, Ontario K1H 7W9

II. A Gene map of pCMV6-CD127

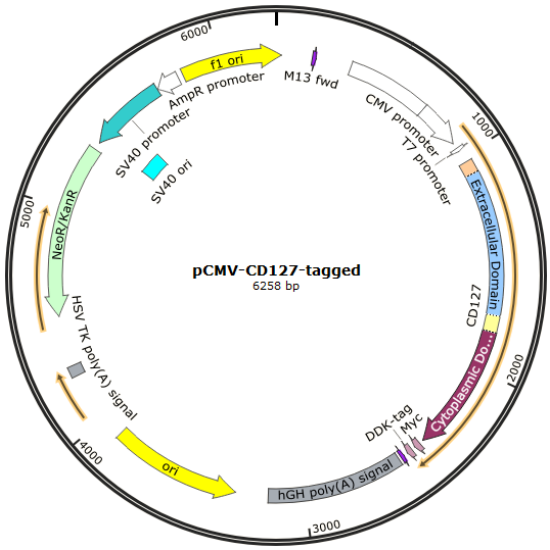

Schematic of pCMV6-CD127 gene map.

pCMV6-CD127 plasmid (Plasmid Clone # RC209687; OriGene USA; Rockville, MD). Expression of Human CD127 cDNA is driven from a CMV promoter. Neomycin resistance gene is driven from an SV40 promoter.

II. B Transfection and selection approach

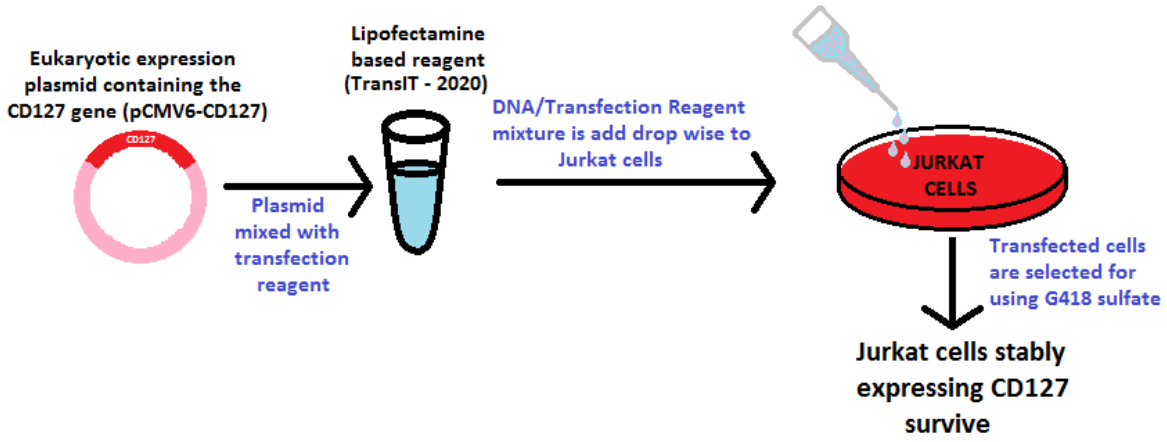

Schematic of the transfection and selection approach to make stably expressing CD127 cell lines.

Originally, I attempted to use the transfection and selection approach to develop a Jurkat cell line that stably expressed CD127. In this approach, I first pre-warmed the transfection reagent TransIT-2020 (Mirus Bio, LLC.; Madison, WI) and the purified pCMV6-CD127 plasmid to room temperature. I then mixed 25µg of the plasmid DNA with 100µL of serum free DMEM. I then added 6µL of TransIT-2020 directly into the diluted DNA, mixed and incubated at room temperature for 20 minutes. The DNA and TransIT-2020 form lipid based complexes. The DNA/TransIT-2020 mixture was then added drop-wise to 1E6 Jurkat cells. These cells were then incubated for 24 hours at 37°C. After 24 hours the media was replaced with RPMI-10 and incubated for another hours. 48 hours post transfection, I began to select for cells using complete media supplemented with 750µg/mL of G418 sulfate.

II. C Jurkat cells transfected with pCMV6-CD127 express CD127

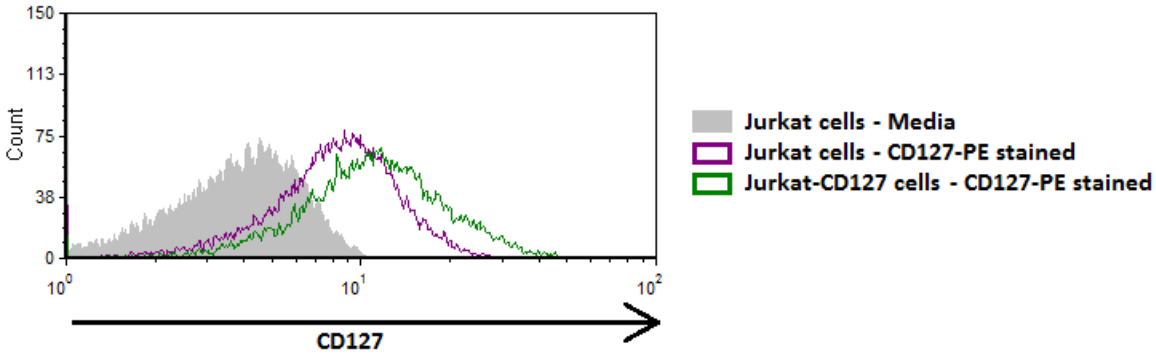

Histogram shows transfected Jurkat cells express higher CD127 levels then untransfected cells.

Jurkat cells were transfected with 25µg of pCMV6-CD127 plasmid using 6µL of TransIT-2020. 24 hours after the transfection, the cells were stained with PE conjugated anti-CD127 antibody. Flow analysis was done using FCS express 3.

III. G418 sulfate kill curve

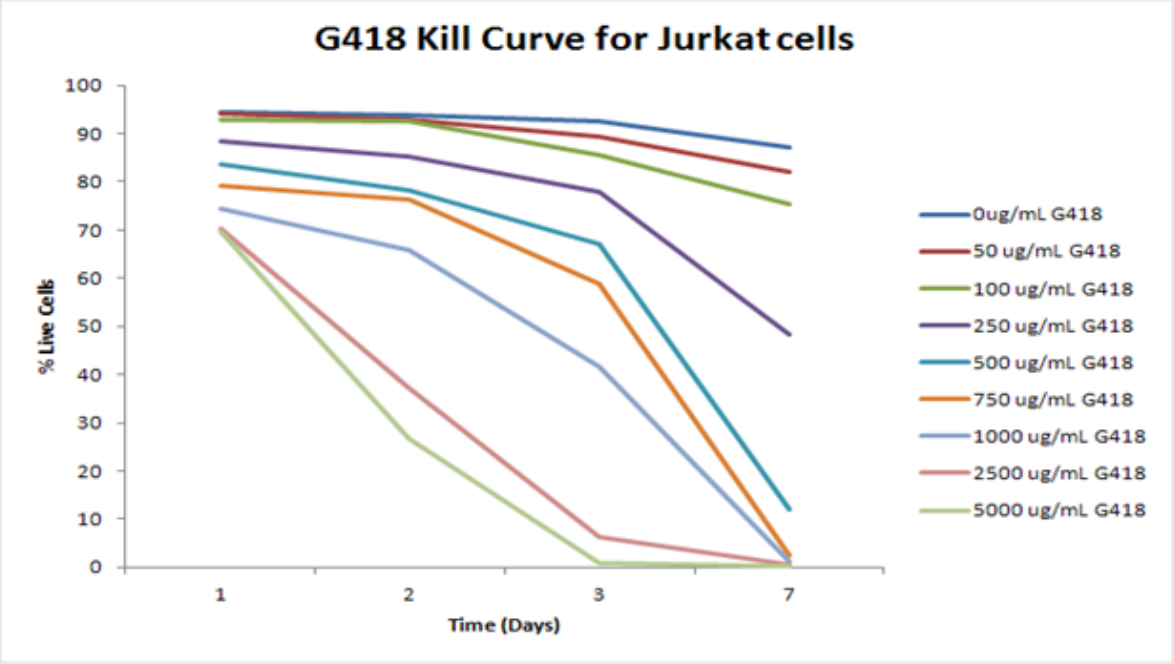

Kill curve for Jurkat cells indicates that the optimal concentration of G418 sulfate in complete media for selecting cells transduced or transfected with the neomycin resistance gene should be between 750-1000µg/mL.

Jurkat cells were cultured in complete media supplemented with 0, 50, 100, 250, 500, 750, 1000, 2500, 5000µg/mL of G418 sulfate for seven days at 37°C. On days 1, 2, 3 and 7, 100µL of sample was removed from each culture, stained with propidium iodine (PI) and analyzed by flow cytometry for cell viability. The percentage of live cells from each reading was graphed. The concentration of 750-1000µg/mL is considered optimal because it smallest concentration that allows for 100% cell death by seven days, but allows cells to survive the first three days of selection.

IV. A Gene map for lentiviral envelope vector, pMD2.G (Addgene plasmid # 12259)

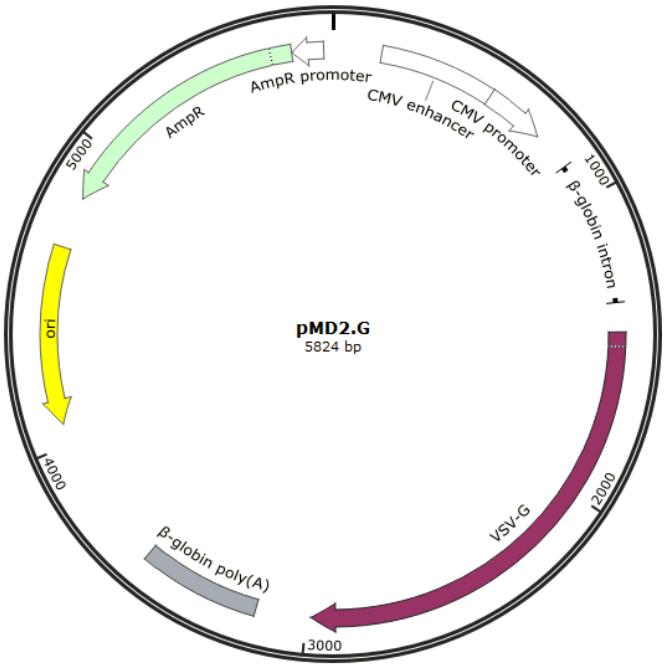

IV. B Gene map for lentiviral packaging vector, psPAX2 (Addgene plasmid # 12260)

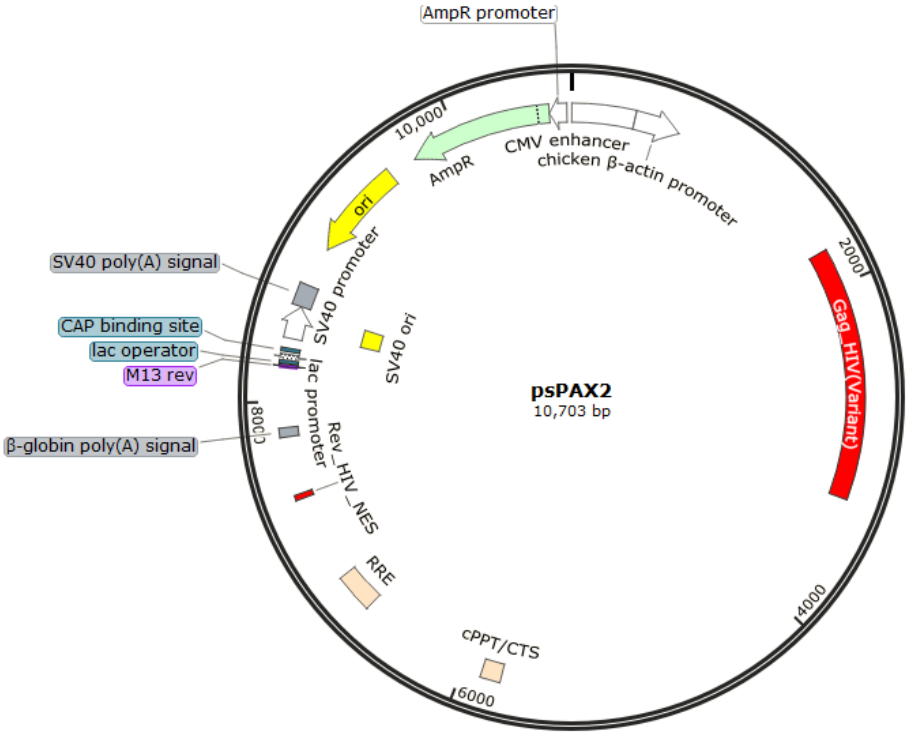

IV. C Gene map for lentiviral transfer vector, pWPI/hPLK2WT/Neo (Addgene plasmid # 35385)

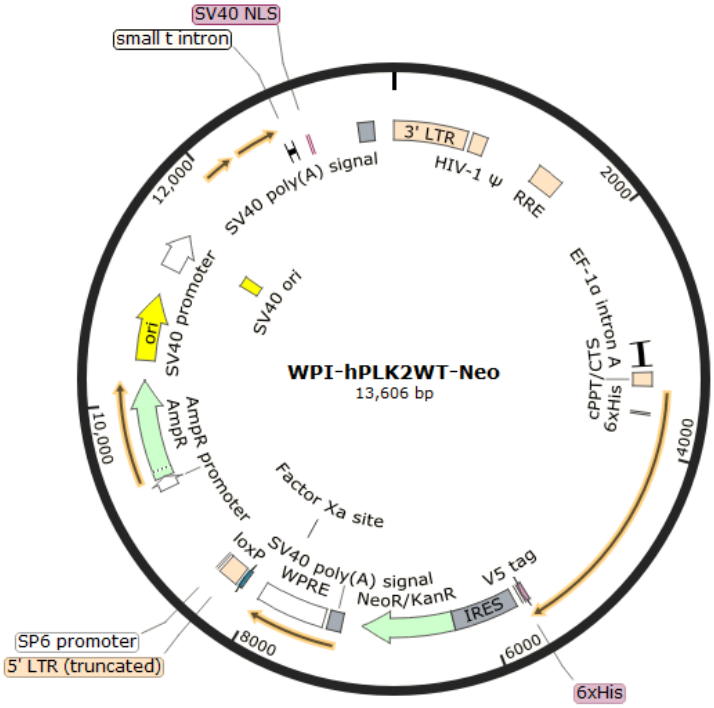

IV. D Gene map for modified lentiviral transfer vector, pWPI/MOCK/Neo

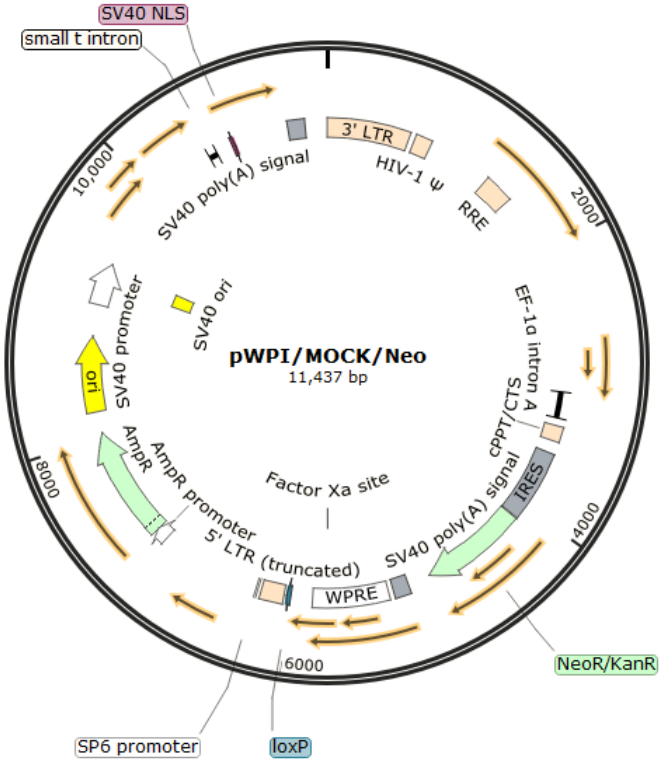

IV. E Gene map for modified lentiviral transfer vector, pWPI/CD127WT/Neo

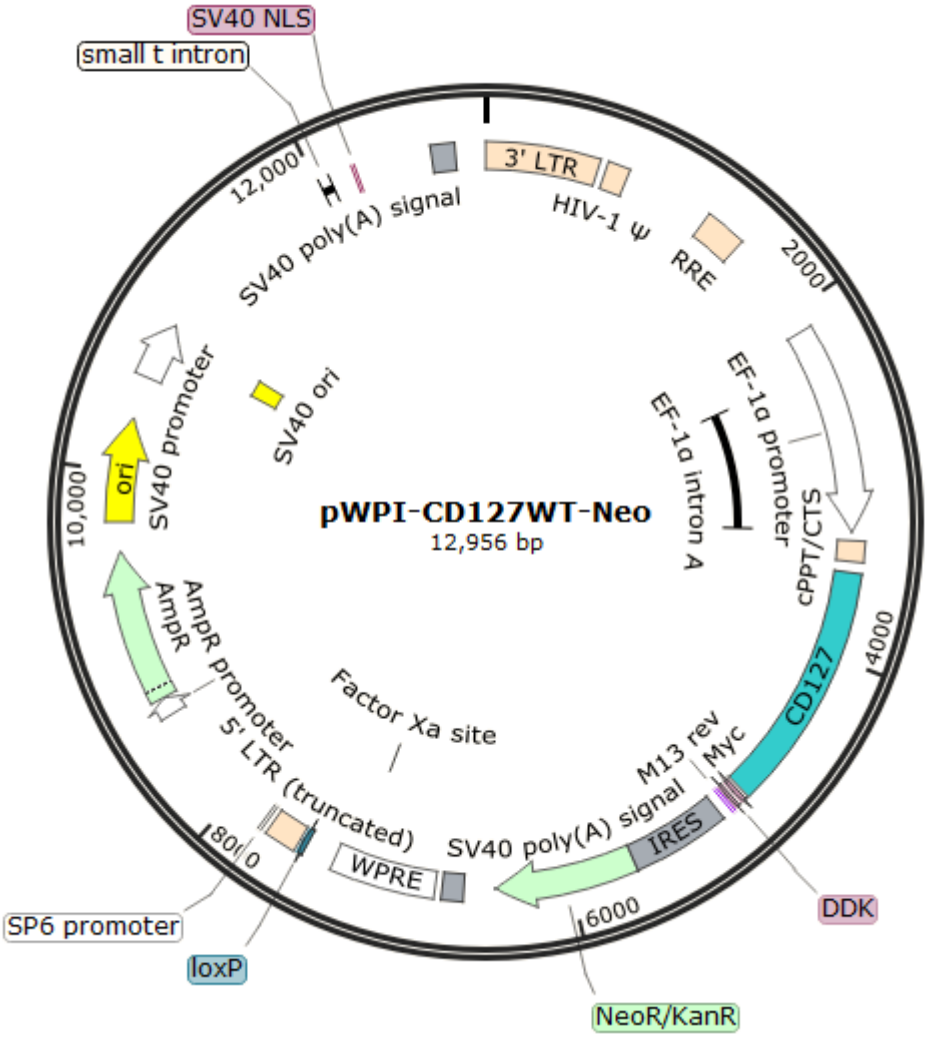

Note all gene maps were made using SnapGene® Viewer Version 2.8 (GSL Biotech LLC; Chicago, IL) and the sequences provided on www.addgene.com or www.origene.com.

V. Prediction of splice sites in CD127 cDNA (Exon 5 to 7)

Online tool to predict splice site acceptor and donors

<http://spliceport.cbcb.umd.edu/>

Input:

> Sequence spanning CD127 exon 5 to exon 7

1 - atgtaaaagttttaatgcacgatgtagcttaccgccaggaaaaggatgaaaacaaatggacgcatgtgaatttatccagcacaaaact
89 -
gacactcctgcagagaaagctccaaccggcagcaatgtatgagattaaagttcgatccatccctgatcactattttaaaggcttctgga
g
179- tgaatggagtccaagttattacttcagaactccagagatcaataatagctcaggggagatggatcctatcttactaaccatcagcattttg
270- agtttttctctgtcgctctgttggtcatcttggcctgtgtgttatggaaaaaaaggattaagcctatcgtatggcccagtctccccgatcat
363- aagaagactctggaacatctttgtaagaaaccaagaaaaaatttaaatgtgagtttcaatcctgaaagtttcctggactgccagattcat
452- agggtggatgacatt

EXON 5
EXON 6
EXON 7

Output:

(A)cceptor Or (D)onor	Location in Input sequence	Splice Site Sequence
A	101	cctgcagagaaa
A	103	tgcagagaaagc
A	107	gagaaagctcca
A	120	ccggcagcaatg
D	124	gcaatgtatgag
A	131	gtatgagattaa
A	138	attaaagttcga
D	137	ttaaagttcgat
A	168	tttaaaggcttc
A	178	tctggagtgaat
D	177	ctggagtgaatg
A	187	aatggagtccaa
D	186	atggagtccaag
A	193	gtccaagttatt
D	192	tccaagttatta
A	205	acttcagaactc
A	213	actccagagatc
A	215	tccagagatcaa
A	226	ataatagctcag
A	231	agctcaggggag
A	236	aggggagatgga
A	262	ccatcagcattt
A	271	ttttgagttttt
D	270	tttgagttttt
D	281	tctctgtcgctc
D	289	gctctgttggtc

(A)cceptor Or (D)onor	Location in Input sequence	Splice Site Sequence
D	293	tgttggtcatct
D	306	ggcctgtgtgtt
D	308	cctgtgtgttat
D	310	tgtgtgttatgg
A	325	aaaaaaggatta
A	332	gattaagcctat
D	338	ctatcgtatggc
A	349	ggcccagtctcc
D	348	gcccagtctccc
A	365	tcataagaagac
A	368	taagaagactct
D	384	tctttgtaagaa

Acceptor site in red is at the end of exon 6 and beginning of exon 7
Donor site in green is at the end of exon 5
Donor site in blue is at the beginning of exon 6

CURRICULUM VITAE

Marko Cavar

Education

University of Ottawa, Ottawa, ON
Candidate for Master of Science degree in Microbiology and Immunology *05/2013-08/2015*
Major Research Project: Mutational analysis of CD127 and its role in immunological diseases; under the supervision of Dr. Paul A. MacPherson at the Ottawa Hospital Research Institute-Department of Chronic Diseases

University of Ottawa, Ottawa, ON
B.Sc. (Hons.) in Biochemistry with MIC option *09/2006-05/2013*
Major Research Project: Aptamer Based Detection Technique for Viruses: Latex Agglutination; under the supervision of Dr. Maxim Berezovski at the University of Ottawa

Work Experience

Biochemistry Undergraduate Teaching Lab, Ottawa, ON
Assistant Lab Technician *09/2012-04/2013*
Part-time position that involved preparing reagents and bacterial cultures for biochemistry and molecular biology labs; optimizing PCR protocols used by students; sub-cloning genes that encode different fluorescent proteins into expression plasmids for use in future labs.

Environment Canada, Gatineau, QC
Risk Assessor *05/2012-08/2012*
Performed searches on azo-based chemicals for toxicity data and for possible structural and functional analogues. Developed a database of toxicity information on various azo-based chemicals and guidance documents to analyze toxicity data.

Environment Canada, Gatineau, QC
Junior Regulatory Specialist & Program Officer *05/2010-05/2012*
Provided support to multiple departments with regards to Chemical Management Plan (CMP) related files. Maintained and updated CMP databases. Developed analyses of various reports related to chemical files such as Bisphenol A and Cyclotetrasiloxane, octamethyl-(D4).

Health Canada, Ottawa, ON
Scientific Evaluator *09/2008-10/2008*
01/2009-08/2009
Evaluated the chemical composition of food packaging materials for toxicity safety. Created and updated a database of information on chemicals including the common uses and toxicity data.

Other Experience

Canadian Cancer Society, Ottawa, ON
Volunteer-Project Leader *01/ 2007-11/ 2008*

- Converse with and comfort chemotherapy patients in English or French
- Work with staff of the cancer centre as a team to improve patients sessions by delivering or gathering patients files
- Maintain and set up a new patient chemotherapy teaching session
- Provide guide tours of the centre and try to ease patients into their new settings

Jadran Croatian Soccer Club, Ottawa, ON
Manager of Men's Competitive and Recreational Team *03/2008-11/2008*

- Acted as registrar for the 2008 winter season by collecting and processing applications and registrations
- Assisted in the organization of fundraisers and functions to help support the club and team

Awards

University of Ottawa - Graduate Studies Entrance Scholarship *09/2013-08/2015*
University of Ottawa BMI Research Day - Best Poster *05/2014*
University of Ottawa - Deans Honour List *09/2012-04/2013*
Admission Scholarship of the University of Ottawa *09/2006-04/2007*

Publications

1. "Mutational analysis of CD127 and its role in immunological diseases" *08/2015*
   Marko Cavar and Paul A. MacPherson
   M.Sc. Thesis
2. "IL-7 induces clathrin-mediated endocytosis of CD127 and subsequent degradation by the proteasome in primary human CD8 T cells" *08/2015*
   Elliot M. Faller, Feras M. Al-Ghazawi, **Marko Cavar** and Paul A. MacPherson
   Immunology and Cell Biology 2015; doi: 10.1038/icb.2015.80.
   [Epub ahead of print]
3. "Aptamer based detection technique for Viruses: Latex agglutination" *04/2013*
   Marko Cavar and Dr. Maxim Berezovski
   B.Sc. (Hons.) Thesis

Abstracts

1. "Autoimmune Disease Associated Mutational Analysis of CD127 Signaling, Expression & Regulation" *03/2015*
   Marko Cavar and Dr. Paul A. MacPherson
   Faculty of Medicine, BMI seminar day - Ottawa
2. "Disease Specific Mutational Analysis of CD127 Signaling, Expression & Regulation" *10/2014*
   Marko Cavar and Dr. Paul A. MacPherson
   Ontario HIV Treatment Network Back2Basic Conference - Toronto
3. "Development of an *In Vitro* Model to Study Interleukin 7 Signaling" *05/2014*
   Marko Cavar and Dr. Paul A. MacPherson
   Faculty of Medicine, BMI poster day - Ottawa
4. " Determining the optimal cell line for the transfection of pCMV-CD127 plasmid, for the purpose of studying IL-7 signaling in vitro." *10/2013*
   Marko Cavar and Dr. Paul A. MacPherson
   Ottawa Hospital Research Institute (OHRI) Annual Poster Day - Ottawa